

©[2013]

Ariel Martin

ALL RIGHTS RESERVED

DEVELOPMENT OF A DECISION SUPPORT SYSTEM TO
OPERATE THE GREENHOUSE LIGHTING AND SHADING
SYSTEMS POWERED BY A DISTRIBUTED GENERATOR

by

ARIEL MARTIN

A dissertation submitted to the

Graduate School-New Brunswick

Rutgers, The State University of New Jersey

In partial fulfillment of the requirements

For the degree of

Doctor of Philosophy

Graduate Program in Environmental Sciences

Written under the direction of

Dr. Arend-Jan Both

And approved by

New Brunswick, New Jersey

OCTOBER, 2013

ABSTRACT OF THE DISSERTATION

DEVELOPMENT OF A DECISION SUPPORT SYSTEM TO OPERATE THE GREENHOUSE LIGHTING AND SHADING SYSTEMS POWERED BY A DISTRIBUTED GENERATOR

By ARIEL MARTIN

Dissertation Director:

Dr. Arend-Jan Both

A Decision Support System (DSS) was developed to manage the use of the electricity generated by a landfill gas-fired 250 kW microturbine system installed at the Rutgers EcoComplex Research and Demonstration Greenhouse located at the Burlington County Resource Recovery Complex near Columbus, NJ. The approximately 220 kW of available power (30 kW are parasitic losses) can be used on-site for supplemental lighting of the greenhouse crop, or it can be exported to the local electricity grid.

In order to maintain sufficiently high crop production during the winter months and darker stretches during other times of the year, supplemental lighting is necessary particularly in the Northern regions of the country. Due to the relatively high light intensity required, supplemental lighting of greenhouse crops can be expensive. The DSS minimizes the cost of the electricity associated with supplemental lighting and guarantees that the harvest date and yield targets are achieved.

The DSS can be implemented at any location within the geographic area of PJM (regional transmission organization that coordinates the wholesale electricity market in 13 states, including NJ) and it was validated by simulation using five years of historic hourly values of electricity prices from PJM and hourly values of solar radiation and other meteorological variables from the National Solar Radiation Database (NSRDB).

The simulation results show that the DSS is able to effectively manage different possible configurations of the supplemental lighting and shading systems to meet a predetermined harvest date and yield while minimizing the use of the on-site generated electricity. All of the excess electricity is exported to the grid in such a way as to maximize the additional income from electricity sales.

Acknowledgements

Many have contributed to the completion of this dissertation and to all of them I wish to express my gratitude and appreciation.

I am specially grateful to my advisor and mentor Arend-Jan Both who gave me the freedom to pursue my ideas and provided the guidance, thoughtful advice, and patience that made possible the development of this research.

To Daniel Gimenez, whose wisdom and ability to point me into the right direction have been invaluable throughout these years of graduate school.

To the Strom family, who have welcomed us and made us part of their own.

To the other members of my graduate committee: Dr. Chris Uchrin, Dr. Frank Felder.

Finally, I am most grateful to my husband, Luis. Without his love and support this research wouldn't have been possible.

Table of Contents

Table of Contents	v
Abstract	ii
Acknowledgements	iv
List of Tables	ix
List of Figures	xi
1. Introduction	1
2. Literature Review	6
2.1. Prediction of Solar Radiation	6
2.2. Prediction of Electricity Prices	9
2.3. Crop Modeling	11
2.4. Decision Support System	13
3. DSS Variables Initialization and Preliminary Calculations	17
3.1. Parameter Initialization	17
3.1.1. Global Variables	17
3.1.2. Local Variables and their Values for the Present Project	18
3.1.3. Operational Variables and their Values for the Present Project	18

3.2. Preliminary Calculations	19
3.2.1. Selection of the nearest NSRDB station	19
3.2.2. Solar Altitude and Azimuth as Functions of Time	21
3.2.3. Sunrise and Sunset Times for a given Julian Day	23
3.2.4. Time Related Operations and Transformations	23
3.2.5. Greenhouse Transmittance	25
4. Prediction of Solar Radiation	29
4.1. National Solar Radiation Database (NSRDB)	30
4.2. Solar Radiation for a Clear Sky	30
4.2.1. Direct-Beam Radiation	31
4.2.2. Diffuse Radiation	32
4.2.3. Reflected Radiation	33
4.2.4. Clear Sky Total Radiation	34
4.3. Prediction of Solar Radiation	34
4.3.1. Validation of Assumptions	36
4.3.2. Long Term Prediction of PAR Energy Inside the Greenhouse .	40
5. Prediction of Electricity Prices	42
5.1. Introduction	42
5.2. Modeling Day-Ahead LMPs	43
5.2.1. Quantitative Variables	45
5.2.2. Qualitative Variables	46
5.2.3. Linear Regression Model for Day-Ahead LMPs	49
5.2.4. Linear Regression Results	49
5.3. Modeling Real-Time LMPs	50
5.4. Prediction of Electricity Prices	53
6. Decision Module	55

6.1.	Update of Prediction of Solar Radiation	56
6.2.	Crop Model	58
6.2.1.	General model assumptions	59
6.2.2.	Equation for Days to Flowering (Seedling Stage)	59
6.2.3.	Equation for Fruit Yield (Production Stage)	60
6.2.4.	Variables for the Crop Model Section	60
6.2.5.	Crop Model Implementation	61
6.3.	Decision Submodule	62
6.4.	Update of the Prediction of Electricity Prices	62
6.5.	Update of the History File	64
7.	Decision Submodule	65
7.1.	Calculation of the Radiation Gap	66
7.2.	Shade Screen Selection	69
7.2.1.	Selection of a Combination of Shade Screens	71
7.3.	Supplemental Lighting Algorithm	71
7.3.1.	Basic Definitions	71
7.3.2.	Available Hours for Supplemental Lighting	72
7.3.3.	Matrix Representation of the Available Hours for Supplemental Lighting	74
7.3.4.	Reduction of the Matrix Representing the Available Hours for Supplemental Lighting	77
7.3.5.	Hourly Distribution of R_{gap}	78
7.3.6.	Supplemental Lighting Decision	81
8.	Results	82
8.1.	Simulations Rationale and Definitions of Performance Metrics	82

8.2. Performance of the DSS while Providing Supplemental Lighting. Minimum Time from Sowing to Final Harvest and Maximum Crop Yield Targets.	90
8.3. Performance of the DSS while Using the Shade Screens for the Hypothetical case of Maximum Time from Sowing to Final Harvest and Minimum Crop Yield Targets.	110
9. Discussion	123
9.1. Performance of the DSS at Providing Supplemental Lighting. Minimum Time from Sowing to Final Harvest and Maximum Crop Yield Targets.	123
9.2. Performance of the DSS while Using the Shade Screens for the Hypothetical case of Maximum Time from Sowing to Final Harvest and Minimum Crop Yield Targets.	138
10. Summary and Conclusions	145
10.1. Future Work	150
Appendices	152
A. Cost and Greenhouse Gas (GHG) Emissions Analysis	153
B. Decision Support System Programming Code	169
C. DSS Auxiliary Data and Simulation Results	171
References	175

List of Tables

3.1. Analysis of Variance for Solar Radiation Transmittance Regression . .	27
3.2. Parameter Estimates for Solar Radiation Transmittance Regression . .	27
4.1. Analysis of Variance for Solar Radiation Transmittance Regression . .	35
4.2. Parameter Estimates for sky cover Model	36
4.3. National Solar Radiation Database NJ Stations	39
4.4. Coefficient of Determination and Coefficient of Variation of the Root-Mean-Square-Error for NJ Stations	40
5.1. Analysis of Variance for Day-Ahead Electricity Prices Regression . . .	50
5.2. Analysis of Variance for Real-Time Electricity Prices Regression . . .	52
5.3. Parameters Estimates for Solar Radiation Transmittance Regression .	53
7.1. Possible combinations in which a set of three screens can be selected.	70
8.1. Lamps per Area and Power per Area vs. Lighting Intensity for two Cases of mounting height.	87
8.2. Selection of set points for the Reference Case new control strategy . .	112
9.1. Ratio of energy use for DSS to energy use for Reference Case during summer	132
9.2. Ratio of energy use for DSS to energy use for Reference Case during winter	134
9.3. Ratio of lighting cost for DSS to lighting cost for Reference Case during summer	136
9.4. Ratio of lighting cost for DSS to lighting cost for Reference Case during winter	137
A.1. LED, HPS, and CMH fixtures for the cost and GHG emissions analysis.	155

A.2. Lamps per Area vs. Lighting Intensity when mounting height is 5 feet for 400 W HPS lamps.	156
A.3. Power per Area vs. Lighting Intensity when mounting height is 5 feet for selected lamps.	156
A.4. Configuration, energy use, and cost for LED and HPS lighting systems	161
A.5. Lighting fixtures purchase cost for LED and HPS lighting systems . .	162
A.6. Return on investment for LED lighting system. Reference: HPS system	163
A.7. Configuration, energy use, and cost for LED and CMH lighting systems	164
A.8. Lighting fixtures purchase cost for LED and CMH lighting systems .	165
A.9. Return on investment for LED lighting system. Reference: CMH system	166

List of Figures

1.1. Flow Chart of the Main Components of the Decision Support System	5
3.1. Distance between the station and the location.	20
3.2. Solar position as a function of time.	22
3.3. Greenhouse inside and outside solar PAR values used for the <i>Transmittance</i> Linear Model	26
3.4. Solar radiation transmittance regression. Four common regression diagnostics plots based on the R-Student residuals	28
4.1. Solar radiation striking a surface and the various angles involved. . .	32
4.2. sky cover Regression. Four common regression diagnostics plots based on the R-Student residuals	37
5.1. Wholesale electricity prices and weather variables for PJM PSEG Zone during 2001.	44
5.2. Day-Ahead Electricity Prices Regression. Four common regression diagnostics plots based on the R-Student residuals	51
5.3. Real-Time Electricity Prices Regression. Four common regression diagnostics plots based on the R-Student residuals	54
6.1. Decisions Module flow chart	57
6.2. Crop Model flow chart	63
7.1. Decisions Submodule Algorithm	67
7.2. Examples of Hours Classification: Present Hour, Daytime and Night-time Hours.	73
7.3. Examples of Time Period τ_{double}	74

7.4. Different Possible Positions of the Required Dark Period During the Nighttime Hours.	75
8.1. Power per area vs. lighting intensity for two cases of mounting height.	88
8.2. Performance of DSS while Providing Supplemental Lighting. Time from Sowing to Final Harvest during Summer	94
8.3. Performance of DSS while Providing Supplemental Lighting. Time from Sowing to Final Harvest during Winter	95
8.4. Performance of DSS while Providing Supplemental Lighting. Total Fruit Yield during Summer	96
8.5. Performance of DSS while Providing Supplemental Lighting. Total Fruit Yield during Winter	97
8.6. Performance of DSS while Providing Supplemental Lighting. Lighting Energy Use during Summer	98
8.7. Performance of DSS while Providing Supplemental Lighting. Ratio of Lighting Energy Use during Summer	99
8.8. Performance of DSS while Providing Supplemental Lighting. Lighting Energy Use during Winter	100
8.9. Performance of DSS while Providing Supplemental Lighting. Ratio of Lighting Energy Use during Winter	101
8.10. Performance of DSS while Providing Supplemental Lighting. Lighting Cost during Summer	102
8.11. Performance of DSS while Providing Supplemental Lighting. Ratio of Lighting Cost during Summer	103
8.12. Performance of DSS while Providing Supplemental Lighting. Lighting Cost during Winter	104
8.13. Performance of DSS while Providing Supplemental Lighting. Ratio of Lighting Cost during Winter	105

8.14. Performance of DSS while Providing Supplemental Lighting. Radiation Budget during Summer. Day-Ahead Market	106
8.15. Performance of DSS while Providing Supplemental Lighting. Radiation Budget during Summer. Real-Time Market	107
8.16. Performance of DSS while Providing Supplemental Lighting. Radiation Budget during Winter. Day-Ahead Market	108
8.17. Performance of DSS while Providing Supplemental Lighting. Radiation Budget during Winter. Real-Time Market	109
8.18. Performance of the DSS while Using the Shade Screens. Time from Sowing to Final Harvest during Summer	115
8.19. Performance of the DSS while Using the Shade Screens. Total Fruit Yield during Summer	116
8.20. Performance of the DSS while Using the Shade Screens. Lighting Energy Use during Summer	117
8.21. Performance of the DSS while Using the Shade Screens. Ratio of Lighting Energy Use during Summer	118
8.22. Performance of the DSS while Using the Shade Screens. Lighting Cost during Summer	119
8.23. Performance of the DSS while Using the Shade Screens. Ratio of Lighting Cost during Summer	120
8.24. Performance of DSS while Using the Shade Screens. Radiation Budget. Day-Ahead Market	121
8.25. Performance of DSS while Using the Shade Screens. Radiation Budget. Real-Time Market	122
A.1. Lamps and Power per unit floor area vs. lighting intensity for HPS selected lamp.	158
A.2. Lamps and Power per unit floor area vs. lighting intensity for LED selected lamp.	158

A.3. Lamps and Power per unit floor area vs. lighting intensity for CMH
selected lamp. 159

Chapter 1

Introduction

It is estimated that greenhouse tomatoes represent around 37% of the fresh tomatoes sold at U.S. retail outlets, making the North American greenhouse tomato industry a major player on the larger fresh tomato market. Canada is the largest producer of greenhouse tomatoes in North America (42 percent), followed by the U.S. (30 percent), and Mexico (28 percent). Although Canada is the industry leader in the region, as of 2005 it did not produce greenhouse tomatoes during the winter months profitably, leaving the U.S. market available to U.S. and Mexican producers during this period when the prices of fresh tomatoes are higher (Cook & Calvin, 2005).

Because of climate conditions, the largest U.S. greenhouse tomato operations are located in the Southwest and West. However, there are several factors that make the production of greenhouse tomatoes in the Northeast during the winter an attractive opportunity: high prices during the winter, year around demand for fresh tomatoes, and the relative high cost of transportation to bring fresh tomatoes from different areas. Albright (2005) showed that less energy is needed to produce winter greenhouse tomatoes in New York State than to transport them to the state from the winter production areas (Florida, California, Mexico).

Due to low temperatures and solar radiation, the production of greenhouse tomatoes in the Northeast during the winter requires the use of energy for heating and supplemental lighting, making the cost associated with supplemental lighting a big expense for tomato growers in the region.

Managing the use of supplemental lighting to achieve the grower's goals while minimizing the cost of electricity is a challenging task for a greenhouse operator

because the present crop needs (depending on the yield and harvest time targets) are functions of the past and future values of the different environmental factors that have an effect on the crop development, among them: photosynthetically active radiation (PAR, radiation with wavelengths between 400 and 700 nm), carbon dioxide concentration, nutrients, temperature, and relative humidity.

The changing price of electricity is another factor that adds complexity to the management of the greenhouse supplemental lighting system. In the particular case of the present project, the electricity is generated by a 250 kW landfill gas-fired microturbine system installed at the Rutgers EcoComplex Research and Demonstration Greenhouse located at the Burlington County Resource Recovery Complex in Columbus, NJ.

The approximately 220 kW of available power (30 kW are required for the operation of the micro-turbine and fuel conditioning system, the so called parasitic losses) is used in the greenhouse mainly for supplemental lighting, otherwise it is exported to the grid. The exported electricity and the renewable energy credits (1 renewable energy credit, REC, is generated for every MWh of electricity produced) generate secondary revenue for the greenhouse operator.

In this new scenario, the goals of the greenhouse operator are not only to meet the crop needs according to the time and yield targets, but also to maximize the secondary income from the exported electricity. Unfortunately, these goals act in opposite ways: the more electricity is exported to the grid the less is available for supplemental lighting necessary to achieve the time and yield targets and vice versa.

Several optimization problems can be defined in this case depending on the final goal. If the goal is to maximize the total economic benefits from the greenhouse operation, including the income from the exported electricity and the income resulting from selling the harvest, then it is necessary not only to predict the electricity prices but also the crop prices.

Because of the uncertainty associated with the prediction of crop prices, the approach in the present study has been to reduce the optimization problem to the case when the harvest date and yield targets are constrained to fixed values imposed by the grower and the goal is just to maximize the value of the exported electricity by providing supplemental lighting during the hours when the electricity prices are the lowest.

To find the optimal lighting schedule that makes possible that both goals are met, a decision support system (DSS) with the following elements is required:

- A model that relates crop parameters (e.g., crop growth period and yield) to environmental variables such as cumulative PAR energy, carbon dioxide concentration, nutrients, temperature, and relative humidity,
- Predicted values of incoming solar radiation and electricity prices,
- An optimization algorithm that uses the output from the crop growth model and the predicted values of the environmental variables and electricity prices to make a decision on a defined time step basis to provide a specific amount of supplemental light to the crop.

The DSS program was written in the MATLAB language and consists of a main program whose components are individual functions related to the three previously mentioned elements. Several reasons make the MATLAB language appropriate for the present work:

- The possibility to create custom functions facilitates the use of functional programming that fits naturally with the logic of the DSS,
- The individual functions are written independently and have a flexible structure: given an argument or input, an output is generated through a defined process. The input and output are not restricted to a single value and the process is a series of permissible operations on the argument,

- The present DSS is based on operations and transformations on data in the form of vectors and matrices. MATLAB provides a high level programming environment oriented to the work with matrices and arrays, algorithm development, and data analysis, which makes it appropriate for this study.

Figure 1.1 shows a flow chart of the main modules of the DSS. The role and the structure of the operations of each of those parts will be described in the next chapters.

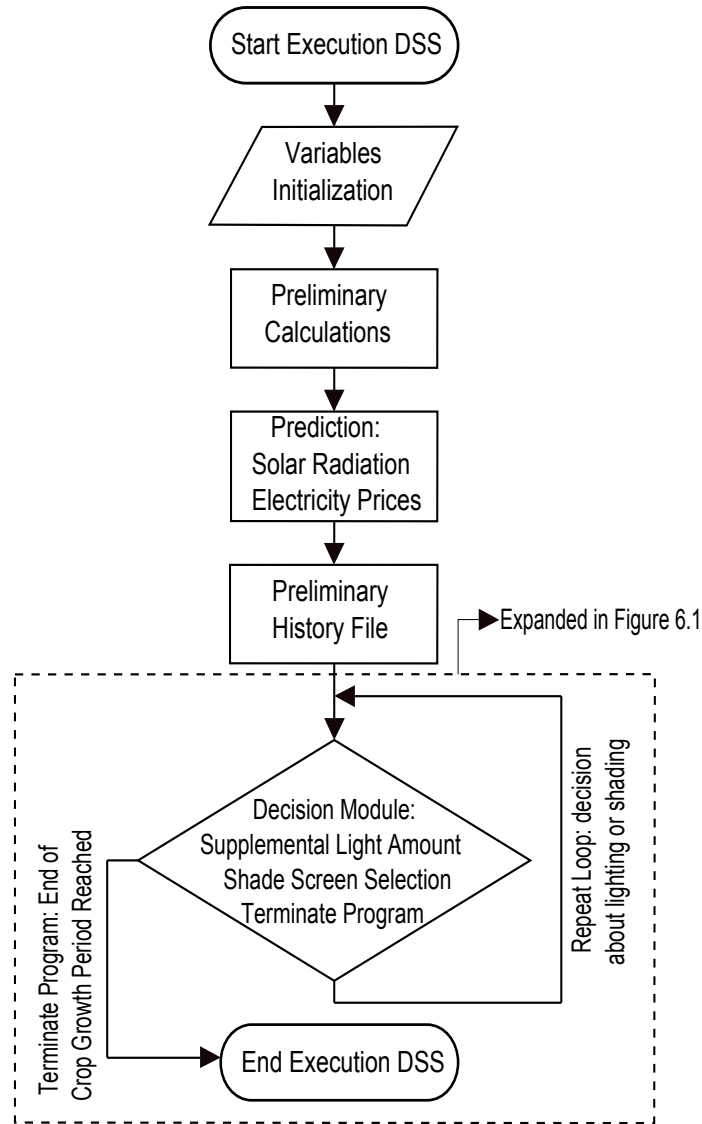


Figure 1.1: Flow chart of the main components of the Decision Support System (DSS). The arrows represent the order of execution of the different operations. The Parameters Initialization and Preliminary Calculations sections are discussed in the first chapter. The second chapter comprises the Prediction of Solar Radiation and the third one the Prediction of Electricity Prices. The Preliminary History File section is introduced at the beginning of the fourth chapter. The Decision Module section is explained in the fourth and fifth chapters.

Chapter 2

Literature Review

2.1 Prediction of Solar Radiation

Solar radiation models for agricultural applications usually fall in two broad categories:

- Stochastic models
- Regression models

The goal of the stochastic models is to generate weather data (precipitation, temperature, solar radiation) with the same statistical characteristics (distribution, mean, standard deviation) as the observed data (Hoogenboom, 2000). The data generated by these models, usually called synthetic data, is particularly useful in climate and agriculture when historic weather data is missing and it is necessary to evaluate the effects of the variability of the weather variables (Wilks & Wilby, 1999).

The best known stochastic weather models or *weather generators*, as they are usually referred to in the literature, are the GWEN (Richardson, 1981, 1984), USCLIMATE (Hanson et al., 1994), and CLIGEN (Nicks & Gander, 1993) models. A generalized version of the GWEN model was evaluated by Wilks (1999) in 62 weather stations in the USA northwest. Wilks (1999) showed that the GWEN model can be used to simultaneously generate meteorological time series for a large collection of locations preserving the spatial correlation observed in recorded data. Johnson et al. (1996) compared and evaluated the USCLIMATE and CLIGEN models at six widely dispersed stations across the USA and concluded that USCLIMATE is superior to

CLIGEN at simulating variability and correlation of meteorological variables making USCLIMATE a better choice for biological and hydrological applications and also for applications that estimate electrical power demand using modeled meteorological data.

It is important to mention that the weather generators are not forecasting models and that the time resolution of the data generated is usually a day (24 hour period). These two facts prevent their use in our present work. As will be explained in chapters 6 and 7, the DSS requires prediction of hourly values of solar radiation and electricity prices to take a decision, depending on harvest and yield targets set by the grower, about providing supplemental lighting or deploying the screens.

An alternative to the stochastic models are the solar radiation regression models that offer the possibility of generating forecast values of solar radiation using measurements or forecast of other weather variables. The model developed by Ångström (1924) predicts daily total solar radiation from the daily fraction of sunshine hours. Bristow and Campbell (1984) and Hargreaves et al. (1985) use daily maximum and minimum temperature to predict daily total solar radiation while Reddy (1987) uses precipitation.

Hunt et al. (1998) fitted two linear models to predict daily total solar radiation (one using maximum and minimum temperature, and the other using maximum and minimum temperature, and precipitation), and compared them to the models developed by Bristow and Campbell (1984), Hargreaves et al. (1985), and Reddy (1987) using data for eight sites in Ontario, Canada. Hunt et al. (1998) concluded that the results corresponding to the method described by Reddy (1987) were poor, while the two linear regressions were superior to the Bristow and Campbell (1984) or Hargreaves et al. (1985) approaches.

The solar radiation regression models based on temperature and precipitation are among the most commonly used in agricultural applications for several reasons: the weather stations commonly used as sources of data for modeling are usually located

near airports and poorly represent the conditions of the locations where the models are intended to be used; measurement of solar radiation is frequently missing even at these stations, and measurement of temperature and precipitation is relatively easy and frequently done in stations located at agricultural sites (Hoogenboom, 2000).

The previously mentioned regression models, however, forecast solar radiation daily totals and the present DSS requires forecast of hourly values of solar radiation. Although forecasting hourly values of solar radiation is challenging (Albright et al., 2000), it is possible to build simple regression models that perform relatively well at forecasting hourly values of solar radiation using forecast values of sky cover (Perez et al., 2007).

Several models have been developed to predict solar radiation using sky cover as predictor. Davies and McKay (1988) predict hourly values of solar radiation based on extraterrestrial solar radiation, cloud layer information, and landscape and atmospheric albedo. Brinsfield et al. (1984) predict daily total solar radiation based only on hourly values of total opaque sky cover. Supit and Van Kappel (1998) estimate global radiation from mean daytime sky cover and maximum and minimum temperature. The model developed by Kasten and Czeplak (1980) predicts solar radiation using solar radiation for a clear sky and ground observed sky cover measured in octas (fraction of the sky covered by clouds, in eighths).

The Perez et al. (2007) model follows closely the model introduced by Kasten and Czeplak (1980), but instead of using ground observed sky cover it uses forecasted values of sky cover from the National Digital Forecast Database. The solar radiation model developed in the present project also relies on forecasted values of sky cover from the National Digital Forecast Database, however, the form of the regression function is not predefined but adopts a general linear form whose parameters are determined through local calibration. The values of solar radiation for a clear sky used in the solar radiation model for the present project are determined according to Threlkeld and Jordan (1958) as discussed in Chapter 4.

2.2 Prediction of Electricity Prices

The ranking of the future hours according to their corresponding forecasted values of electricity prices is a factor that influences the decision about providing supplemental lighting or deploying the shade screens. For this reason, the DSS requires a prediction of electricity prices that makes possible to rank the future hours.

The wholesale electricity market and the movement of electricity in Delaware, the District of Columbia, Maryland, New Jersey, Ohio, Pennsylvania, Virginia, West Virginia, and parts of Indiana, Illinois, Kentucky, Michigan, North Carolina and Tennessee are managed and controlled by the Regional Transmission Organization (RTO) and the Independent System Operator (ISO) PJM Interconnection.

The market consists of two distinct markets: the Day-Ahead Market and the Real-Time Market. PJM uses Locational Marginal Prices (LMP) to reflect the varying energy costs within the region depending on the transmission constraints. The Day-Ahead LMPs depend on generation offers and demand bids and are calculated for each hour of the next operating day. The Real-Time LMPs are calculated every five minutes according to the actual grid operation conditions.

For the present project the electricity is generated by an on site distributed generation unit and is used mostly for supplemental lighting. Only the excess power that is not needed to meet the crop needs is exported to the wholesale electricity market. The developed DSS is designed to maximize the revenue from the exported electricity while meeting the crop targets set by the grower.

The system can be used when the exported electricity is sold in any of the LMP zones of the PJM Day-Ahead or Real-Time Markets, but the simulation is done for the PSEG (Public Service Electric and Gas Company) zone since PSEG is the power utility that serves the geographic area where the greenhouse and the power generation unit (the microturbine) are located.

Because the Day-Ahead LMPs are settled for the next day and are available from

the ISO website, the design of the DSS is such that it relies on those posted Day-Ahead LMPs to make the decisions. However, for the exceptional situations when the Day-Ahead LMPs are not available (e.g., server unavailable, no internet connection, power outage) the DSS uses predicted Day-Ahead LMPs.

Among the most commonly used approaches to model electricity prices are statistical methods and intelligent-based techniques (Weron, 2006; Aggarwal et al., 2009). The statistical methods are based on time series analysis and comprise some of the different techniques that are used to study time-oriented data with correlated errors: dynamic regression and transfer function (Nogales et al., 2002), autoregressive integrated moving average (ARIMA) models (Contreras et al., 2003; Conejo et al., 2005), and generalized autoregressive conditionally heteroskedastic (GARCH) models (Guirguis & Felder, 2004).

The intelligence-based techniques used to model electricity prices are comprised mostly of the artificial neural network (ANN) models, overparameterized nonlinear regression models that perform better at predicting future values than regular linear regression or time series techniques (Kutner et al., 2004a). Works published in this area include Szkuta et al. (1999); Yamin et al. (2004); Catalao et al. (2007); Mandal et al. (2006), and Mandal et al. (2007). In particular, the studies by Mandal et al. (2006, 2007) focus on the application of these techniques to the prediction of electricity prices in the PJM area.

In the present project, however, the Day-Ahead electricity prices are modeled using a multiple linear regression using time and weather variables as predictors. Although Real-Time electricity prices are more erratic than Day-Ahead electricity prices, the fact that Real-Time electricity prices follow a similar trend to Day-Ahead electricity prices was used to model Real-Time electricity prices as a single linear regression using Day-Ahead electricity prices as the predictor variable.

Although this method is less robust than ANN models to capture the non-linearity

observed in the data, it allows easier interpretation of the model parameter and statistical results, reflects the effect that some environmental factors (temperature, humidity, wind speed) have on electricity prices, and accounts for the patterns exhibited by electricity prices at the hourly, daily, and seasonal levels. This choice of price modeling was also determined by the facts that the DSS depends on modeled prices only marginally, the models can be easily calibrated with local data and, considering that the DSS does not require accurate values of electricity prices but instead accurate ranking of the hours according to the prices, the linear regression models provide an adequate fit.

A similar approach has been used by PJM interconnection to forecast electricity loads in the region with the goal of supporting regional transmission expansion planning and reserve margin study (*PJM LOAD/ENERGY FORECASTING MODEL*, 2007; *PJM Manual 19: Load Forecasting and Analysis*, 2012). PJM's load forecasting model is a multiple linear regression that uses time (day of the week, atypical days, months), weather (winter weather parameter, temperature and humidity index), and economic explanatory variables such as the Real Gross Metropolitan Product (a measure of the size of the economy of a metropolitan area).

2.3 Crop Modeling

Since the goal of the present project was to design a DSS to manage the supplemental lighting in a greenhouse when the crop is tomato, a model for this particular crop was needed. The crop model was required to include timing of production and harvest yield as output variables so that the grower can set the harvest time and yield to desired levels.

Crop models are usually classified as explanatory or descriptive (Marcelis et al., 1998). Explanatory models are developed with the objective of understanding and explaining the system by relating the crop growth development to physiological processes (photosynthesis, respiration, transport of water and nutrients). Descriptive

models, on the contrary, have the goal of predicting the system behavior without explaining the underlying principles (Lentz, 1998; Gary et al., 1998).

Several explanatory tomato crop models for a greenhouse environment have been developed. The model of greenhouse tomato growth by Kano and Van Bavel (1988) is based on leaf assimilation and respiration. The TOMGRO model (Jones et al., 1991; Dayan et al., 1993a, 1993b) explains crop development and yield based on the potential growth rate of the different plant organs (sink strength approach) and a series of differential equations to represent the changes in the different plant structures (leaves, fruits, stem segments). The TOMSIM model (E. Heuvelink, 1996, 1999) also explains crop development based on the sink strength approach.

Because explanatory models are based on fundamental processes of the crop biology, they offer some flexibility regarding the set of conditions under which they can be applied. This fact was one reason why the possibility of using an explanatory model was considered for the present project. However, explanatory models tend to be excessively complex and their over parametrization adds more noise than precision (Monteith, 1996). Indeed, although a reduced version of the TOMGRO model has only five variables, the first version contained sixty nine variables, and another version 574 state variables (Jones et al., 1999; Kenig & Jones, 1997). For a tactical DSS like the present one, it is preferable that the crop model is relatively simple and able to provide just what is necessary: a relationship for timing of production and another for harvest yield.

Therefore, and because most of the models for timing of production are not explanatory models (Marcelis et al., 1998), a descriptive model was chosen for the present project. Models to predict production timing of tomato are less common. Liebig (1989) proposes a general approach for modeling timing of production based on a general form for the growth curve and mean growth rate using temperature and solar radiation as input variables, but the model is not calibrated or validated for tomato. The models by Perry et al. (1997) and Wolf et al. (1986) predict tomato

harvest time based on temperature but these models were developed for field crops and not for greenhouse environments where temperature is typically kept within a narrow range of values. The model selected for this project was developed by Giniger et al. (1988) for a single truss tomato cropping system (McAvoy, 1988; McAvoy et al., 1989; Ting et al., 1993).

The single truss tomato cropping system was developed by plant scientists and agricultural engineers at Rutgers University as an alternative to the traditional greenhouse tomato production systems where the plants are kept at fixed locations and the fruits are harvested from the different clusters throughout the plant life cycle that can last as long as 11 months.

In the single truss tomato cropping system the plants are grown on top of movable benches and after harvesting a single fruit cluster (the apical meristem of each plant is pinched two leaves above the first fruit truss), the plants are discarded and replaced. Plants of the same development stage, are kept in crop sections and once transplanted to the crop block corresponding to the next development stage the spacing among them is increased. The single truss cropping system facilitates mechanization and guarantees a continuous production of quality fruits.

The crop model assumes that cumulative PAR energy is the only input variable and the values of the other factors are kept within determined ranges (a valid assumption for a greenhouse environment). It consists of a set of two equations, one for the duration of the seedling or vegetative stage (period from emergence to flowering), and the other for yield during the production stage (period from flowering to harvest).

2.4 Decision Support System

The goal of the present DSS is to manage the use of the electricity generated by a landfill gas-fired 250 kW microturbine system installed at the Rutgers EcoComplex Research and Demonstration Greenhouse. Most of the available power can be used on-site for supplemental lighting of the greenhouse crop, or it can be exported to the

local electricity grid.

The DSS prioritizes the grower's harvest date and yield targets and then minimizes the cost of the electricity associated with the supplemental lighting needed to achieve these goals. By minimizing the cost of supplemental lighting, the DSS maximizes the value of the exported electricity since the power that is not used in the greenhouse is exported to the local electricity grid.

In order to achieve the grower's harvest and yield targets and minimize the cost of electricity associated with supplemental lighting, the DSS requires a yield and production timing crop model and the possibility to control not only the supplemental lighting system, but also the greenhouse shade screens so that the radiation levels inside the greenhouse are finely tuned according to the crop needs and solar radiation and electricity price predictions.

Several studies have been dedicated to dynamic optimization, the use of crop modeling to control the greenhouse supplemental lighting according to certain optimization criteria. E. P. Heuvelink and Challa (1989) developed a strategy to control supplemental lighting based on the break even point between the future economic benefit from the additional yield resulting from providing supplemental lighting and the cost of that supplemental lighting.

A similar approach is followed by Carrier et al. (1994). The strategy they proposed is based on a series of *if-then-else* rules to decide the optimal amount of radiation inside the greenhouse. The two rules with the lowest priorities determine the profitability of supplemental lighting similarly to the criteria proposed by E. P. Heuvelink and Challa (1989).

None of these previous approaches offer the possibility of controlling the greenhouse shade screens, an essential element to control the greenhouse light environment. Contrary to the DSS developed as part of this study, these strategies are not aimed at achieving specific production timing and yield targets, but to decide when it is economically advantageous to provide supplemental lighting based on the future value

of the crop.

Considering these elements, the rationale of the present DSS is closer to the strategy proposed by Albright et al. (2000) to control a greenhouse light to a consistent daily integral. However, there are fundamental differences between the two approaches. The strategy developed by Albright et al. (2000) consists of a series of *if-then-else* rules to control the supplemental lighting system and the shade screens, without using prediction of solar radiation, so that the integrated daily PAR is consistent throughout the crop growth period. The present DSS also controls the supplemental lighting and the shade screens, but instead of relying on rules, it uses prediction of solar radiation and electricity prices and a crop model that determines the optimal level of radiation to achieve predetermined harvest time and yield targets rather than a consistent daily light integral.

Different commercial products, DSS generators, are available to generate Decision Support Systems that are capable of solving decision problems that are beyond the capabilities offered by spreadsheets (Bhargava et al., 1999). However, the algorithms of these DSS generators are mostly based on regression trees and are not able to accommodate the complexity that the present DSS requires, in particular, the integration of a very specific crop model with different databases. The integration of data warehousing in web-based DSS has been reported in the literature (Shim et al., 2002; Bhargava et al., 2007); however, the application of these DSS is in areas vastly different from the intended application of the present DSS and fall short of offering a guide that could be followed in this case.

The algorithm of the present DSS is similar to the model predictive control strategy described by Garcia et al. (1989) and used by Marsh and Albright (1991) and Seginer and McClendon (1992) to determine economically optimum temperature set-points for greenhouse lettuce. On a time step period defined by the user (one hour for simulation purposes in the present study), the system uses past data and prediction values of independent variables to determine the possible decisions that will

provide the desired results (specific harvest time and yield in the present case). From the possible decisions, the system selects the decision to be executed according to an optimization criterion (lowest cost in the present case) and then the system proceeds to the next iteration. The DSS was implemented in MATLAB using a functional programming paradigm.

Chapter 3

DSS Variables Initialization and Preliminary Calculations

3.1 Parameter Initialization

In this section of the DSS the values of the different input variables that are used are entered. The input variables are classified as global, local, or operational. Global variables are constants whose values are independent of any possible variation of the conditions on which the DSS is executed. That is, global variables are independent of factors such as the geographical location, the regional transmission organization, and the type of electricity prices market. Local variables, on the other hand, are specific to the geographic location, and operational variables vary according to the operations that the DSS executes.

For clarity, throughout the present work the terms *PAR energy* or *PAR* refer to radiation energy in the PAR waveband (400-700 nm) per unit area and is expressed in mol/m^2 (*mol* refers to moles of photons in the PAR waveband) while *PAR flux* or *Intensity* refer to radiation energy in the PAR waveband per unit area per unit time and is expressed in $mol/m^2 \cdot sec$. If the radiation energy is not in the PAR range, *radiation energy* or *radiation* is used instead and is expressed in J/m^2 , while *radiation flux* is used instead of *PAR flux* and is expressed in $J/m^2 \cdot sec$ or W/m^2 .

3.1.1 Global Variables

In the present case the global variables include constants related to the crop growth model used:

- Duration of the germination stage: 7 *days*
- Minimum duration of the seedling stage: 38 *days*
- Maximum duration of the seedling stage: 58 *days*
- Duration of the production stage: 60 *days*
- Maximum allowable daily amount of PAR energy: 30 mol/m^2
- Conversion factor for the hourly solar radiation energy in J/m^2 to the hourly solar radiation energy in the PAR waveband in mol/m^2 : $2.0699 \cdot 10^{-6} mol/J$ (Ting & Giacomelli, 1987)

3.1.2 Local Variables and their Values for the Present Project

- Latitude of greenhouse location: 40.0752° *N*
- Longitude of greenhouse location: 74.7736° *W*
- Standard meridian corresponding to the time zone of the present geographic location: 75° *W*
- Regional Transmission Organization (RTO): PJM Interconnection (organization that manages the wholesale electricity market in the area)
- Zone within the RTO: PSEG gas and electric utility company

The DSS was developed for locations within the continental USA, for which there is readily available historic weather and electricity price data.

3.1.3 Operational Variables and their Values for the Present Project

- Frequency of readings from solar radiation sensors. For simulation purposes this value was chosen as 60 minutes since the historic data used for simulation

is available on an hourly basis.

- Execution Period or frequency at which the DSS takes a decision. The Execution Period can not be less than 60 minutes because 60 minutes is the frequency at which the electricity prices are reported by the RTO for its different zones.
- Types of Electricity Price Markets. The present simulation analyzes the sensitivity of the DSS to both the Day-Ahead and the Real-Time Markets (the difference between these two types of markets will be discussed in Chapter 5.1)

3.2 Preliminary Calculations

The preliminary calculations module is comprised of the operations whose results will be used in the remaining parts of the DSS. There are four main groups of preliminary calculations:

1. Selection of nearest NSRDB (National Solar Radiation Database) station
2. Calculation of solar variables for the location and the selected station
3. Time related transformations and operations
4. Greenhouse transmittance

3.2.1 Selection of the nearest NSRDB station

The algorithm for long term forecast of hourly values of solar radiation requires the identification of the station from the updated NSRDB that is closest to the greenhouse location. Using the greenhouse latitude and longitude (these values were entered in the local variables section) as well as the latitude and longitude for each NSRDB station (a spreadsheet contains the metadata for all the stations, including their geographic location), the program identifies the closest station by calculating the distance between each station and the greenhouse. The distance between a given

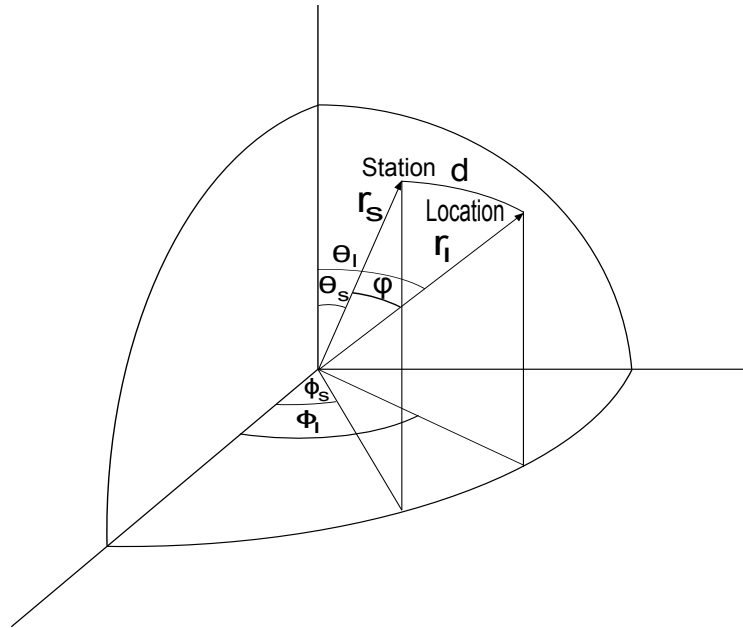


Figure 3.1: Distance between the station and the location.

station and the greenhouse is calculated using their geographic coordinates (latitude and longitude) and assuming that the earth is a sphere at whose center is the origin of the coordinate system.

In this model the distance between the station and the location, d , is just the product of the radius of the earth, R , and the angle (in radians), φ , between the position vectors representing the station and the location, \mathbf{r}_s and \mathbf{r}_l , respectively:

$$d = \varphi R \quad (3.1)$$

The angle φ can be determined through the scalar product between \mathbf{r}_s and \mathbf{r}_l :

$$\mathbf{r}_l \cdot \mathbf{r}_s = \|\mathbf{r}_l\| \cdot \|\mathbf{r}_s\| \cos \varphi \quad (3.2)$$

$$\varphi = \arccos \left\{ \frac{\mathbf{r}_l \cdot \mathbf{r}_s}{\|\mathbf{r}_l\| \cdot \|\mathbf{r}_s\|} \right\} \quad (3.3)$$

where:

$|| \cdot ||$ is used to represent the length of a vector

On the other hand:

$$\mathbf{r}_l = R(\cos \theta_l \cos \phi_l \mathbf{e}_x + \cos \theta_l \sin \phi_l \mathbf{e}_y + \sin \theta_l \mathbf{e}_z) \quad (3.4)$$

$$\mathbf{r}_s = R(\cos \theta_s \cos \phi_s \mathbf{e}_x + \cos \theta_s \sin \phi_s \mathbf{e}_y + \sin \theta_s \mathbf{e}_z) \quad (3.5)$$

From these last two equations:

$$\begin{aligned} ||\mathbf{r}_l|| &= ||\mathbf{r}_s|| = R = \text{Radius of the Earth (assumed constant and equal to 6,371 Km)} \\ \mathbf{r}_l \cdot \mathbf{r}_s &= R^2(\cos \theta_l \cos \phi_l \cos \theta_s \cos \phi_s + \cos \theta_l \sin \phi_l \cos \theta_s \sin \phi_s + \sin \theta_l \sin \theta_s) \\ \varphi &= \arccos(\cos \theta_l \cos \theta_s \cos(\phi_l - \phi_s) + \sin \theta_l \sin \theta_s) \end{aligned} \quad (3.6)$$

where:

θ_s, ϕ_s : station latitude, station longitude

θ_l, ϕ_l : location latitude, location longitude

3.2.2 Solar Altitude and Azimuth as Functions of Time

The solar altitude and azimuth as functions of time and the sunrise and sunset times for a given Julian Day (days of the year numbered from 1 to 365 for a regular year and from 1 to 366 for a leap year) for both the location and the nearest station are used in the prediction of solar radiation.

The solar altitude, β , is the angle between the horizontal plane and a line from the observer to the position of the sun in the sky. The solar azimuth, ϕ , is the angle between the projection of this line in the horizontal plane and a line that goes from

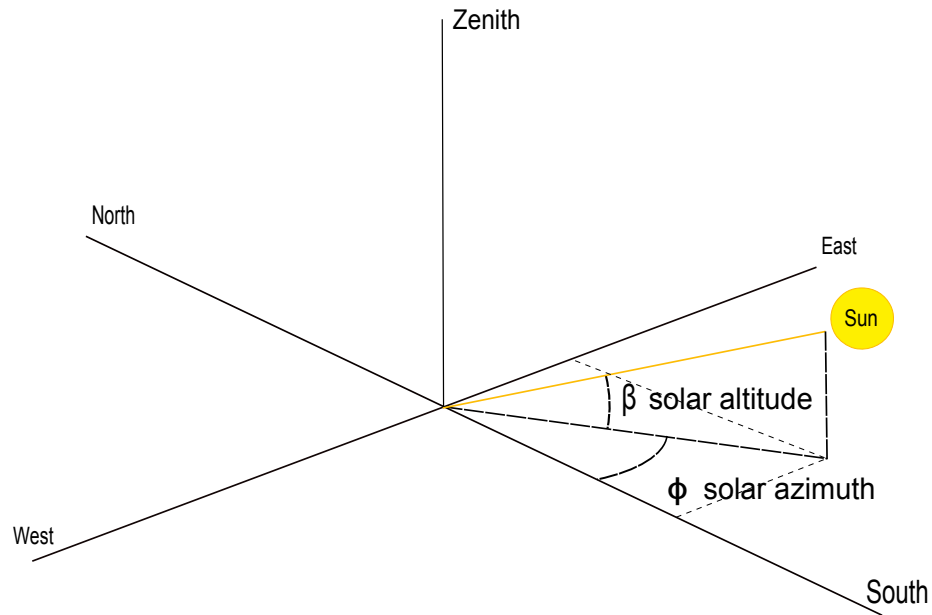


Figure 3.2: Solar position as a function of time.

north to south (positive and negative values before and after solar noon, respectively; Figure 3.2). Both the solar altitude and azimuth are functions of the latitude and longitude of the location, the day of the year, and the time of the day (Duffie & Beckman, 2006, p. 11):

$$\sin \beta = \cos L \cos \delta \cos H + \sin L \sin \delta \quad (3.7)$$

$$\sin \phi = \frac{\cos \delta \sin H}{\cos \beta} \quad (3.8)$$

$$\delta = 23.45^\circ \sin \left[\frac{360^\circ}{365} (n + 284) \right] \quad (3.9)$$

$$H = \frac{360^\circ}{24 \text{ hours}} (\text{Solar Time} - 12 \text{ hours}) \quad (3.10)$$

$$\begin{aligned} \text{Solar Time} = & \text{Standard Local Time (hours)} + \\ & + \frac{4 \text{ min}}{\text{degree}} (\text{Local Time Meridian} - \text{Local Longitude}) / 60 \text{ min/hour} + \\ & + \text{ET (min)} / 60 \text{ min/hour} \end{aligned} \quad (3.11)$$

$$ET(min) = 229.2(0.000075 + 0.001868 \cos B - 0.032077 \sin B - 0.014615 \cos 2B - 0.04089 \sin 2B) \quad (3.12)$$

$$B = \frac{360^\circ}{365}(n - 1) \quad (3.13)$$

where:

- β : Solar altitude
- ϕ : Solar azimuth
- L : Location latitude (degrees)
- δ : Solar declination angle (degrees)
- H : Hour angle (degrees)
- $ET(min)$: Equation of Time in minutes
- n : Julian day number ($1 \leq n \leq 366$)
(366 is used instead of 365 to consider leap years)

Solar Time: Time based on the motion of the sun across the sky with solar noon defined as the time when the sun crosses the local meridian of the location of the observer.

3.2.3 Sunrise and Sunset Times for a given Julian Day

The geometric sunrise and sunset times are the times that correspond to the hour angles in Equation 3.7 such that $\beta = 0$ and are based on the center of the solar disk. The lowest time value corresponds to the geometric sunrise and the highest to the geometric sunset. The sunrise and sunset times for the present project were based on the geometric sunrise and sunset times, respectively.

3.2.4 Time Related Operations and Transformations

Almost all the operations in the DSS are related to time so keeping track of it in a simple and clear manner is important. For convenience, a time and date representing

an event in time will simply be called *event*. For any event in Standard Time (local time without the daylight savings adjustment) a Time Distance or Distance is defined using as reference or origin the event 00:00:00 on January 1st of the year corresponding to the planting date.

To a given event past the origin corresponds a positive distance equals to the time past from the origin to the given event while to a given event prior to the origin corresponds a negative distance equals to the time past from the given event to the origin. By definition, the distance of the origin is zero.

Different functions were programmed to move back and forth from the *time distance format* to the regular *time and date format*:

- A function to transform a time and date from Daylight Savings to Standard Time. This function operates by using the date and time of transition between Standard Time to Daylight Savings established by Congress in the Energy Policy Act of 2005 (109th US Congress, 2005).
- A function to find the Distance that corresponds to an event expressed in Standard Time. This function first finds the Julian day and the year that correspond to the event and then calculates the time that passed from the event to the origin.
- The inverse of the previous two functions (the time related operations are performed by the DSS using the metric Distance, but the output results are provided in Daylight Savings Time).

To account for the PAR energy that the crop has received at any given time and to plan the amount that will need in the future depending on the prediction of weather variables, it is necessary to create a function that for any given event identifies the sunrises right before or at the event and right after the event as well as the sunset between these two consecutive sunrises. Once these two sunrises and the sunset in-between are identified, it is possible to know if the given event belongs

to the night (dark) or day (light) period, which will be essential at the moment of making a decision about the use of supplemental lighting or the shade screens.

3.2.5 Greenhouse Transmittance

Unless otherwise specified, any future reference to radiation inside the greenhouse (solar or from supplemental lighting) is understood as the value of radiation at the top of the crop's canopy. In the present work, the greenhouse transmittance will be defined as the linear relation between the values of solar PAR flux ($mol/m^2 \cdot sec$) inside the greenhouse and the solar PAR flux outside the greenhouse, the solar altitude, and the solar azimuth. This approach takes into account that the solar PAR flux inside the greenhouse not only depends on the outside values but also on the time of the day and the greenhouse structure.

This linear relation was obtained through a regression using inside and outside solar PAR values measured using LI-COR Quantum PAR sensors during a time period when neither the supplemental lighting nor the greenhouse screens were used (Figure 3.3). The resulting relation will be called Greenhouse Solar Radiation *Transmittance* Linear Model and it is specific for a particular location and greenhouse. Equation 3.14 represents the model, and Tables 3.1 and 3.2 contain the results. Figure 3.4 contains four common regression diagnostics plots based on the R-Student residuals: histogram (upper left), Normal Q-Q plot (upper right), Residuals vs. Fitted Values (lower left), and Cook's Distance (lower right).

$$In = \beta_0 + \beta_1 \cdot Out + \beta_2 \cdot Az + \beta_3 \cdot Al + \varepsilon \quad (3.14)$$

<i>In:</i>	Inside PAR flux ($mol/m^2 \cdot sec$)
<i>Out:</i>	Outside PAR flux ($mol/m^2 \cdot sec$)
<i>Az:</i>	Solar Azimuth (Degrees)
<i>Al:</i>	Solar Altitude (Degrees)

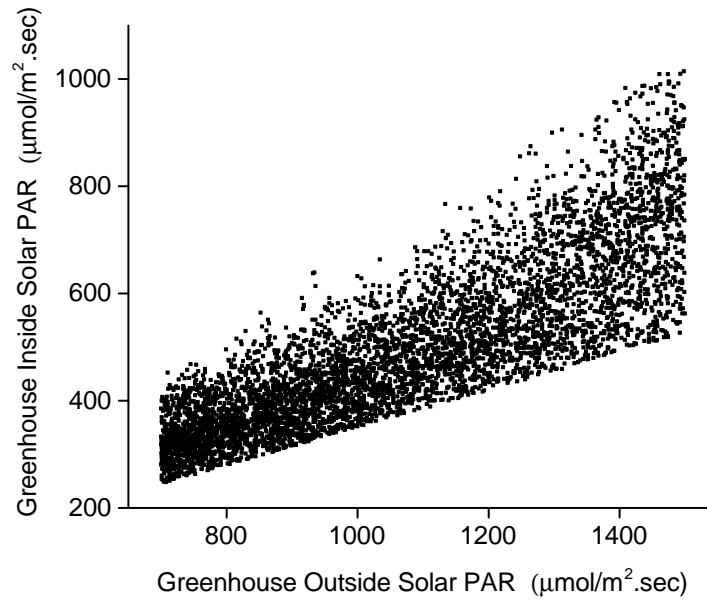


Figure 3.3: Greenhouse inside and outside solar PAR values used for the *Transmittance* Linear Model.

$\beta_0, \beta_1, \beta_2, \beta_3$: Linear Model Parameters

ε : Error term

A value of R^2_{PRESS} close to R^2 (as in the previous linear regression) serves as a validation of the model for prediction purposes. By definition (Kutner et al., p. 74, Montgomery et al., p. 39):

$$R^2 = 1 - \frac{\sum_i (y_i - \hat{y}_i)^2}{\sum_i (y_i - \bar{y})^2} \quad (3.15)$$

Here y and \hat{y} refer to the response variable and fitted values for the response variable, respectively, and \bar{y} is the average of the response variable.

Similarly:

$$R^2_{PRESS} = 1 - \frac{\sum_i (y_i - \hat{y}_{(-i)})^2}{\sum_i (y_i - \bar{y})^2} \quad (3.16)$$

Table 3.1: Analysis of Variance for Solar Radiation *Transmittance* Regression. *PRESS*: Prediction Error Sum of Squares.

Source of Variation	Sum of Squares	Degrees of Freedom	Mean Square	F Score	P Value
Regression	$9.19 \cdot 10^{-5}$	3	$3.06 \cdot 10^{-5}$	4962.37	0.00
Error	$3.48 \cdot 10^{-5}$	5636	$6.18 \cdot 10^{-9}$		
Total	$1.27 \cdot 10^{-4}$	5639			
R^2	R^2_{Adj}	<i>PRESS</i>	Mean <i>PRESS</i>	<i>PRESS</i> R^2	<i>PRESS</i> R^2_{Adj}
0.73	0.73	$3.48 \cdot 10^{-5}$	$6.19 \cdot 10^{-9}$	0.72	0.72

Table 3.2: Parameter Estimates for Solar Radiation *Transmittance* Regression.

Parameters	Parameter Values	Standard Deviation	t values	P value
β_0 (<i>mol/m² · sec</i>)	$-9.48 \cdot 10^{-5}$	$5.09 \cdot 10^{-6}$	-18.62	0.00
β_1 (<i>unitless</i>)	0.52	$4.84 \cdot 10^{-3}$	107.13	0.00
β_2 (<i>mol/m² · sec · degree angle</i>)	$8.67 \cdot 10^{-7}$	$8.31 \cdot 10^{-8}$	10.43	0.00
β_3 (<i>mol/m² · sec · degree angle</i>)	$-9.18 \cdot 10^{-8}$	$2.11 \cdot 10^{-8}$	-4.35	$1.39 \cdot 10^{-5}$

In this case $\hat{y}_{(-i)}$ is a predicted value of the response variable obtained by deleting the i -th observation, fitting a model with the remaining observations, and evaluating this model at the i -th level of the regressors. Since $\hat{y}_{(-i)}$ is a predicted value, the term *PRESS* (predicted error sum of squares) is used to refer to $\sum_i (y_i - \hat{y}_{(-i)})^2$ (Montgomery et al., 2001, p. 134))

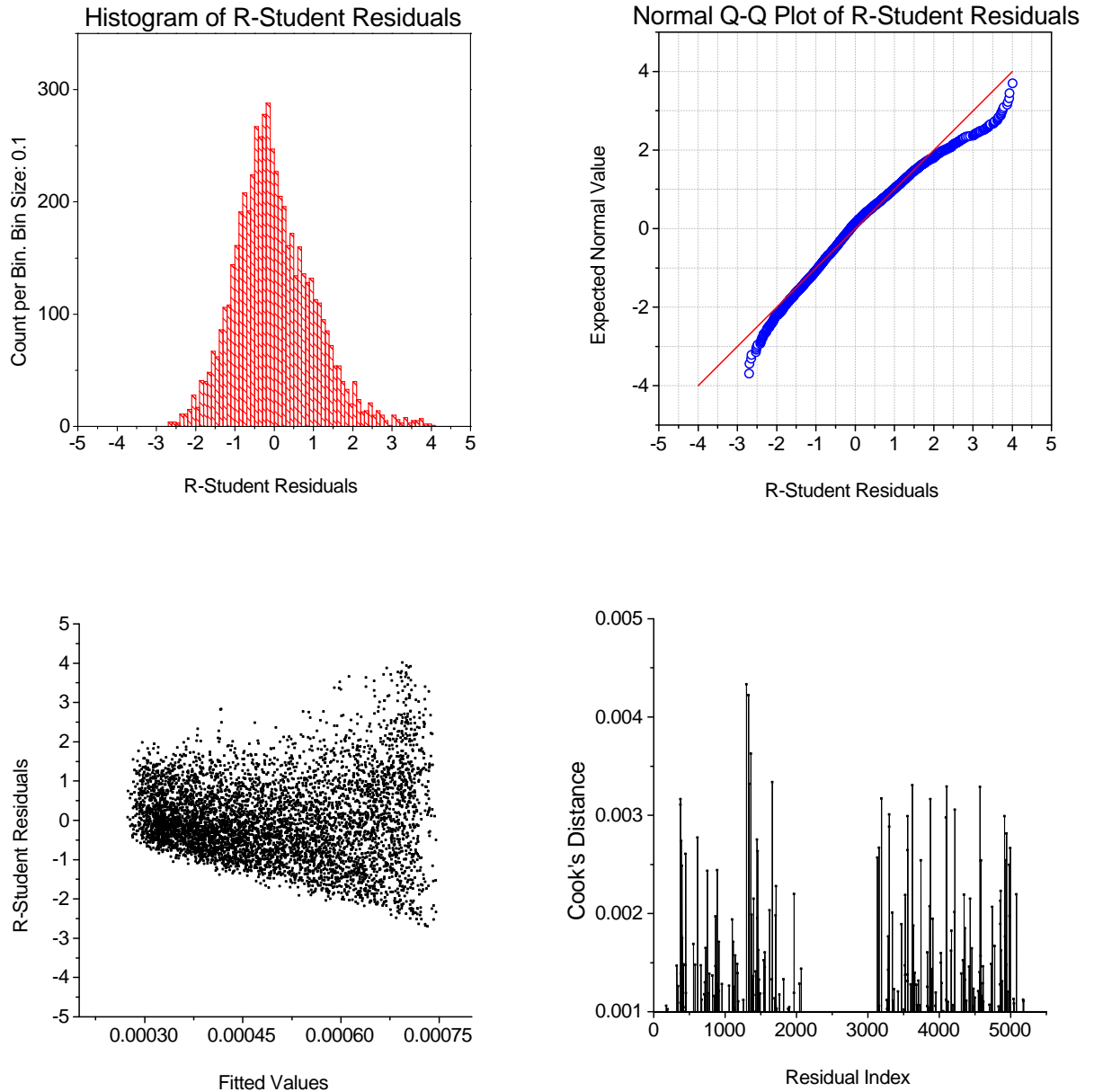


Figure 3.4: Solar radiation transmittance regression. Four common regression diagnostics plots based on the R-Student residuals: histogram (upper left), Normal Q-Q plot (upper right), Residuals vs. Fitted Values (lower left), and Cook's Distance (lower right). The residuals are fairly normally distributed (upper plots) and although many residuals present large values (residuals with values above 1 in lower left plot), there are no influential observations (Cook's Distance values are always below 1). The lower left plot also shows that the variance is an increasing function of the solar radiation. When the variance is not constant the estimate of the model parameters is still unbiased but they do not have the smallest standard errors. However, because of the simplicity of the model and its ability to explain more than 70% of the variation in the data, it was retained in its present form.

Chapter 4

Prediction of Solar Radiation

Prediction of hourly values of solar radiation is an essential element of the DSS. To make a decision about providing supplemental lighting or deploying the shade screens, the present decision support system depends on the PAR energy received by the crop, the goals set by the grower (harvest date and yield), and predicted values of solar radiation and electricity prices.

Modeling solar radiation is usually based on meteorological variables such as temperature, precipitation, or sky cover. Solar radiation models could be stochastic, whose goal is to generate solar radiation sequential data (*synthetic data*) with the same statistical properties as the validation data, or based on a regression function and produce forecast values of solar radiation using measurements or estimates of other meteorological variables.

In the present project, a regression model is used to generate predicted values of solar radiation based on calculated values of solar radiation for a clear sky and forecasted values of sky cover. This approach has the advantage that predicting solar radiation values for a clear sky requires only the latitude and longitude of the location while forecast values of sky cover are readily available from the National Digital Forecast Database for any location in the United States.

In the present work, a long term prediction of hourly values of solar radiation for the different Julian days of the year is based on values of sky cover generated using the National Solar Radiation Database (NSRDB); while a short term prediction is based on forecasted values of sky cover readily available from the National Digital Forecast Database through the National Oceanic and Atmospheric Administration

(NOAA). For every execution of the Decisions Module, the long term prediction of solar radiation is updated with the short term prediction.

4.1 National Solar Radiation Database (NSRDB)

The NSRDB is a set of two databases: the National Solar Radiation Database 1961-1990 and the National Solar Radiation Database 1991-2005 update. The updated NSRDB also comprises two databases (Wilcox, 2012):

- a discrete database spanning from 1991 to 2005 for 1,454 stations throughout the United States. This database was produced using the meteorological-based model METSTAT (Meteorological-Statistical) (Maxwell, 1998), a model developed by the National Renewable Energy Laboratory (NREL) using observations of sky cover from the National Weather Service (NWS) and solar radiation measurements from the Solar Radiation Network (SOLRAD). Less than 1 % of the records in this database correspond to measured data.
- a 10-km gridded database spanning from 1998 to 2005 for all 50 states excluding a region of Alaska where the geostationary satellites cannot accurately resolve sky cover (northwest of 60°N and 160°W). This gridded database was generated by a model developed by the State University of New York at Albany (SUNY) that uses Geostationary Operational Environmental Satellite (GOES) imagery to estimate solar radiation (Wilcox, 2012).

For the long term forecast of hourly values of solar radiation the discrete database from the updated NSRDB was used.

4.2 Solar Radiation for a Clear Sky

The solar radiation energy flux (W/m^2) that a surface on the ground receives is comprised of three components:

- Direct-Beam Radiation: radiation that passes through the atmosphere in a straight line from the position of the sun in the sky to the surface,
- Diffused Radiation: radiation that is diffused by particles and molecules in the atmosphere,
- Reflected Radiation: radiation that is reflected by the surroundings.

The estimation of the different components of the solar radiation for a clear sky for the present work is based on the Clear Day Solar Flux Model from the American Society of Heating, Refrigeration, and Air Conditioning Engineers (ASHRAE), developed by Threlkeld and Jordan (1958) for a moderately dusty atmosphere with a water vapor content equal to the average monthly values in the United States.

4.2.1 Direct-Beam Radiation

The direct-beam radiation striking a surface whose normal forms an angle θ with the radiation beam (Figure 4.1) is given by (Masters, 2004, p. 413):

$$I_{BC} = I_B \cos \theta \quad (4.1)$$

$$I_B = Ae^{-km} \quad (4.2)$$

$$A = 1160 + 75 \sin \left[\frac{360^\circ}{365} (n - 275) \right] \quad (4.3)$$

$$k = 0.174 + 0.035 \sin \left[\frac{360^\circ}{365} (n - 100) \right] \quad (4.4)$$

$$m = \frac{1}{\sin \beta} \quad (4.5)$$

where:

I_{BC} : Direct-beam radiation striking the collector (W/m^2)

I_B : Direct-beam radiation (W/m^2)

A : Apparent extraterrestrial flux (W/m^2)

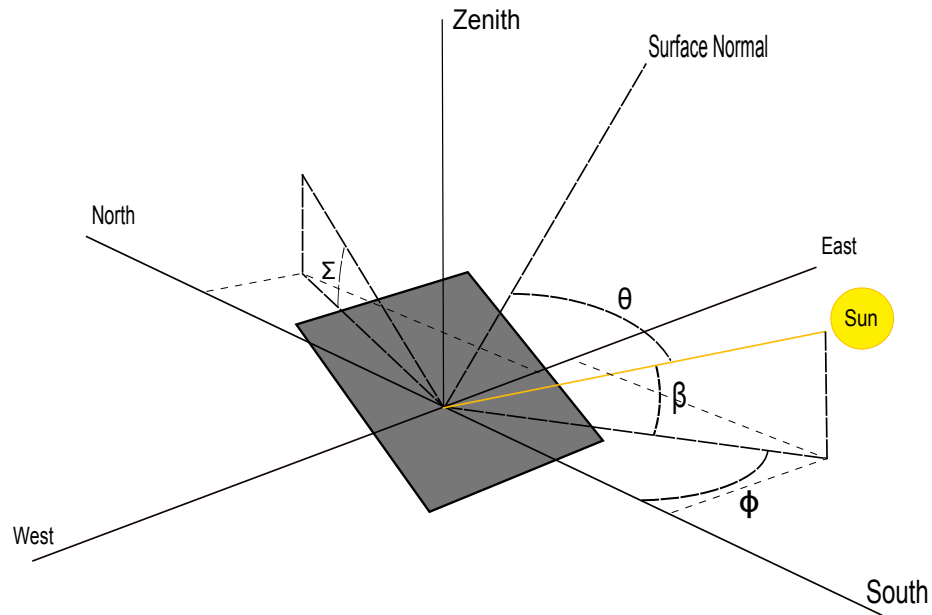


Figure 4.1: Solar radiation striking a surface and the various angles involved.

- k : Optical depth (dimensionless)
- m : Air mass ratio (dimensionless)
- β : Solar altitude angle (degrees)
- n : Julian day number ($1 \leq n \leq 366$)
(366 is used instead of 365 to consider leap years)
- Σ : Surface tilt angle

For the particular case of a horizontal collector:

$$I_{BH} = I_B \sin \beta \quad (4.6)$$

4.2.2 Diffuse Radiation

In ASHRAE's Clear Day Solar Flux Model, the sky is assumed to be isotropic for diffuse radiation. In that case, the amount of the diffuse radiation striking a collector surface whose normal forms an angle Σ (Figure 4.1) with the normal to a horizontal

surface is:

$$I_{DC} = C I_B \left(\frac{1 + \cos \Sigma}{2} \right) \quad (4.7)$$

$$C = 0.095 + 0.04 \sin \left[\frac{360^\circ}{365} (n - 100) \right] \quad (4.8)$$

I_{DC} : diffuse radiation striking the collector (W/m^2)

I_B : direct-beam radiation (W/m^2)

C : sky diffuse factor (dimensionless)

n : day number ($1 \leq n \leq 366$)

(366 is used instead of 365 to consider leap years)

For the particular case of a horizontal collector ($\Sigma = 0$):

$$I_{DH} = C I_B \quad (4.9)$$

4.2.3 Reflected Radiation

The reflected radiation is estimated through a simple model that considers that the reflected radiation is emitted in all directions as diffuse radiation by an infinite horizontal surface (not a valid assumption in the presence of large nearby vertical structures) that reflects the direct-beam and diffuse radiation coming from the sky. Assuming a reflectance ρ for this hypothetical surface, the reflected radiation that strikes a collector whose normal forms an angle Σ (see Figure 4.1) with the normal to a horizontal surface is:

$$I_{RC} = \rho(I_{BH} + I_{DH}) \left(\frac{1 - \cos \Sigma}{2} \right) \quad (4.10)$$

I_{RC} : reflected radiation striking the collector (W/m^2)

For the particular case of a horizontal collector ($\Sigma = 0$):

$$I_{RH} = 0 \text{ W}/\text{m}^2 \quad (4.11)$$

4.2.4 Clear Sky Total Radiation

Using the previous results, the total radiation on a horizontal surface for a clear sky (I_{TH}) can be estimated:

$$\begin{aligned} I_{TH} &= I_{BH} + I_{DH} \\ I_{TH} &= Ae^{-\frac{k}{\sin\beta}} (\sin\beta + C) \end{aligned} \quad (4.12)$$

Since parameters A , k , and C are given by Equations 4.3, 4.4, and 4.8 respectively; I_{TH} is a function of only the day of the year and the solar altitude. On the other hand, the solar altitude, β , is a function of the latitude and longitude of the location, the day of the year, and the time of the day (Equations 3.7 to 3.13). Using all previously mentioned equations and Equation 4.12, it is possible to estimate the total solar radiation on a horizontal surface for a clear day for a given location at any time for any day of the year.

4.3 Prediction of Solar Radiation

The prediction of hourly values of solar radiation on a horizontal surface at the location of the greenhouse rest on two assumptions:

- During the daylight hours the total solar radiation is linearly related to the direct solar radiation, the diffuse solar radiation, and the total sky cover.
- Predicted values of solar radiation for the closest NSRDB station can be used as predicted values of solar radiation at the greenhouse location.

The assumed linear relation between total solar radiation, direct solar radiation, diffuse solar radiation, and total sky cover is of the form:

$$\begin{aligned} I_{TH} &= \beta_0 + \beta_1 \cdot I_{BH} + \beta_2 \cdot CC \cdot I_{BH} + \beta_3 \cdot I_{DH} \\ &+ \beta_4 \cdot CC \cdot I_{DH} + \varepsilon \end{aligned} \quad (4.13)$$

where:

$$\begin{aligned}
 I_{TH} &= \text{total radiation on a horizontal surface (W/m}^2\text{)} \\
 \beta_0, \dots, \beta_4 &= \text{model parameters} \\
 I_{BH} &= \text{direct beam radiation on a horizontal surface (W/m}^2\text{)} \\
 I_{DH} &= \text{diffuse radiation on a horizontal surface (W/m}^2\text{)} \\
 CC &= \text{total sky cover (percent)} \\
 \varepsilon &= \text{error term}
 \end{aligned}$$

Once the closest station to the greenhouse location is identified from the updated NSRDB, it is possible to import the corresponding files containing historic solar radiation and meteorological data and fit the previous model to the data. The regression results for station 724096 (MCGUIRE AFB), the closest station to the greenhouse location of the current project (11 miles east from the greenhouse), are contained in Tables 4.1 and 4.2. Figure 4.2 contains four common regression diagnostics plots based on the R-Student residuals: histogram (upper left), Normal Q-Q plot (upper right), Residuals vs. Fitted Values (lower left), and Cook's Distance (lower right).

Table 4.1: Analysis of Variance for sky cover Model at MCGUIRE AFB Station. *PRESS*: Prediction Error Sum of Squares.

Source of Variation	Sum of Squares	Degrees of Freedom	Mean Square	F Score	P Value
Regression	$3.37 \cdot 10^9$	4	$8.42 \cdot 10^8$	67559	0.00
Errors	$8.33 \cdot 10^8$	66890	12463.36		
Total	$4.2 \cdot 10^9$	66894			
R^2	R^2_{Adj}	<i>PRESS</i>	Mean <i>PRESS</i>	<i>PRESS</i> R^2	<i>PRESS</i> R^2_{Adj}
0.80	0.80	$8.34 \cdot 10^8$	12465	0.80	0.80

Table 4.2: Parameter Estimates for sky cover Model at MCGUIRE AFB Station.

Parameters	Parameter Values	Standard Deviation	t values	P value
β_0 (W/m^2)	-6.10	1.03	-5.93	0.00
β_1 (<i>unitless</i>)	1.20	0.08	157	0.00
β_2 (<i>unitless</i>)	0.71	0.00	-72	0.00
β_3 (<i>unitless</i>)	0.53	0.05	10.68	0.00
β_4 (<i>unitless</i>)	0.17	0.06	2.76	0.00

The data files are available in comma delimited format on an hourly basis for the 1,454 stations comprising the NSRDB update for each year from 1991 until 2005 at the NREL website. Although for the present simulation purposes the data for all the available years is imported, the program allows the selection of the years for which the data is to be imported for the selected station.

Using the previous model it is possible to generate predicted values of solar radiation for the closest station. According to the second assumption these predicted values can also be used as predicted values for the greenhouse location. The need for this assumption arises from the fact that a grower rarely has historic solar radiation or meteorological data for the greenhouse location.

4.3.1 Validation of Assumptions

To test and validate these two assumption the linear regression shown in Equation 4.13 was fitted for each j – th NSRDB station in New Jersey and the corresponding coefficient of determination R_j^2 and coefficient of variation of the root-mean-square-error $CV(MRSE)_j$, as defined by equations 4.16 and 4.18, were calculated. These coefficients are measures of how well the linear model, as proposed by equation 4.13, predicts solar radiation values at each station. Large values of R_j^2 and small values

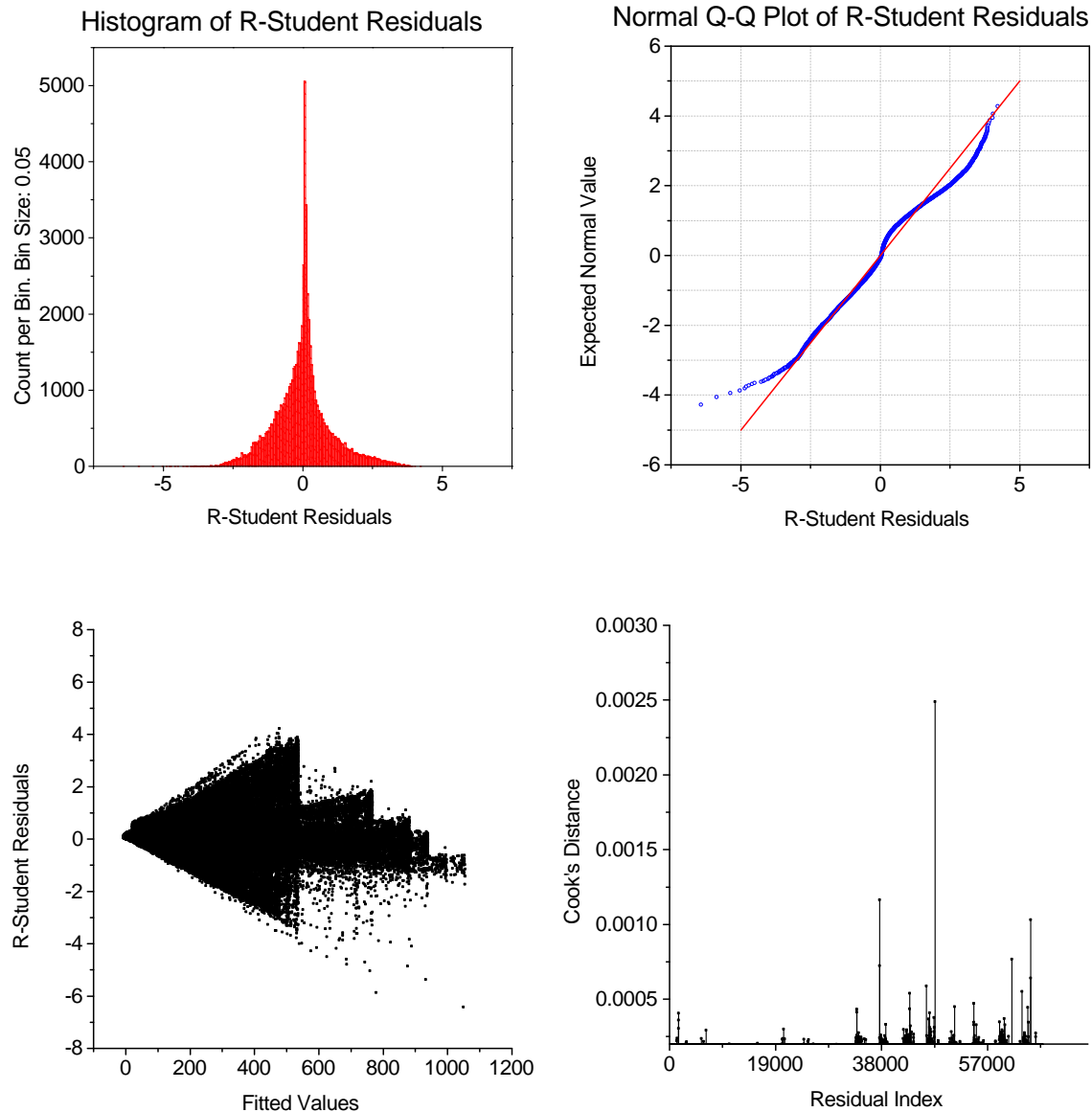


Figure 4.2: Sky cover regression. Four common regression diagnostics plots based on the R-Student residuals: histogram (upper left), Normal Q-Q plot (upper right), Residuals vs. Fitted Values (lower left), and Cook's Distance (lower right). The presence of large residual values (lower left plot) produces some departure from normality (fat left tail of histogram and Q-Q plots) but there are no influential observations (Cook's Distance values are always below 1). The unusual shape of the plot of the residuals vs. fitted values made it challenging to choose a transformation to stabilize the variance that would make physical sense. When the variance is not constant the estimate of the model parameters is still unbiased but they do not have the smallest standard errors. However, because of the simplicity of the model and its ability to explain 80% of the variation in the data, it was retained in its present form.

of $CV(MRSE)_j$ indicate the validity of the first assumption:

$$I_{TH}^j = \beta_0^j + \beta_1^j \cdot I_{BH}^j + \beta_2^j \cdot CC^j \cdot I_{BH}^j + \beta_3^j \cdot I_{DH}^j + \beta_4^j \cdot CC^j \cdot I_{DH}^j + \varepsilon \quad (4.14)$$

$$\hat{I}_{TH}^j = \hat{\beta}_0^j + \hat{\beta}_1^j \cdot I_{BH}^j + \hat{\beta}_2^j \cdot CC^j \cdot I_{BH}^j + \hat{\beta}_3^j \cdot I_{DH}^j + \hat{\beta}_4^j \cdot CC^j \cdot I_{DH}^j \quad (4.15)$$

$$R_j^2 = 1 - \frac{\sum_i (I_{TH}^j(i) - \hat{I}_{TH}^j(i))^2}{\sum_i (I_{TH}^j(i) - \bar{I}_{TH}^j)^2} \quad (4.16)$$

$$RMSE_j = \sqrt{\frac{\sum_i (I_{TH}^j(i) - \hat{I}_{TH}^j(i))^2}{n_j}} \quad (4.17)$$

$$CV(RMSE)_j = \frac{RMSE_j}{\bar{I}_{TH}^j} \quad (4.18)$$

where:

$\beta_0^j, \dots, \beta_4^j$: regression parameters for the $j - th$ station

$\hat{\beta}_0^j, \dots, \hat{\beta}_4^j$: estimated values of regression parameters
for the $j - th$ station

I_{BH}^j, I_{DH}^j : direct beam and diffuse radiation, respectively,
for the $j - th$ station

I_{TH}, \hat{I}_{TH} : total and estimated total radiation, respectively,
for the $j - th$ station

i : index used to refer to the different hourly values

\bar{I}_{TH}^j : average, over the different hourly values,
of the total radiation for the $j - th$ station

Then, based on the linear model developed for the closest station to the $j - th$ station, $k - th$ station, a prediction coefficient of determination $R_{pred,j}^2$ and a prediction coefficient of variation of the root-mean-square-error $CV(MRSE)_{pred,j}$ are calculated:

$$R_{pred,j}^2 = 1 - \frac{\sum_i (I_{TH}^j(i) - \hat{I}_{TH}^k(i))^2}{\sum_i (I_{TH}^j(i) - \bar{I}_{TH}^j)^2} \quad (4.19)$$

$$RMSE_{pred,j} = \sqrt{\frac{\sum_i (I_{TH}^j(i) - \hat{I}_{TH}^k(i))^2}{n_j}} \quad (4.20)$$

$$CV(RMSE)_{pred,j} = \frac{RMSE_{pred,j}}{\bar{I}_{TH}^j} \quad (4.21)$$

$R_{pred,j}^2$ and $CV(MRSE)_{pred,j}$ are measures of how well the k – th station predicts solar radiation values at the j – th station. Values of $R_{pred,j}^2$ and $CV(MRSE)_{pred,j}$ close to R_j^2 and $CV(MRSE)_j$, respectively, indicate the validity of the second assumption. Table 4.3 shows information about New Jersey stations and their relative distance. The results of the regression analyses are shown in Table 4.4.

Table 4.3: NSRDB NJ Stations. USAF: United States Air Force

Station Name	Station USAF number	Closest Station USAF number	Distance (miles)
ATLANTIC CITY INTL AP	724070	724075	28.1
S JERSEY RGNL ARPT	724074	724096	13.6
MILLVILLE MUNICIPAL AP	724075	724088	26.1
BELMAR ASC	724084	724090	18.2
LAKEHURST NAS	724090	724096	13.3
CALDWELL/ESSEX CO.	724094	725025	11.5
TRENTON MERCER CO. AP	724095	725113	16.2
MCGUIRE AFB	724096	724090	13.3
SOMERSET ARPT ASOS	724104	724095	25.4
NEWARK INTL ARPT	725020	725025	11.0
TETERBORO AIRPORT	725025	725033	7.0
CAPE MAY CO	725966	724075	26.9

The relatively large values of R^2 in Table 4.4 are an indication of the validity of the first assumption while the proximity of R_{pred}^2 to R^2 is an indication of the validity of the second assumption.

Table 4.4: Coefficient of Determination and Coefficient of Variation of the Root-Mean-Square-Error for NJ Stations

Station Name	R^2	$CV(RMSE)$	R^2_{pred}	$CV(RMSE)_{pred}$
ATLANTIC CITY INTL AP	0.82	0.35	0.72	0.45
S JERSEY RGNL ARPT	0.60	0.50	0.72	0.42
MILLVILLE MUNICIPAL AP	0.83	0.33	0.75	0.41
BELMAR ASC	0.82	0.33	0.64	0.48
LAKEHURST NAS	0.62	0.50	0.72	0.43
CALDWELL/ESSEX CO.	0.80	0.39	0.71	0.47
TRENTON MERCER CO. AP	0.62	0.51	0.48	0.60
MCGUIRE AFB	0.80	0.37	0.62	0.50
SOMERSET ARPT ASOS	0.45	0.61	0.63	0.50
NEWARK INTL ARPT	0.81	0.37	0.72	0.45
TETERBORO AIRPORT	0.63	0.51	0.48	0.60
CAPE MAY CO	0.82	0.35	0.65	0.48

4.3.2 Long Term Prediction of PAR Energy Inside the Greenhouse

Once the linear regression model is developed for the closest station to the greenhouse location, a long term prediction of solar radiation energy flux (W/m^2) hourly values, for the outside of the greenhouse, is generated for each Julian day. To generate this long term prediction, the value of total sky cover assigned to a given hour is the average total sky cover, over the 15 years of data contained in the NSRDB, that correspond to that hour.

However, the development of the crop depends, among other factors, on the cumulative PAR energy that it receives and for this reason, measured inside the greenhouse. By using the long term prediction of solar radiation energy flux hourly values it is possible to obtain, after several basic operations, the long term prediction of solar PAR energy inside the greenhouse that corresponds to a given time period.

First, the long term prediction of solar radiation energy flux hourly values are converted to the time resolution of the PAR sensors located inside the greenhouse in

order to facilitate their update with the measurements from the PAR sensors. This conversion is straightforward: if the time resolution of the PAR sensors is less than an hour, then for a given time interval in the new time resolution the long term prediction of solar radiation energy flux value is the same as that of the hour to which the time interval belongs. If the new time resolution is more than an hour, then for a given time interval in the new time resolution the long term prediction of solar radiation energy flux value is the average over the hours contained in the time interval.

Once the long term prediction of solar radiation energy flux hourly values have been converted to the time resolution of the PAR sensors, they are transformed to solar PAR flux in $mol/m^2 \cdot sec$ by using the conversion factor $2.0699 \cdot 10^{-6} mol/J$ (Ting & Giacomelli, 1987). The resulting solar PAR flux values still refer to the outside of the greenhouse, but using the Transmittance model previously introduced and the solar azimuth and altitude for the location, the corresponding solar PAR flux values inside the greenhouse are found.

Finally, to obtain the long term prediction of solar radiation energy inside the greenhouse in mol/m^2 that correspond to a given time interval of the time resolution of the PAR sensors, the corresponding long term prediction of solar radiation energy flux values inside the greenhouse in $mol/m^2 \cdot sec$ is multiplied by the number of seconds contained in the time interval. Every time the Decisions Module is executed, the long term prediction of solar radiation energy values inside the greenhouse is updated with a short term prediction of solar radiation energy values based on forecasted values of total sky cover for the next 48 hours for the closest station obtained from the National Digital Forecast Database (<http://www.nws.noaa.gov/ndfd/>).

Chapter 5

Prediction of Electricity Prices

5.1 Introduction

The decision about providing supplemental lighting is based on yield and harvest targets, resulting crop growth, past and predicted values of solar radiation, and predicted values of electricity prices in the market where the power is sold. In the present case the power is sold in the wholesale electricity market corresponding to PJM Interconnection, a Regional Transmission Organization (RTO) and Independent System Operator (ISO) that manages and controls the wholesale electricity market and the movement of electricity in Delaware, District of Columbia, Maryland, New Jersey, Ohio, Pennsylvania, Virginia, West Virginia, and parts of Indiana, Illinois, Kentucky, Michigan, North Carolina and Tennessee.

To reflect the varying energy costs within the region depending on the transmission constraints, the PJM market uses Locational Marginal Prices (LMP), electricity prices that reflect the value of energy at a specific location at the time that it is delivered. The wholesale electricity market consists of two distinctive markets: the Day-Ahead Market and the Real-Time Market. The Day-Ahead LMPs depend on generation offers and demand bids and are calculated for each hour of the next operating day. The Real-Time LMPs are calculated every five minutes according to the actual grid operation conditions.

The developed decision support system is designed to maximize the revenue from the exported electricity while meeting the crop targets set by the grower. The electricity is generated by an on-site distributed generation unit and is used mostly for

supplemental lighting. Only the excess power that is not needed to meet the crop needs is exported to the wholesale electricity market. Although the system can be used when the exported electricity is sold in any of the LMP zones of the PJM Day-Ahead or Real-Time Markets, the simulation is done for the PSEG (Public Service Electric and Gas Company) zone since PSEG is the power utility that serves the geographic area where the greenhouse and the power generation unit (the microturbine) are located.

5.2 Modeling Day-Ahead LMPs

Because of the lack of storability of power in the wholesale market, its price is strongly correlated with the demand and exhibits a pattern that fluctuates hourly, daily, and seasonally. The price of power also reflects the effect that some environmental factors (temperature, humidity, wind speed) have on the power demand. This dependence of the electricity prices on the weather conditions and the fact that the transmission capacity is physically limited and also influenced by environmental factors, are elements that contribute to its spiky nature, varying abruptly from one hour to the next in certain cases (Figure 5.1).

Day-Ahead LMPs, have a smoother behavior than Real-Time LMPs and different techniques have been used for their modeling and forecasting: multiple linear regression, time series, and neural networks. For the present work a multiple linear regression was fitted between Day-Ahead LMPs and a set of predictor variables that include quantitative variables (Heating Degree Hours, HDH , and Cooling Degree Hours, CDH), qualitative variables (season, weekday, holidays, and hour), as well as the interactions between the quantitative and qualitative variables. The different variables for this multiple linear regression were defined following the PJM model for load forecasting and analysis.

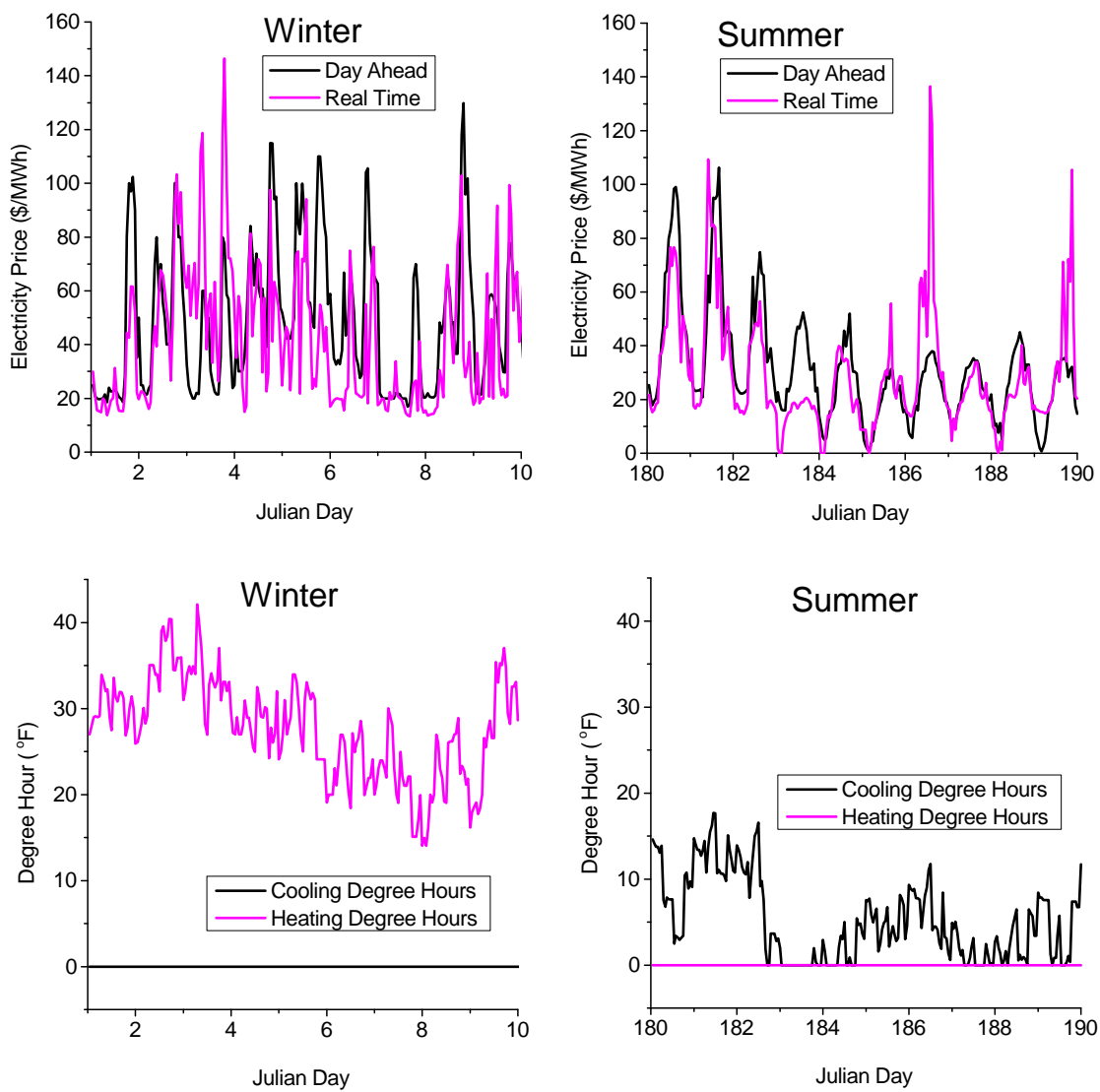


Figure 5.1: Wholesale electricity prices and weather variables for PSEG Zone for 10 consecutive days during the summer and winter of 2001.

5.2.1 Quantitative Variables

Cooling Degree Hours (*CDH*) and Heating Degree Hours (*HDH*) are the two quantitative variables of the multiple regression model. Both variables are functions of the hour of the day and the season through a base temperature that varies hourly and a weather parameter that is defined according to the season. The weather parameter for the summer months or cooling season (June, July and August) is the Temperature and Humidity Index (*THI*) while for the winter months or heating season (December, January and February) the weather parameter is the Winter Weather Parameter (*WWP*). For the remaining months the weather parameter is the dry bulb temperature in $^{\circ}F$ (*DB*).

Definitions of Weather Parameters:

$$THI = DB - 0.55 \cdot (1 - RH) \cdot (DB - 58) \cdot (1 + \text{sign}(DB - 58))/2 \quad (5.1)$$

$$WWP = DB - 0.5 \cdot (WIND - 10) \cdot (1 + \text{sign}(WIND - 10))/2 \quad (5.2)$$

where:

$$\text{sign}(x) = \begin{cases} 1 & \text{for } x > 0 \\ 0 & \text{for } x = 0 \\ -1 & \text{for } x < 0 \end{cases}$$

RH: relative humidity (decimal)

WIND: wind speed (*mph*. Measured at 10 meters height)

Definitions of Quantitative Variables:

$$\begin{aligned} CDH &= \text{maximum}(THI - CBaseTemp(hour), 0) \Rightarrow & (5.3) \\ &\Rightarrow CDH \geq 0 \end{aligned}$$

$$\begin{aligned} HDH &= \text{maximum}(HBaseTemp(hour) - WWP, 0) \Rightarrow & (5.4) \\ &\Rightarrow HDH \geq 0 \end{aligned}$$

where:

$CBaseTemp$: Cooling Base Temperature ($^{\circ}F$)

$HBaseTemp$: Heating Base Temperature ($^{\circ}F$)

If $0 \leq hour < 6$:

$$CBaseTemp = 60$$

$$HBaseTemp = 50$$

If $6 \leq hour < 12$:

$$CBaseTemp = 65$$

$$HBaseTemp = 55$$

If $12 \leq hour < 18$:

$$CBaseTemp = 72$$

$$HBaseTemp = 62$$

If $18 \leq hour < 24$:

$$CBaseTemp = 65$$

$$HBaseTemp = 55$$

For a given utility provider, the quantitative variables THI and WWP are generated using weighted meteorological data for the weather stations assigned to that particular utility provider according to PJM's assignment of weather stations per zone for Load Forecasting and Analysis (*PJM Manual 19: Load Forecasting and Analysis*, 2012). For the present case, PSEG is the power utility provider and the only station assigned to this provider is Newark International Airport Weather Station 72502.

5.2.2 Qualitative Variables

It is expected that the multiple linear regression model between Day-Ahead LPMs and the quantitative variables (CDH and HDH) will vary across seasons, days of the week, and even hours of the day. To avoid having to fit a different model for each of these different cases, qualitative variables are defined for the seasons, days

of the week, hours of the day, and holidays. With these newly defined qualitative variables it is possible to model all the different cases through a single multiple linear regression that includes the quantitative variables, the qualitative variables, and the interactions between the quantitative and the qualitative variables.

There are several sets of qualitative variables in the linear regression model. The first set correspond to an indicator variable for the summer (I_{summ}) and another for the winter (I_{wint}). During the summer months (June, July, August) I_{summ} has a value of *one* and *zero* otherwise. Similarly, during the winter months (December, January, February) I_{wint} has a value of *one* and *zero* otherwise.

The second set of qualitative variables consists of six indicator variables for the first six days of the week:

- I_{sund} : indicator variable for Sunday
- I_{mond} : indicator variable for Monday
- I_{tues} : indicator variable for Tuesday
- ...
- I_{frid} : indicator variable for Friday

For a given hour, only the day of the week indicator that corresponds to the day of the week of that hour has a value of *one*, the rest of the indicators have a value of *zero*. For this reason there is no need to define an indicator for the seventh day of the week: the seventh day of the week corresponds to the case when all the day of the week indicators have a value of *zero*.

A third set of indicator variables is defined for the different hours of the day (I_{hour1} , $I_{hour2}, \dots, I_{hour23}$). The definition of these *hourly* indicators is similar to the definition of the day of the week indicators: for a given hour, only the hourly indicator that correspond to that hour has a value of *one*, the rest of the hourly indicators have a value of *zero*.

An indicator variable is also used for the different holidays and atypical days through the year (I_{hold}) since it is expected that the different demand of electricity during these days will affect the price of the electricity.

Holidays considered:

- New Year's Day (January First)
- Martin Luther King Day (Third Monday in January)
- Washington's Birthday or President's Day (Third Monday in February)
- Memorial Day (Last Monday in May)
- Independence Day (Fourth of July)
- Labor Day (First Monday in September)
- Columbus Day (Second Monday in October)
- Veteran's Day (November 11)
- Thanksgiving Day (Fourth Thursday in November)
- Christmas Eve (December 24)
- Christmas Day (December 25)
- New Year's Eve (December 31)

Atypical days considered:

- Super Ball Sunday (First Sunday of February)
- Valentine's day (February 14)
- Mother's Day (Second Sunday of May)

5.2.3 Linear Regression Model for Day-Ahead LMPs

The proposed multiple linear regression between the response variable (Day-Ahead LMPs, DA) and the predictor variables (quantitative and qualitative variables as well as their interactions) has the following form:

$$DA = \beta_0 + Quant_terms + Qual_terms + Interactions + \varepsilon \quad (5.5)$$

where:

$$Quant_terms = \beta_H HDH + \beta_C CDH$$

$$Qual_terms = Seasons + Weekdays + Hours + Holidays$$

$$Seasons = \beta_{summ} I_{summ} + \beta_{wint} I_{wint}$$

$$Weekdays = \beta_{sund} I_{sund} + \beta_{mond} I_{mond} + \dots + \beta_{frid} I_{frid}$$

$$Hours = \beta_{hour1} I_{hour1} + \beta_{hour2} I_{hour2} + \dots + \beta_{hour23} I_{hour23}$$

$$Holidays = \beta_{hold} I_{hold}$$

$$Interactions = Quantitative \cdot Qualitative$$

$$\varepsilon = \text{Error term}$$

In this equation there are a total of 99 terms. One term corresponds to the intercept (β_0), two terms to the quantitative variables ($\beta_H HDH$, $\beta_C CDH$), 32 terms to the indicator variables ($\beta_{summ} I_{summ}$, ..., $\beta_{hold} I_{hold}$) and 64 terms to the interactions between the quantitative and qualitative variables ($\beta_H \beta_{summ} HDH \cdot I_{summ}$, ..., $\beta_C \beta_{hold} CDH \cdot I_{hold}$)

5.2.4 Linear Regression Results

Table 5.1 contains the results from the Day-Ahead LMPs multiple linear regression. The linear regression model is significant (The F score is over 300 and the corresponding p value is below 10^{-15}) and is able to explain around 40 percent of

Table 5.1: Analysis of Variance for Day-Ahead Electricity Prices Regression. *PRESS*: Prediction Error Sum of Squares.

Source of Variation	Sum of Squares	Degrees of Freedom	Mean Square	F Score	P Value
Regression	$1.78 \cdot 10^7$	98	181756	358	0
Errors	$2.48 \cdot 10^7$	48862	508.3		
Total	$4.26 \cdot 10^7$	48960			
R^2	R_{Adj}^2	<i>PRESS</i>	Mean <i>PRESS</i>	<i>PRESS</i> R^2	<i>PRESS</i> R_{Adj}^2
0.42	0.42	$2.49 \cdot 10^7$	511.4	0.41	0.41

the variation of the Day-Ahead LMPs. The model performance at prediction is also around 40 percent as can be seen from the Coefficient of Determination for the Prediction Sum of Square Errors (*PRESS* R^2). Figure 5.2 contains four common regression diagnostics plots based on the R-Student residuals: histogram (upper left), Normal Q-Q plot (upper right), Residuals vs. Fitted Values (lower left), and Cook's Distance (lower right).

The fraction variation of the Day-Ahead LMPs that the model explains is not high; however, the DSS does not rely on the predicted values of Day-Ahead LMPs generated by this model, but on the Day-Ahead LMPs provided by the Independent System Operator (ISO) for the next day. The predicted values of Day-Ahead LMPs generated by the model only serve as back up values for the unexpected situations when the Day-Ahead LMPs from the ISO are not available.

5.3 Modeling Real-Time LMPs

Since the behavior of the Real-Time LMPs is more erratic than that of Day-Ahead LMPs, the prediction of Real-Time LMPs could be particularly challenging when the predictors are weather and indicator variables. However, the Real-Time LMPs follow

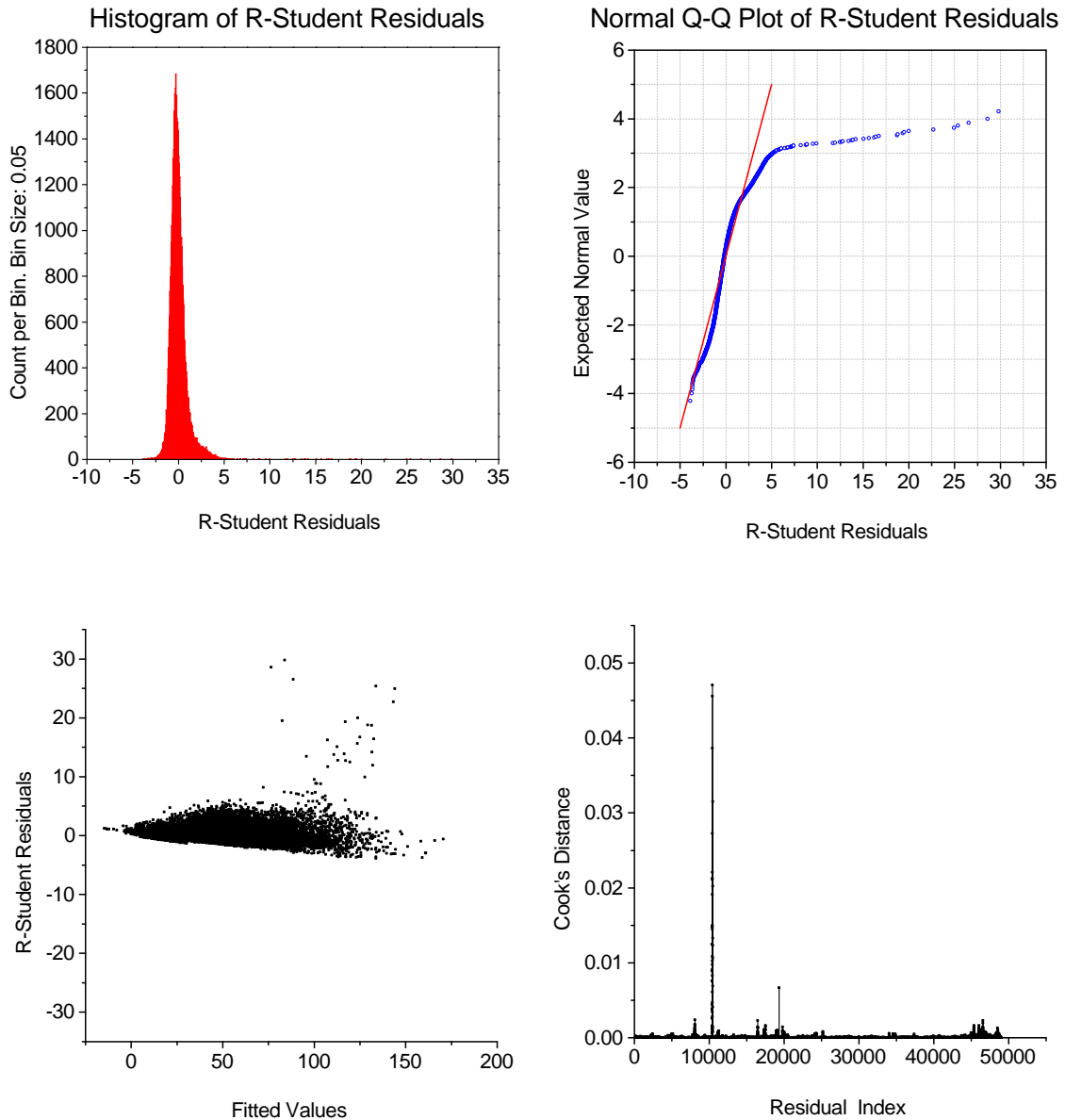


Figure 5.2: Day-Ahead Electricity Prices Regression. Four common regression diagnostics plots based on the R-Student residuals: histogram (upper left), Normal Q-Q plot (upper right), Residuals vs. Fitted Values (lower left), and Cook's Distance (lower right). The presence of large residual values (lower left plot) produces some departure from normality (fat right tail of histogram and Q-Q plots) but these are not influential observations (Cook's Distance values are always below 1). The plot of the residuals vs. fitted values does not reveal a particular pattern, however, some large residuals are present. Since the DSS relies on predicted values of Day-Ahead electricity prices only on exceptional conditions (e.g., outage, RTO site down), the model was retained in its present form.

a trend similar to the Day-Ahead LMPs and this fact can be used to model Real-Time LMPs using Day-Ahead LMPs as the predictor variable. The results of a single linear regression of Real-Time LMPs in terms of Day-Ahead LMPs (Equation 5.6) are shown in Tables 5.2 and 5.3. Figure 5.3 contains four common regression diagnostics plots based on the R-Student residuals: histogram (upper left), Normal Q-Q plot (upper right), Residuals vs. Fitted Values (lower left), and Cook's Distance (lower right).

$$RT = \text{intercept} + \text{slope} \cdot DA + \varepsilon \quad (5.6)$$

where:

RT = Real-Time Electricity Prices (\$/MWh)

DA = Day-Ahead Electricity Prices (\$/MWh)

ε = Error term

Table 5.2: Analysis of Variance for Real-Time Electricity Prices Regression

Source of Variation	Sum of Squares	Degrees of Freedom	Mean Square	F Score	P Value
Regression	$8.82 \cdot 10^7$	1	$8.82 \cdot 10^7$	146384	0
Errors	$5.72 \cdot 10^7$	94942	602.51		
Total	$1.45 \cdot 10^8$	94943			
R^2	R_{Adj}^2	$PRESS$	Mean $PRESS$	$PRESS R^2$	$PRESS R_{Adj}^2$
0.61	0.61	$5.72 \cdot 10^7$	602.85	0.61	0.61

The significance of the regression (the p value corresponding to the F score is below 10^{-15}) and the relatively high Coefficient of Determination ($R^2 = 0.61$) confirm the validity of this approach. By using the predicted values of Day-Ahead LMPs available

Table 5.3: Parameters Estimates for Real-Time LMPs Regression

Parameters	Parameter Values	Standard Deviation	t values	P value
<i>intercept</i> (\$/MWh)	-0.3572	0.1548	2.3079	0.0210
<i>slope</i> (unitless)	1.0114	0.0026	382.6012	0.0000

for the whole crop growth period, the previous model also provides a continuous set of predicted Real-Time LMP values for the decision support system. Since the predicted values of Day-Ahead LMPs are updated hourly for the remaining hours of any given present day with Day-Ahead LMPs from the ISO, the Real-Time LMPs model will predict 61 percent of the Real-Time LMPs for those hours.

5.4 Prediction of Electricity Prices

The previously discussed linear regression models are used to generate a long term prediction of Day-Ahead and Real-Time LMP hourly values for the different Julian days. To generate the long term prediction of Day-Ahead LMPs, the values of the meteorological variables assigned to a given hour are the averages of the corresponding meteorological variables, over the 15 years of data contained in the NSRDB, that correspond to that hour. The long term prediction of Real-Time LMPs is generated from the long term prediction of Day-Ahead LMPs.

Every time the Decisions Module is executed the long term prediction of Day-Ahead LMPs is updated: first, with a short term prediction based on the most recent forecast of meteorological variables (available from NOAA website); and second, with the Day-Ahead LMP values determined for the next day (available from the ISO website). The updated prediction of Day-Ahead LMPs is then used to update the long term prediction of Real-Time LMPs.

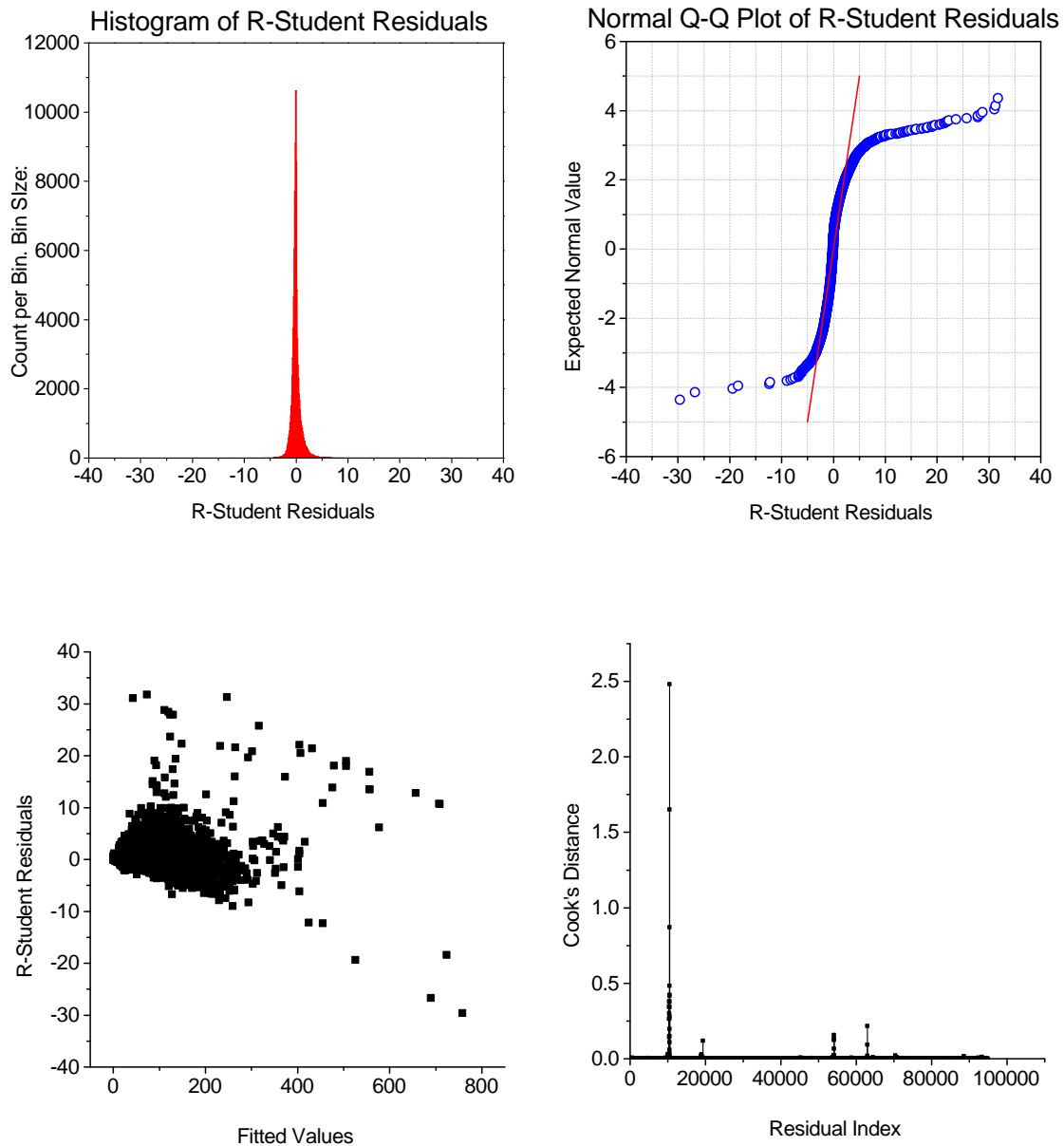


Figure 5.3: Real-Time Electricity Prices Regression Diagnostic Plots. The presence of large residual values (lower left plot) produces significant departure from normality (fat left and right tails of histogram and Q-Q plots). The Cook's distance plot also reveals three influential observations. The plot of the residuals vs. fitted values reveals some underestimation of the response variable as a consequence of the influential observations. These influential observations, however, are not erroneous but observed values resulting from specific conditions. For that reason, because the DSS does not rely directly on electricity prices but on the ranking of the hours according to the prices, and because of the simplicity of the model that is able to explain more than 60% of the variation in the data, the model was retained in its present form including the influential observations.

Chapter 6

Decision Module

Prior to the execution of the Decision Module a *History File* is created to store the output from the different operations executed in the Decisions Module. The program first checks if such a file has been previously created since the system started running, and if that file exists it is then used to create a new *History File*. The data stored in the *History File* is not only for future analysis, but it is also the back up data automatically used in case of unexpected termination of the program (e.g., power outage, system malfunction).

Once the *History File* has been generated the program proceeds to a loop of execution of the Decision Module with a time period defined by the user. The time period of execution of the Decision Module, or execution period, can not be less than an hour since the electricity prices are reported not more frequently than on an hourly basis. For simulation purposes the execution period was chosen as one hour.

The Decision Module comprises the operations shown in Figure 6.1:

- Update of prediction of solar radiation: a more accurate short term forecast of solar radiation and measured values from the sensors are used to update the long term forecast of solar radiation,
- Crop model: using the values of cumulative PAR energy, updated prediction of solar radiation, harvest date and yield targets, and time passed since planting; a crop model calculates the crop radiation need for a certain future time period and makes a decision about terminating the program (the program is terminated when the end of the crop growth period is reached) or continuing to the next

task,

- Update of electricity prices: the most recent prediction of meteorological variables and the available values of electricity prices in the Day-Ahead market for the next day at the time of execution are used to update the long term forecast of electricity prices in the Day-Ahead or Real-Time markets,
- Decision: using the output from the crop model subsection and the updated prediction of electricity prices, a decision is made about providing supplemental lighting, deploying the shade screens, or not performing any action,
- Update of history file: the output from the different operations is stored in a file that is updated every time the Decision Module is executed,
- Return to the beginning of the Decision loop.

6.1 Update of Prediction of Solar Radiation

The long term prediction of solar PAR energy inside the greenhouse described in Chapter 4 is updated every time the Decision Module is executed. The values that belong to the past are updated with the values that correspond to the available measurements from the PAR sensors while the values that belong to the future are updated with the short term predicted values.

The short term predicted values of PAR energy values inside the greenhouse are generated using the greenhouse transmittance and forecasted values of total sky cover, available on an hourly basis for any location in the U.S.A from the National Digital Forecast Database, NDFD (<http://www.nws.noaa.gov/ndfd/>). For the present project, the short term prediction is done for the next 48 hours from any given present hour, but since the reported values of total sky cover from NDFD are available for a longer period of time, it is possible to increase the time span of this short term prediction.

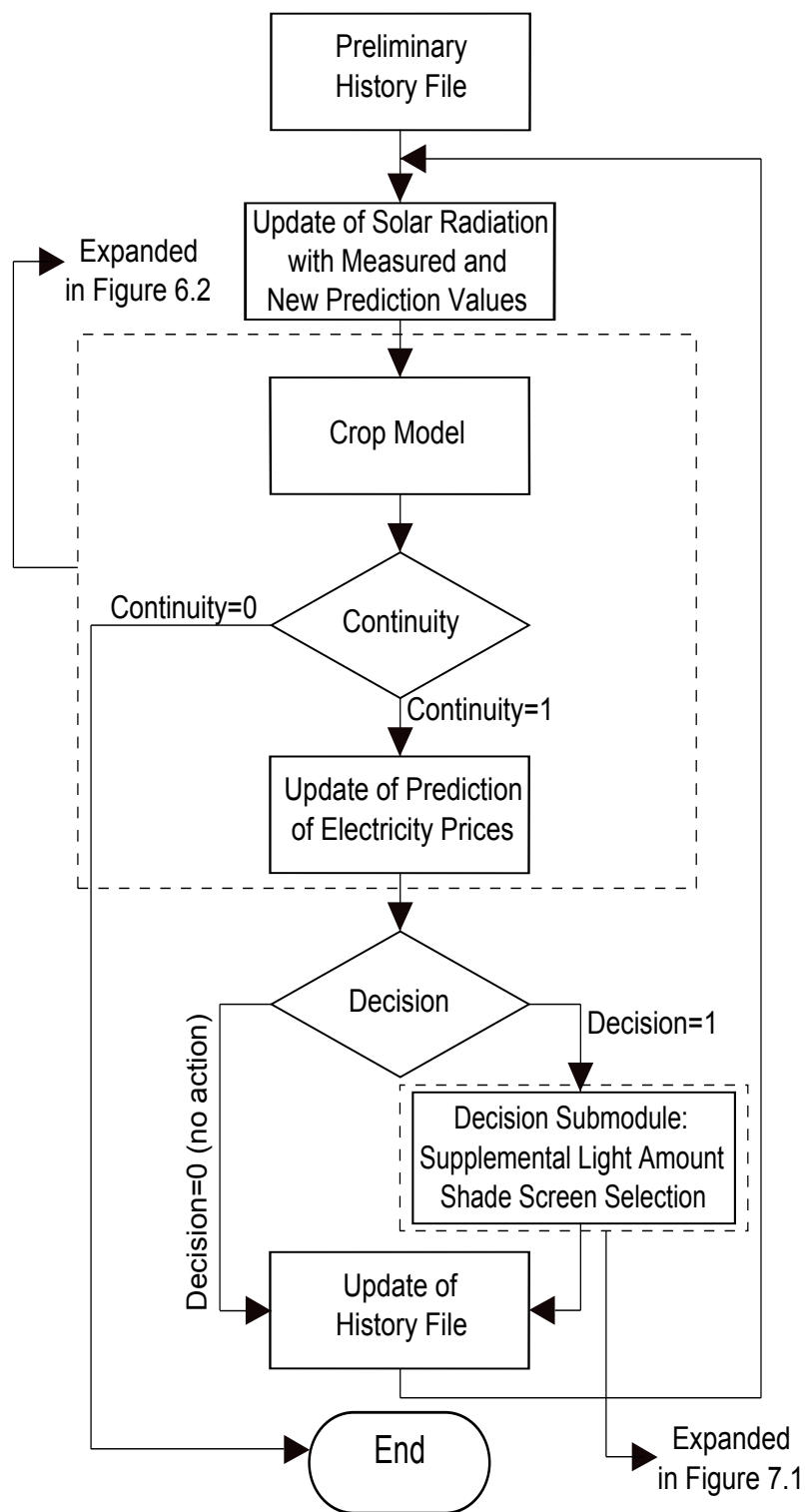


Figure 6.1: Decisions Module flow chart.

6.2 Crop Model

Crop models can be classified as descriptive or explanatory models (Marcelis et al., 1998). Descriptive models typically consist of regression functions between the crop variables of interest and variables corresponding to different environmental factors. Explanatory models, on the other hand, relate the crop growth development with physiological processes and are more complex than descriptive models (Marcelis et al., 1998; Lentz, 1998). For tactical decision support systems such as the present one, a descriptive crop model is preferred because its implementation is relatively simple and provides just what is necessary: a relationship between crop variables of interest (growth period and yield) and the environmental factors (cumulative PAR energy in the present case).

For this project the model selected was developed by Giniger et al. (1988) for a single truss tomato cropping system (McAvoy, 1988; McAvoy et al., 1989). The single truss tomato cropping system was developed by plant scientists and agricultural engineers at Rutgers University as an alternative to the traditional greenhouse tomato production systems where the plants are kept at fixed locations and the fruits are harvested from the different clusters throughout the plant life cycle that can last as long as 11 months.

In the single truss tomato cropping system the plants are grown on top of movable benches and after harvesting a single fruit cluster (the apical meristem of each plant is pinched two leaves above the first fruit truss), the plants are discarded and replaced. Plants of the same development stage, are kept together and during transplanting to the crop block corresponding to the next development stage, the plant spacing is increased. The single truss cropping system facilitates mechanization, more easy plant maintenance, and guarantees a continuous production of quality fruits.

The crop model assumes that cumulative PAR energy is the only input variable and the values of the other factors are kept within determined ranges (a valid assumption for a greenhouse environment). It consists of a set of two equations, one for

the seedling or vegetative stage (period from emergence to flowering), and the other for the production stage (period from flowering to harvest):

6.2.1 General model assumptions

- Model developed for *Lycopersicon esculentum* cv. Dombito
- Day/night temperatures were kept at $21^{\circ}C$ and $17^{\circ}C$, respectively
- Carbon dioxide concentration was maintained at $600 \mu mol/mol$ during non-venting hours
- Supplemental lighting (if needed) provided between 4:00 and 22:00 hours
- Daily PAR during the seedling stage was maintained between $10 mol/m^2$ and $30 mol/m^2$ at the top of the plant canopy
- Cumulative PAR received during the production stage was between $300 mol/m^2$ and $1200 mol/m^2$
- The germination period, from seeding to germination, takes approximately one week

6.2.2 Equation for Days to Flowering (Seedling Stage)

$$D = 86 - 0.049 \cdot X \tag{6.1}$$

$R^2 = 0.75$, slope standard error 0.007, intercept standard error 5.4.

D : Days to first flowering after germination. $38 \leq D \leq 58$

X : Cumulative PAR, measured at the top of the canopy level, during the seedling stage.

6.2.3 Equation for Fruit Yield (Production Stage)

$$Y = 0.82 \cdot X - 194 \quad (6.2)$$

$R^2 = 0.90$, slope standard error 0.05, intercept standard error 36

Y : Total fruit yield in *g/plant* during the production stage

X : Cumulative PAR, measured at the top of the canopy level, during the production stage.

The duration of the production stage, from first flowering to final harvest, is 60 days independently of the cumulative PAR received during that period. Harvesting is scheduled over the two weeks period before the end of the production period (immature fruit is allowed to stay on the plant a little longer).

6.2.4 Variables for the Crop Model Section

The crop model developed by Giniger et al. (1988) was selected for this project for its simplicity and its dependence on only one variable, cumulative PAR, one of the main limiting factors for tomato production in the northeast region of the USA during the winter months. By keeping track of time and the accumulated amount of PAR that the crop receives, it is possible to predict the number of days to flowering using Equation 6.1.

The amount of accumulated PAR that the crop receives is recorded in the updated long term prediction of solar PAR inside the greenhouse since the energy values that correspond to the measurements from the PAR sensors are substituted for the past prediction of solar PAR values every time the Decision Module is executed. To facilitate this update, the prediction of solar radiation was transformed from an hourly basis to a time resolution equal to the measuring period of the PAR sensors.

Once the long term prediction of solar PAR inside the greenhouse has been updated and before they are used by the crop model, they are transformed to a time

resolution equal to the execution period to facilitate the calculations. These final values, the time past since seeding, the expected harvest date and yield, and the different model parameters, become the input variables for the crop model section. While the input variables are specific to the crop model used, the output variables are not model specific.

Crop Model Section Output Variables:

- Continuity: binary variable indicating if the program proceeds to the end (value 0) or to the next task (value 1),
- Decision: binary variable indicating whether the Decision Submodule will be executed (value 1) or not (value 0),
- Available Time: remaining time (*days*) of the present stage of the crop, vegetative or production,
- Radiation Need: amount of accumulated PAR needed during a time period determined by *Available Time*,
- Predicted Duration of Crop Growth: predicted duration (*days*) of crop growth according to the model and the input variables,
- Predicted Crop Yield: predicted crop yield (*g/plant*) according to the model and the input variables.

6.2.5 Crop Model Implementation

The algorithm that corresponds to the crop model consists of a series of conditions about the developmental stage of the crop according to the model: germination, vegetative, or production. Using the time past since seeding, the amount of cumulative PAR that the crop has received, and Equation 6.1, it is possible to determine the number of days to flowering.

If the crop is in the germination period the output value of the variable *Decision* from the crop model section is 0 and although the Decision Submodule is bypassed, the loop corresponding to the whole Decision Module continues to be executed (Figure 6.1). The crop model section calculates *Radiation Need* and *Available Time* using Equation 6.1 and the target final harvest date if the crop is in the vegetative (seedling stage). If the crop is in the production stage, the crop model section calculates *Radiation Need* and *Available Time* using Equation 6.2 and the target harvest yield. The program ends when the stage of the crop is past the production stage. These processes are represented in Figures 6.1 and 6.2.

6.3 Decision Submodule

Because of the complexities of the Decision Submodule and importance in the DSS, it will be described in a separate chapter (Chapter 7).

6.4 Update of the Prediction of Electricity Prices

In Chapter 5.1 it was described how to generate long term predictions of Day-Ahead and Real-Time electricity prices using the linear models developed for each of them and historic values of certain meteorological variables. Similarly to the long term prediction of solar radiation, these long term predictions of electricity prices are updated every time the Decision Module is executed.

The long term predictions of electricity prices that correspond to the past are updated with the values that were reported by the ISO while the values that correspond to the future are updated in two steps. First, a short term prediction of Day-Ahead LMPs is generated using the corresponding linear model and the most recent meteorological data from NOAA for the weather stations assigned to the geographic area of the power utility provider. The long term prediction of Day-Ahead LMPs is then updated with the available values from this short term prediction.

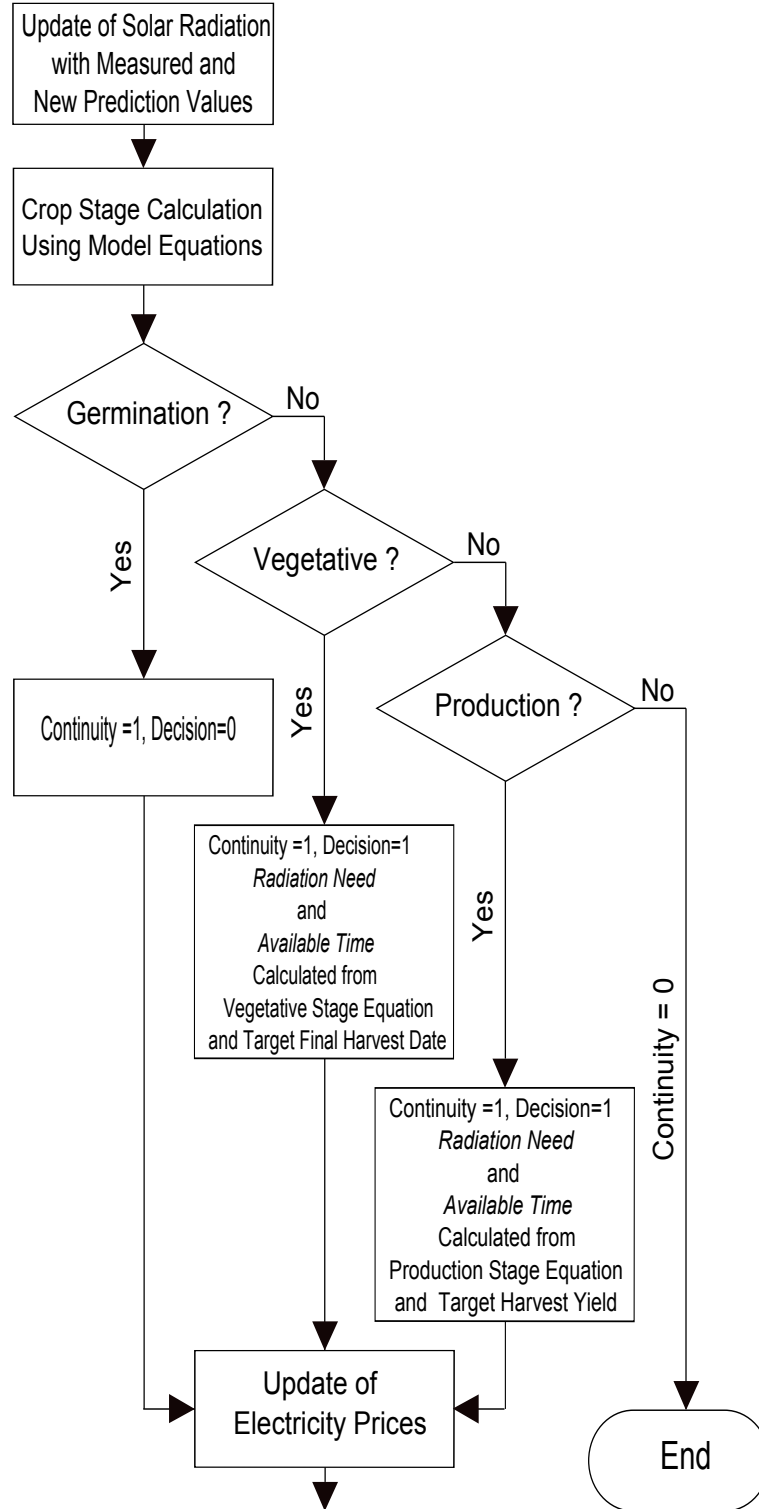


Figure 6.2: Crop Model flow chart. See Figure 6.1 to see the Crop Model section in relation to the other components of the overall Decision Module.

A second update of the long term prediction of Day-Ahead LMPs is done using the values of Day-Ahead LMPs for the next day, available from the ISO website. The updated prediction of Day-Ahead LMPs is then used to update the long term prediction of Real-Time LMPs. Before executing the Decision Submodule the updated long term prediction of electricity prices is transformed from an hourly time resolution to a time resolution equal to the execution period.

6.5 Update of the History File

The history file records the output from the operations performed in the Decision Module and it is updated every time this module is executed. This file not only serves as a validation of the whole program but also as a back up data repository in case of an unexpected termination of the program. The values of the following variables are recorded in this file in a time resolution equal to the execution period:

- Date and Time in Daylight Savings Time Format
- Predicted and Received PAR
- Supplemental Lighting Decision (1 for lights on, 0 for lights off)
- Shade screen Selection (1 for deployed , 0 for retracted)
- Predicted and Actual Electricity Prices
- Target and expected Final Harvest Date and Harvest Yield

Chapter 7

Decision Submodule

The Decisions Submodule is the section of the DSS program responsible for making the decision to provide supplemental lighting, to deploy the shade screens, or take no action. Because the Decision Submodule is a section of the larger Decision Module, it is also executed (depending on the output from the crop model) in a time loop with a period equal to the execution period. The output or decision resulting from the execution of this submodule at a given time is valid until the next execution, when a new decision is made. For example, if the execution period is chosen as 1 hour and at a given time the decision taken is to provide supplemental lighting, this decision will remain valid for the next hour starting at the time the decision was made.

Throughout the present chapter the Decision Submodule will be described by explaining the algorithm and structure of its different sections. First of all it is necessary to define its input and output variables.

Input Variables:

- Available Time (output variable from the crop model): remaining time of the present stage of the crop, vegetative or production
- Radiation Need (output variable from the crop model): amount of PAR needed during a time period determined by *Available Time*
- Updated Prediction of Solar Radiation
- Updated Prediction of Electricity Prices

- Price Sensitivity: value from 0 to 1 to indicate the priority or weight of considering the electricity prices during the decision process. A 1 corresponds to the highest priority and 0 to no priority (how this variable is incorporated in the calculations is explained in section 7.3.5).
- Duration of dark period: duration, in hours, of a required dark period during the night (for a tomato crop, a minimum of 6 hours is required).

Output Variables:

- Amount of Supplemental Light to be Provided: if the lights are dimmable, the amount of supplemental lighting can vary from zero to the maximum intensity that the lighting system can provide. If the lights are not dimmable, the amount of supplemental lighting can be zero or the intensity that the lighting system can provide.
- Selected Combination of Screens to be Deployed: depending on the number of screens available, this value can vary from zero (no screens are selected) to the number of possible combinations of screens (see section 7.2).

Figure 7.1 represents the different sections of the Decision Submodule and their relation to the previously defined variables.

7.1 Calculation of the Radiation Gap

According to the Crop Model, if the crop receives an amount of accumulated PAR energy equal to *Radiation Need* (R_{need}) during the time determined by *Available Time* ($\tau_{avblble}$) the harvest time and yield targets are achieved. However, providing this amount of radiation in that specific time interval is challenging because the radiation that the crop will receive in that time period will be coming from supplemental light and/or solar radiation, and the future values of solar radiation are not known with certainty.

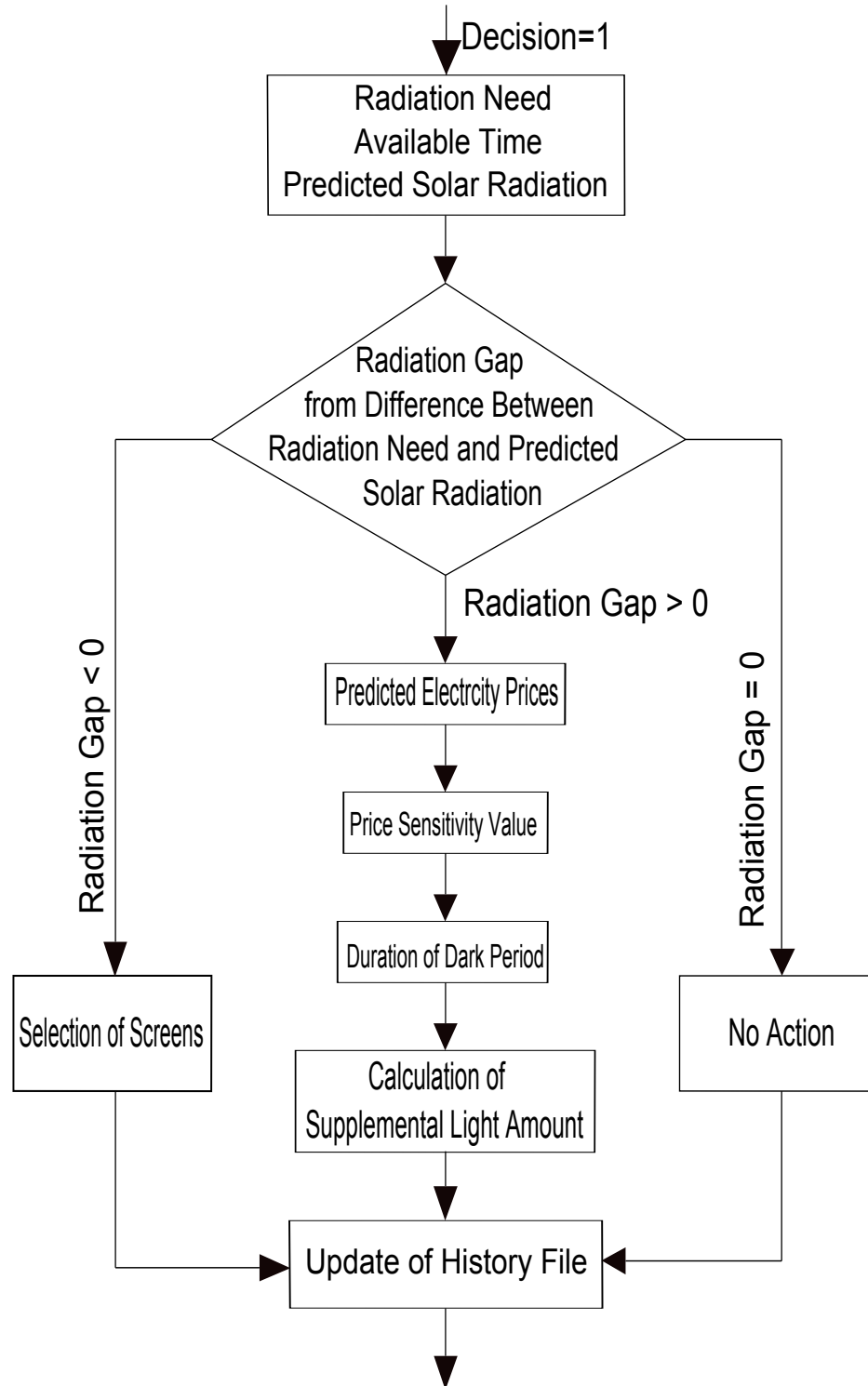


Figure 7.1: Decisions Submodule Algorithm. See Figure 6.1 to see the Decisions Submodule Algorithm in relation to the other components of the encompassing Decision Module Algorithm.

The more accurate the prediction of future values of solar radiation, the more likely it is that the crop receives an amount of PAR energy equal to *Radiation Need* during the time determined by *Available Time*. For this reason, and because the prediction of solar radiation for a given location for the next 48 hours from a given time are based on the most recent forecast of sky cover from NOAA while the prediction values further than 48 hours from the present are based on historic values of solar radiation from the NSRDB, the decision about providing supplemental lighting or deploying the shade screens will be based on a future *decision time interval*, τ_{dec} (the subindex *dec* stands for *decision*), that starts at the present hour and is not longer than 48 hours or *Available Time*.

In a similar way, the more accurate the prediction of future values of electricity prices, the better the performance of the DSS at optimizing the electricity cost of the supplemental lighting system. For this reason, the *decision time interval* will not exceed the number of future hours for which the Day-Ahead LMPs are available from the Regional Transmission Organization (RTO) website. If the present hour is before 4:00 PM, the time at which the RTO reports the Day-Ahead LMPs for each hour of the next day, the number of future hours for which the Day-Ahead LMPs are available, n_{DH} , is equal to the number of remaining hours of the day. If the present hour is after or at 4:00 PM, n_{DH} is equal to the number of remaining hours of the day plus 24 (number of hours of the next day).

$$\tau_{dec} = \text{minimum}(n_{DH} \text{ hours}, \tau_{avblle}) \quad (7.1)$$

A partial amount of cumulative PAR energy $R_{partial}$ is assigned to τ_{dec} according to:

$$R_{partial} = R_{need} \cdot \tau_{dec} / \tau_{avblle} \quad (7.2)$$

Then the Radiation Gap, R_{gap} , is defined as the difference between the partial cumulative PAR energy, $R_{partial}$, and the predicted cumulative solar PAR energy,

R_{dec} , calculated in a time period equal to τ_{dec} :

$$R_{gap} = R_{partial} - R_{dec} \quad (7.3)$$

Depending on $R_{partial}$ and R_{dec} , R_{gap} can have positive or negative values, or even be zero. If R_{gap} is negative, the section that selects the appropriate combination of screens is executed. If R_{gap} is positive, the section that calculates the necessary intensity of supplemental lighting is executed. When R_{gap} is zero no action is taken.

7.2 Shade Screen Selection

If the predicted cumulative solar radiation during τ_{dec} is larger than what the crop will need (according to the time and harvest yield targets) during that same period, $R_{gap} < 0$, the DSS executes the *shade screen selection algorithm* to make a decision about blocking solar radiation during the next hour. The algorithm is developed for an arbitrary number of screens n_s . Each screen is represented by a set of three numbers indicating the percentages of direct, diffuse, and reflective solar radiation that the screen is able to block (information provided by the manufacturer for specific conditions; in the present study these values are assumed to remain constant):

$$S^i = (S_{dir}^i, S_{dif}^i, S_{ref}^i), \quad i = 1, 2, \dots, n_s \quad (7.4)$$

where:

$S_{dir}^i, S_{dif}^i, S_{ref}^i$: percentages of direct, diffuse, and reflective solar radiation, respectively, that the i -th screen is able to block.

The total number of possible combinations in which the different n_s screens can be selected is $2^{n_s} - 1$ and will be represented by n_c . Table 7.1 shows the possible combinations, 7, in which a set of three screens can be selected.

		Screens		
		1	2	3
Selection		X	X	X
		X	X	
			X	X
		X		X
		X		
			X	
				X

Table 7.1: Possible combinations in which a set of three screens can be selected.

$$n_c = \sum_{k=1}^{n_s} \binom{n_s}{k} = 1 + \sum_{k=1}^{n_s} \binom{n_s}{k} - 1 = 2^{n_s} - 1 \quad (7.5)$$

where:

$$\binom{n_s}{k} = \frac{n_s!}{k! \cdot (n_s - k)!}$$

The notation $\binom{n_s}{k}$ indicates the number of combinations of size k in a population of size n_s . The value of k varies from 1 to n_s because it is possible to have combinations of only one screen (n_s possible combinations), two screens, and so on up to combinations of n_s screens (only one combination that contains all the screens is possible). Every combination represents a subset of screens from all the available screens:

$$C_j = \{S^{i_j}\} \quad (7.6)$$

where:

C_j : j - th combination

$\{S^{i_j}\}$: subset of screens in the j - th combination

The way in which the different combinations are identified is not important as long as every combination is assigned a unique value from $\{1, 2, \dots, 2^{n_s} - 1\}$

7.2.1 Selection of a Combination of Shade Screens

The predicted cumulative solar PAR energy screened during τ_{dec} by the screens contained in the $j - th$ combination is represented by $R_j^{\tau_{dec}}$ and calculated in the following way:

$$R_j^{\tau_{dec}} = R_{dir}^{\tau_{dec}} \cdot \prod_{i_j} (1 - S_{dir}^{i_j}) + R_{dif}^{\tau_{dec}} \cdot \prod_{i_j} (1 - S_{dif}^{i_j}) + R_{ref}^{\tau_{dec}} \cdot \prod_{i_j} (1 - S_{ref}^{i_j}) \quad (7.7)$$

where:

- i_j : indicator for the screens in the $j - th$ combination
- $(S_{dir}^{i_j}, S_{dif}^{i_j}, S_{ref}^{i_j})$: percentages of direct, diffuse, and reflected solar radiation that the i_j screen is able to block
- $(R_{dir}^{\tau_{dec}}, R_{dif}^{\tau_{dec}}, R_{ref}^{\tau_{dec}})$: direct, diffuse, and reflected components of the predicted cumulative PAR energy during τ_{dec}

The screens combination for which the predicted screened-cumulative PAR energy $R_j^{\tau_{dec}}$ value is closest to $R_{dec} + R_{gap}$ is selected, and its screens are the ones that will be deployed in the next execution period. If more than one screen combination satisfies the previous criterion, the combination with less screens is selected.

7.3 Supplemental Lighting Algorithm

7.3.1 Basic Definitions

The hours in a given day can be classified into *daytime* and *nighttime* hours depending on their timing relative to sunrise and sunset for that day. In the classification adopted for the present study, if sunrise takes place right at the start or within a given hour, the hour is classified as *sunrise hour*. If sunset takes place right at the start of

a given hour, the hour is classified as *sunset hour*, otherwise the next following hour is considered the *sunset hour*.

The hours between the *sunrise hour* and the first *sunset hour* that follows the *sunrise hour*, including the *sunrise hour* but excluding the *sunset hour*, are considered *daytime hours*. In the same way, the hours between the *sunset hour* and the first *sunrise hour* that follows the *sunset hour*, including the *sunset hour* but excluding the *sunrise hour* are considered *nighttime hours* (Figure 7.2).

In order to facilitate the explanation of the material that follows, the execution period will be considered as one hour. The moment of execution of the Decision Module will be referred to as the *present event*. The hour during which the present event takes place or that starts at the present event is considered the *present hour* (Figure 7.2).

7.3.2 Available Hours for Supplemental Lighting

The decision about providing a determined amount of supplemental lighting at a given time is the result of a sequence of some basic operations on a matrix that represent the different possibilities in which supplemental lighting can be provided. First, a time period τ_{double} is defined spanning from the sunrise hour that precedes or coincides with the present hour to the last nighttime hour before the second sunrise hour that follows the present hour (Figure 7.3). τ_{double} includes two daytime periods and two nighttime periods and it is defined in this way so that the decision time interval (defined in section 7.1), τ_{dec} , is contained in τ_{double} .

A value of 1 or 0 is used to indicate the possibility of providing supplemental lighting during a given hour of τ_{double} (value 1 for possible and 0 for not possible). To all the hours belonging to the daytime periods a value of 1 is assigned since there are not dark period restrictions during the daytime. The value that can be assigned to the different hours of the nighttime periods, however, depend on the fact that the tomato plants require a predetermined number of consecutive hours of darkness

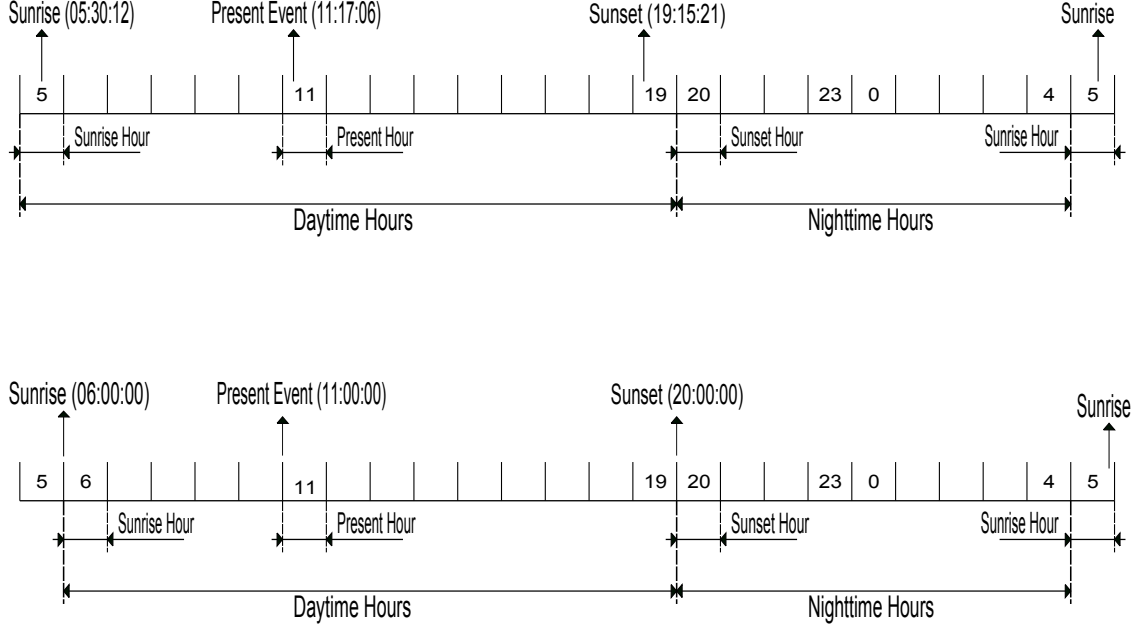


Figure 7.2: Examples of Hours Classification: Present Hour, Daytime and Nighttime Hours.

(required dark period). As a consequence of this, the assignment of a value of 1 or 0 to each hour of τ_{double} can be done in different ways.

The number of hours in the first and second daytime periods are represented by n_d^1 and n_d^2 , respectively. In the same way, the number of hours in the first and second nighttime periods are represented by n_n^1 and n_n^2 , respectively. The sum of the hours from the first daytime and nighttime periods will be represented by n^1 while n^2 represents the sum of the hours from the second daytime and nighttime periods. The number of hours in the dark period is represented by n_k ($n_k \leq n_n^1$, $n_k \leq n_n^2$).

The assignment of a value of 1 or 0 to each hour of τ_{double} will be called *allocation*.

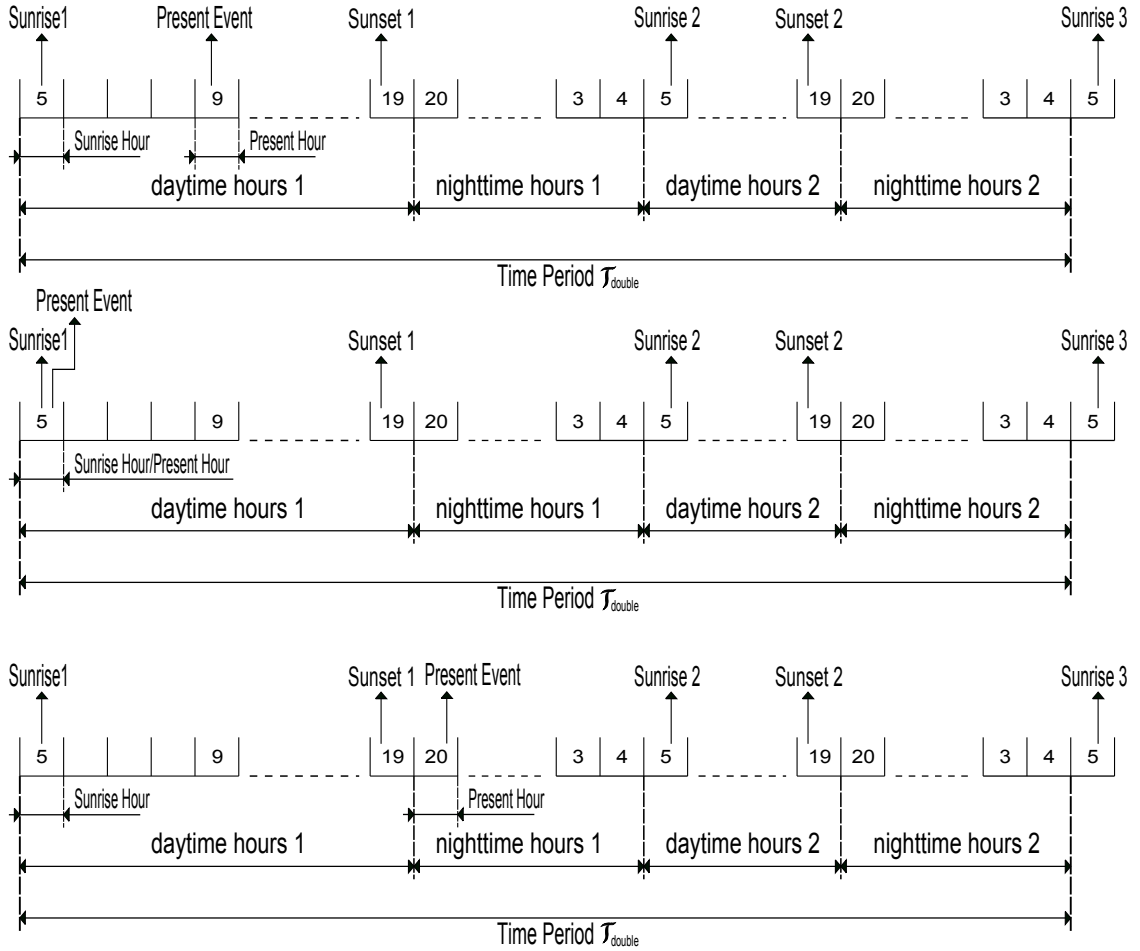


Figure 7.3: Examples of Time Period \mathcal{T}_{double} .

The value n_p represents the number of possible allocations taking into account the dark period restriction:

$$n_p = (n_n^1 - n_k + 1) \cdot (n_n^2 - n_k + 1) \quad (7.8)$$

7.3.3 Matrix Representation of the Available Hours for Supplemental Lighting

Each allocation is represented by a column vector $C_{(n^1+n^2) \times 1}^{\lambda_1, \lambda_2, n_n^1, n_n^2, n_k}$. The lower index n^1+n^2 correspond to the number of rows while the value of 1 to the number of columns

(only one column). The upper indices λ_1 and λ_2 indicate the position of the first hour of the dark period in the first and second nighttime periods, respectively (Figure 7.4). The possible values of λ_1 and λ_2 depend on the number of hours in the dark period, and the number of hours in the first and the second nighttime periods:

$$1 \leq \lambda_1 \leq n_n^1 - n_k + 1 \quad (7.9)$$

$$1 \leq \lambda_2 \leq n_n^2 - n_k + 1 \quad (7.10)$$

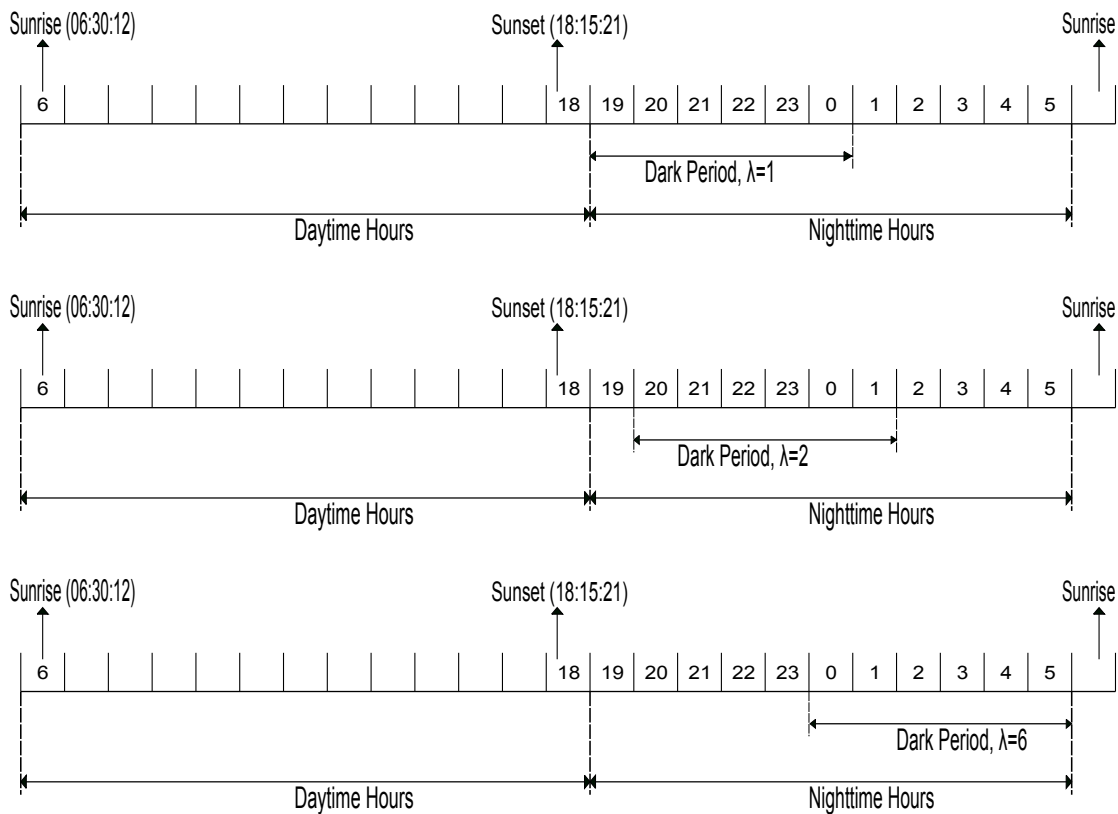


Figure 7.4: Different Possible Positions of the Required Dark Period During the Nighttime Hours.

Using these conventions, the column vector $C_{(n^1+n^2) \times 1}^{\lambda_1, \lambda_2, n_n^1, n_n^2, n_k}$ is represented in the

following way:

$$C_{(n^1+n^2)\times 1}^{\lambda_1, \lambda_2, n_n^1, n_n^2, n_k} = \begin{bmatrix} \mathbf{1}_{(n_d^1+\lambda_1-1)\times 1} \\ \mathbf{0}_{n_k\times 1} \\ \mathbf{1}_{(n_n^1+1-\lambda_1-n_k+n_d^2+\lambda_2-1)\times 1} \\ \mathbf{0}_{n_k\times 1} \\ \mathbf{1}_{(n_n^2+1-\lambda_2-n_k)\times 1} \end{bmatrix} \quad (7.11)$$

where:

$$\mathbf{1}_{n\times 1} = \begin{bmatrix} 1 \\ 1 \\ \vdots \\ 1 \end{bmatrix} \quad \text{Column of } n \text{ 1's} \quad (7.12)$$

$$\mathbf{0}_{n\times 1} = \begin{bmatrix} 0 \\ 0 \\ \vdots \\ 0 \end{bmatrix} \quad \text{Column of } n \text{ 0's} \quad (7.13)$$

$\mathbf{1}_{(n_d^1+\lambda_1-1)\times 1}$ corresponds to the n_d^1 daytime period hours and first $\lambda_1 - 1$ hours from the first nighttime period. The two $\mathbf{0}_{n_k\times 1}$ matrices correspond to the dark period hours during the first and second nights. $\mathbf{1}_{(n_n^1+1-\lambda_1-n_k+n_d^2+\lambda_2-1)\times 1}$ corresponds to the $n_n^1 + 1 - \lambda_1 - n_k$ hours that follow the dark period during the first night, the n_d^2 daytime period hours, and first $\lambda_2 - 1$ hours from the second nighttime period. $\mathbf{1}_{(n_n^2+1-\lambda_2-n_k)\times 1}$ corresponds to the $n_n^2 + 1 - \lambda_2 - n_k$ hours that follow the dark period during the second night.

As expected, the sum of the number of rows of all the five column vectors that $C_{(n^1+n^2)\times 1}^{\lambda_1, \lambda_2, n_n^1, n_n^2, n_k}$ is composed of should equal $n^1 + n^2$:

$$\begin{aligned}
& (n_d^1 + \lambda_1 - 1) + n_k + (n_n^1 + 1 - \lambda_1 - n_k + n_d^2 + \lambda_2 - 1) + n_k \\
& + (n_n^2 + 1 - \lambda_2 - n_k) = n_d^1 + n_n^1 + n_d^2 + n_n^2 = n^1 + n^2
\end{aligned} \tag{7.14}$$

A matrix $M_{(n^1+n^2) \times n_p}^{n_n^1, n_n^2, n_k}$ is then formed whose columns are the column vectors $C_{(n^1+n^2) \times 1}^{\lambda_1, \lambda_2, n_n^1, n_n^2, n_k}$. For simplicity $n^1 + n^2 = n$ and the upper indices n_n^1, n_n^2, n_k from both M and C will be omitted. Only the upper indices λ_1 and λ_2 from C will be kept, resulting in this simplified representation:

$$M_{n \times n_p} = \left[C_{n \times 1}^{1,1} \ C_{n \times 1}^{2,1} \ \dots \ C_{n \times 1}^{n_n^1 - n_k + 1, 1} \ C_{n \times 1}^{1,2} \ \dots \ C_{n \times 1}^{n_n^1 - n_k + 1, n_n^2 - n_k + 1} \right] \tag{7.15}$$

7.3.4 Reduction of the Matrix Representing the Available Hours for Supplemental Lighting

The larger time span determined by the first and last rows from $M_{n \times n_p}$ encompasses the shorter time span τ_{dec} . However, only the rows from $M_{n \times n_p}$ that correspond to the shorter time span determined by τ_{dec} have an impact on the supplemental lighting decision. These rows are referred to as *decision rows*. The number of decision rows will be represented by n_d .

The columns of matrix $M_{n \times n_p}$ represent all the possible allocations or ways in which the hours from τ_{double} are available for supplemental lighting. However, some of these allocations are already invalid at the start of the *present hour*. For example, if during one of the hours belonging to the dark period from a given allocation supplemental lighting was already provided, then the dark period restriction is not valid for that particular allocation.

To identify the invalid columns, each row from each column from $M_{n \times n_p}$ is compared with the corresponding value from the updated prediction of solar radiation. If for certain column there is a row that belongs to the dark period and for which the corresponding value from the updated prediction of solar radiation is not zero,

then that column is considered *invalid* because a non-zero value from the updated prediction of solar radiation during a dark period hour only means that supplemental lighting has been provided during that hour. Columns that are not *invalid* are considered *valid*. The number of valid columns will be represented by n_v .

A new matrix $M_{n_d \times n_v}^{ready}$ is formed including only the decision rows and the valid columns from $M_{n_d \times n_p}$. The assignment of a value of 1 or 0 to each hour from τ_{dec} according to a column from $M_{n_d \times n_v}^{ready}$ will be referred to as a *valid allocation*.

7.3.5 Hourly Distribution of R_{gap}

Although the valid allocations guarantee that the dark period restriction is satisfied, the problem of distributing an amount of PAR energy from supplemental lighting equal to R_{gap} through the different hours of each valid allocation remains unresolved.

The approach adopted in the present study to solve this problem is as follows:

- To each hour of a valid allocation is assigned a *weight* (to be explained later) that will determine the order in which supplemental lighting will be provided throughout the different hours.
- Starting from the hour with the highest weight, to each hour of a valid allocation is assigned the maximum possible amount of supplemental lighting PAR energy until a total amount of supplemental lighting PAR energy equal to R_{gap} is distributed throughout the different hours or until the maximum possible amount of supplemental lighting PAR energy is assigned to the hour with the lowest weight (whichever comes first).

The hourly *weight* values depend on the priority that is placed on minimizing the electricity cost associated with supplemental lighting while achieving the yield and harvest targets. This priority is quantified through an input variable in the DSS called *price sensitivity*, s_p . s_p varies between 0 and 1. $s_p = 0$ means that no priority is placed on minimizing the electricity cost associated with supplemental lighting

while $s_p = 1$ means that minimizing the electricity cost associated with supplemental lighting while achieving the grower targets has the highest priority.

The hourly *weight* values also depend on the ordinal number representing the position of the hour regarding the time, $n_{time}(hour)$; and the ordinal number representing the position of the hour regarding the corresponding electricity price, $n_{price}(hour)$:

$$\begin{aligned} n_{time}(hour\ 1) &= 1, \text{ hour 1 corresponds to the present hour} \\ n_{time}(hour\ 2) &= 2 \\ &\vdots \\ n_{time}(hour\ n_d) &= n_d \end{aligned}$$

n_d is the number of hours in τ_{dec} .

Similarly:

$$\begin{aligned} n_{price}(hour\ with\ lowest\ price) &= 1 \\ &\vdots \\ n_{price}(hour\ with\ highest\ price) &= n_d \end{aligned}$$

The value of the *weight* for a given hour h is then defined as:

$$weight(h) = (1 - s_p) \cdot (n_d + 1 - n_{time}(h)) + s_p \cdot (n_d + 1 - n_{price}(h)) \quad (7.16)$$

According to this definition, when $s_p = 0$ (no sensitivity to electricity prices), $weight(h)$ is determined solely by the relative distance of the hour to the present hour. In this case, the closer an hour to the present hour, the higher the corresponding $weight(h)$. The reason for defining $weight(h)$ in this way is to guarantee immediacy

in achieving the yield and harvest targets. When $s_p = 1$ (maximum sensitivity to electricity prices) $weight(h)$ is determined solely by the ranking that corresponds to the hour regarding the electricity prices. In this case, the lower the electricity price that corresponds to an hour, the higher the corresponding $weight(h)$. For the cases in between, $0 < s_p < 1$, $weight(h)$ is determined by both the relative distance of the hour to the present hour and by the ranking that corresponds to the hour regarding the electricity prices, in a proportion determined by the value of *price sensitivity*, s_p , according to Equation 7.16.

The maximum possible amount of supplemental lighting PAR energy that can be assigned to a given hour, $R(h)$, depends on several factors: the amount of PAR energy from R_{gap} that has not been assigned to previous hours, R_{gap}^{left} (R_{gap}^{left} for the first or present hour is just R_{gap}); the minimum and maximum values of supplemental lighting PAR flux, I_{min}^{sup} and I_{max}^{sup} , respectively; the PAR flux that causes radiation saturation in the crop, (I^{sat}); and on the value from $M_{n\tau \times n\nu}^{ready}$ that correspond to the hour (value of 0 for dark period hours and value of 1 otherwise). By using *Max* and *Min* to represent the functions that select the maximum and minimum, respectively, from a series of values:

$$R(h) = M_{n\tau \times n\nu}^{ready}(hour) \cdot Max\{R_{min}^{sup}, Min(R_{max}^{sup}, R^{sat}, R_{gap}^{left})\} \quad (7.17)$$

where:

$$M_{n\tau \times n\nu}^{ready}(hour) = \text{Value of } M_{n\tau \times n\nu}^{ready} \text{ that correspond to the hour}$$

$$R_{min}^{sup} = I_{min}^{sup} \cdot 3600 \text{ sec}$$

$$R_{max}^{sup} = I_{max}^{sup} \cdot 3600 \text{ sec}$$

$$R^{sat} = I^{sat} \cdot 3600 \text{ sec}$$

$$3600 \text{ sec} = \text{Number of seconds in 1 hour}$$

This equation is expressing that $R(h)$ can not exceed R_{gap}^{left} , or the hourly PAR energy that correspond to the maximum intensity from supplemental lighting, or the saturation radiation. At the same time, if supplemental lighting is to be provided, $R(h)$ can not be less than the hourly PAR energy that correspond to the minimum intensity from supplemental lighting.

7.3.6 Supplemental Lighting Decision

Once a $weight(h)$ and a maximum possible amount of supplemental lighting PAR energy $R(h)$ is assigned to each hour of every valid allocation according to the previous scheme, to every valid allocation is assigned a *return* value according to:

$$return(k) = \sum_h weight_k(h) \cdot R_k(h) \quad (7.18)$$

where:

$$k = \text{subindex to refer to the allocation}$$

The *return* function is defined in such a way to represent the opposite of a cost. The valid allocation with the highest *return* value is selected and the value of $R(hour\ 1)$ for that allocation will determine the amount of supplemental lighting to be provided during the present hour. If more than one valid allocation have the same *return* value, then from these allocations the one for which $weight_k(hour\ 1) \cdot R_k(hour\ 1)$ is maximum is selected.

Chapter 8

Results

8.1 Simulations Rationale and Definitions of Performance Metrics

The DSS has two goals:

1. Guarantee that the grower's harvest time and yield targets are achieved,
2. Depending on the level of sensitivity to electricity prices set by the user (explained in detail in sections 7.3.5 and 8.2), maximize the income from the excess electricity exported to the grid while achieving the first goal.

The adequacy of the DSS at achieving the previous goals was tested, by simulation, using five years (2000-2004) of historic meteorological and solar radiation data from the NSRDB, and electricity price data from PJM. The simulations are divided into *lighting simulations* and *shading simulations*.

In the lighting simulations the grower's harvest time and yield targets are set to their minimum and maximum values, respectively. The lighting simulations are performed during the summer and winter months for each year from 2000 until 2004. The lighting simulations, and in particular the ones performed during the winter months when the available solar radiation is minimum, allow to test the performance of DSS while providing supplemental lighting since the grower's targets in this case require that the crop receives maximum radiation.

In the shading simulations the grower's harvest time and yield targets are set to their maximum and minimum values, respectively. This is a purely theoretical

scenario with the goal of testing the performance of the DSS at using the shade screens to block unwanted radiation. For this reason, the shading simulations are performed only during the summer months for each year from 2000 until 2004, when the available solar radiation is maximum and in order to extend the crop growth period and decrease the harvest yield, it is necessary to make maximum use of the shade screens to block unwanted radiation.

For simulation purposes, an instance of execution refers to the moment of time, within the 2000-2004 simulation period, when the DSS makes a decision about providing supplemental lighting or deploying the shade screens for the next hour. Historic data (meteorological, solar radiation, or electricity price data) that lie back in the past from the instance of execution is referred to as past data while historic data that lie ahead in the future from the instance of execution is referred to as future data.

Future sky cover data are used to predict future values of solar radiation inside the greenhouse (using the sky cover and Transmittance models) while the future Day-Ahead electricity price data is either used to rank the future hours according to the price if the electricity is sold in the Day-Ahead market, or to predict future Real-Time prices otherwise. Past solar radiation data are used, together with the Transmittance Model, to generate synthetic solar radiation values inside the greenhouse since such data do not exist for the simulation period. Past values of electricity price data are used to make the lighting energy and cost estimations.

time and yield metrics

The metrics used to quantify the performance of the DSS at achieving harvest time and yield targets are:

- Time from sowing to final harvest, *time*, in *days*
- Total fruit yield, *yield*, in *g/plant*

These two metrics were chosen because they are affected only by the cumulative PAR received by the crop (based on the plant growth model used) and can be compared across different scenarios independently of the size of the supplemental lighting system.

energy and cost metrics

Choosing the metrics to compare the supplemental lighting energy use or cost across different scenarios required additional analysis because both energy use and cost depend on the size of the supplemental lighting system. The lighting energy use during a time period is a function of the corresponding electric power consumption. In a similar way, the lighting cost is a function of the energy consumption and the associated price:

$$E = \int_{t_0}^{t_f} P_w(t) \cdot dt \quad (8.1)$$

$$C = \int_{t_0}^{t_f} p_e(t) \cdot P_w(t) \cdot dt \quad (8.2)$$

where:

E = Lighting Energy Use (MWh)

P_w = Electric power consumption (MW)

C = Lighting Cost (\$)

p_e = Electricity price ($\$/MWh$)

t_0, t_f = Initial (start) and final (end) times, respectively

For the present case the power and electric prices vary hourly:

$$E = \sum_{\text{lighting hours}} P_w(\text{hour}) \cdot 1 \text{ hour} \quad (8.3)$$

$$C = \sum_{\text{lighting hours}} P_w(\text{hour}) \cdot p_e(\text{hour}) \cdot 1 \text{ hour} \quad (8.4)$$

For a fixed area density of lamps, the power consumption is directly proportional to the lighting area. In a similar manner, for a fixed lighting area, it is expected that the electric power consumption is directly proportional to the area density of lamps and for that reason to the lighting intensity. In the general case, it is assumed that the power consumption is directly related to the lighting area and the lighting intensity (this proposition will be validated in section 8.1):

$$P_w = \lambda \cdot A \cdot S \quad (8.5)$$

where:

λ = Parameter that is specific for the configuration of the supplemental lighting system (type of lamps, lamps/area, and mounting height). λ is the inverse of total PAR efficiency and is expressed in $MW \cdot s/\mu mol$.

A = lighting area (m^2)

S = Lighting intensity measured at the top of the crop canopy ($\mu mol/m^2 \cdot sec$)

From Equations 8.3, 8.4, and 8.5:

$$E = \sum_{\text{lighting hours}} \lambda \cdot A \cdot S(\text{hour}) \cdot 1 \text{ hour} \quad (8.6)$$

$$C = \sum_{\text{lighting hours}} \lambda \cdot A \cdot S(\text{hour}) \cdot p_e(\text{hour}) \cdot 1 \text{ hour} \quad (8.7)$$

For the present case different scenarios are compared for a given greenhouse, so both λ and A are constants:

$$E = \lambda \cdot A \cdot \sum_{\text{lighting hours}} S(\text{hour}) \cdot 1 \text{ hour} \quad (8.8)$$

$$C = \lambda \cdot A \cdot \sum_{\text{lighting hours}} S(\text{hour}) \cdot p_e(\text{hour}) \cdot 1 \text{ hour} \quad (8.9)$$

Equations 8.8, 8.9 can be represented in a different way:

$$E = \rho \cdot E_m \quad (8.10)$$

$$C = \rho \cdot C_m \quad (8.11)$$

$$\rho = \lambda \cdot A \quad (8.12)$$

$$E_m = \sum_{\text{lighting hours}} S(\text{hour}) \cdot 1 \text{ hour} \quad (8.13)$$

$$C_m = \sum_{\text{lighting hours}} S(\text{hour}) \cdot p_e(\text{hour}) \cdot 1 \text{ hour} \quad (8.14)$$

where:

ρ = Parameter that is specific for the configuration of the supplemental lighting system (type of lamps, lamps/area, and mounting height). ρ is the inverse of PAR efficiency per unit area and is expressed in $MW \cdot m^2 \cdot sec/\mu mol$.

E_m = Lighting energy use metric ($h \cdot \mu mol/m^2 \cdot sec$)

C_m = Lighting cost metric ($\$ \cdot \mu mol/MW \cdot m^2 \cdot sec$)

For the present case where ρ is constant (the configuration of the lighting system is assumed to be the same in the different scenarios), the lighting energy use metric (E_m) and the lighting cost metric (C_m) defined by Equations 8.13 and 8.14, respectively, determine the lighting energy use (E) and the lighting cost (C), respectively.

Practical example of the use of the *energy* and *cost* metrics

Since the energy use and cost metrics previously defined are unconventional, it could be helpful to provide an example of their practical use. The estimated values of lighting intensity at the top of the canopy level throughout a 1-acre greenhouse for different lighting configurations of 400 Watt High Pressure Sodium (HPS) lamps, Table 8.1, obtained by Both (2004) can be used for that purpose.

Table 8.1: Lighting intensity at the top of the canopy level throughout a 1-acre greenhouse for different lighting configurations of 400 Watt High Pressure Sodium (HPS) lamps ((Both, 2004)).

floor area/lamp ($m^2/lamp$)	power/fixture* (W)	power/area (W/m^2)	Supplemental Lighting ($\mu mol/m^2 \cdot sec$)	
			Mounting height of 8'	Mounting height of 5'
10.56	443	41.94	49	52
6.92	443	64.01	75	80
5.15	443	86.07	100	107
3.26	443	135.85	149	162
2.54	443	174.67	202	213

* Power consumption for the 400 W HPS fixture with magnetic ballast from the manufacturer Sunlight Supply (Nelson & Bugbee, 2013).

These data show a strong linear relationship between power per area and lighting intensity for both cases of mounting height, which serves as validation of the assumption expressed in Equation 8.5. For each case of mounting height, the slope of the line in Figure 8.1 is the corresponding λ value:

$$\lambda_{8ft} = 0.8761 (W/m^2)/(\mu mol/m^2 \cdot sec) = 0.8761 W \cdot s/\mu mol$$

$$\lambda_{5ft} = 0.8216 W \cdot s/\mu mol$$

Once the mounting height is specified, to find the lighting energy use for this 1 acre greenhouse only the values of the lighting intensity and duration of lighting period are needed. As an example, to calculate the lighting energy use for the case

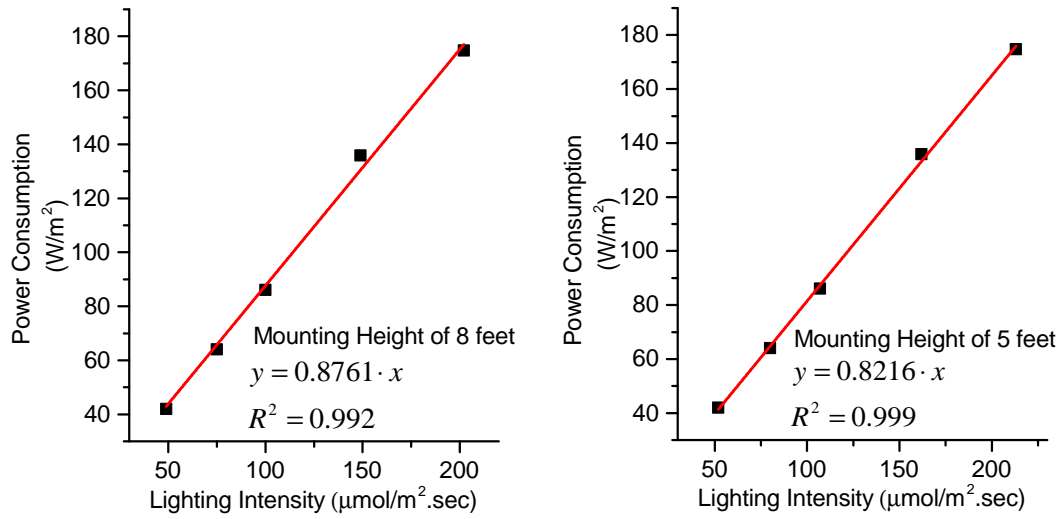


Figure 8.1: Power per area vs. lighting intensity for two cases of mounting height.

of a mounting height of 8 feet and a constant lighting intensity of $100 \mu\text{mol}/\text{m}^2 \cdot \text{sec}$ during 24 hours:

$$\begin{aligned}
 E &= 0.8761 (W \cdot s/\mu\text{mol}) \cdot 100 (\mu\text{mol}/\text{m}^2 \cdot \text{sec}) \cdot 24 (h) \cdot 1 (\text{acre}) \cdot 4046.86 (\text{m}^2/\text{acre}) \\
 &= 3545.45 (W \cdot \text{m}^2 \cdot \text{sec}/\mu\text{mol}) \cdot 2400 (h \cdot \mu\text{mol}/\text{m}^2 \cdot \text{sec}) \\
 &= 8.51 (MWh)
 \end{aligned} \tag{8.15}$$

Since ρ is a constant for the greenhouse for a given mounting height ($\rho = 3545.45 W \cdot \text{m}^2 \cdot \text{sec}/\mu\text{mol}$ for the present example where the mounting height is 8 feet), only the value of the lighting energy use metric, E_m ($E_m = 2400 h \cdot \mu\text{mol}/\text{m}^2 \cdot \text{sec}$ in the present case), is needed to calculate the total lighting energy use for the greenhouse.

A similar analysis applies to the calculation of the lighting energy cost. Using the same example, assuming that the electricity price is constant during the 24 hour period of lighting and equal to $100 \$/MWh$:

$$\begin{aligned}
C &= 3545.45 (W \cdot m^2 \cdot sec/\mu mol) \cdot 2400 (h \cdot \mu mol/m^2 \cdot sec) \cdot 100 \$/MWh = \\
&= 3545.45 (W \cdot m^2 \cdot sec/\mu mol) \cdot 240000 (\$ \cdot \mu mol/MW \cdot m^2 \cdot sec) \quad (8.16) \\
&= 851 (\$)
\end{aligned}$$

Again, since $\rho = 3545.45 W \cdot m^2 \cdot sec/\mu mol$ is constant, only the value of the lighting energy cost metric, C_m ($C_m = 240000 \$ \cdot \mu mol/MW \cdot m^2 \cdot sec$ in the present case), is needed to calculate the total lighting energy cost for the greenhouse.

Cost adjustment for inflation

To make the cost comparable throughout the different simulation years, it is adjusted for inflation to year 2000 dollars using historic Consumer Price Index (CPI) values reported by the Bureau of Labor Statistics (*Archived Consumer Price Index Detailed Report Information*, 2012). The Bureau of Labor Statistics reports different electricity CPI values for the *New York-Northern New Jersey-Long Island* and *Philadelphia-Wilmington-Atlantic City* regions. Because the PJM service area encompasses both regions, the electricity CPI value used was an average of the values reported for these two regions. Although the electricity CPI values reported by the Bureau of Labor Statistics refer to urban consumers, in the present project it is assumed that they reflect the variation of electricity prices in the wholesale power market.

The inflation adjustment is an attempt to remove the effect of inflation so that the lighting cost reflects only the effect of the different strategies to provide supplemental lighting. Because of the challenges of accurately accounting for the electricity inflation rate in the wholesale market, the lighting cost results expressed in dollars show a relatively high standard deviation (close to 20%). On the other hand, the effect of inflation is completely removed from the lighting cost results expressed as a ratio of the lighting cost from the DSS to the lighting cost from a Reference Case (the

Reference Case will be introduced in the following sections).

Radiation usage metrics

The cumulative values of solar radiation, supplemental lighting, and blocked solar radiation during the crop growth period are also used as metrics to evaluate the performance of the DSS. The cumulative values of solar radiation serve as reference level to compare the cumulative values of supplemental lighting and blocked solar radiation during the crop growth period. Large values of cumulative supplemental lighting when the goals are short crop growth period and high yield are indicative of high effectiveness at using supplemental lighting. Large values of blocked solar radiation when the goals are long crop growth period and low yield are indicative of high effectiveness at using the shading system (this purely theoretical scenario will be introduced in the following sections).

8.2 Performance of the DSS while Providing Supplemental Lighting. Minimum Time from Sowing to Final Harvest and Maximum Crop Yield Targets.

The DSS system is designed to handle the general case when the light intensity from the supplemental lighting system can vary from a minimum to a maximum value (explained in section 7.3.5). The cases when the light intensity from the supplemental lighting system is fixed at a certain value (non-dimmable lights) and when it varies from zero to a maximum value (dimmable lights) are particular cases of the general one and both are simulated to test the performance of the DSS for providing supplemental lighting (lighting simulations).

As was explained in Chapter 7, the sensitivity to electricity prices is an input variable that provides the possibility of defining the level of cost optimization. At 100% price sensitivity the ranking of the future hours is solely based on the electricity

prices and maximum emphasis is placed on cost optimization at achieving the crop timing and yield targets. At 0% price sensitivity the ranking of the future hours is solely based on their proximity to the present and maximum emphasis is placed on immediacy at achieving the crop timing and yield targets.

The lighting simulations evaluated three levels of sensitivity to electricity prices (0, 50, and 100 %) for both the non-dimmable and dimmable lighting cases. For each of the resulting six cases, the lighting simulations comprise seven values of supplemental lighting intensity: 0, 50, 100, 150, 200, 250, and 300 $\mu mol/m^2 \cdot sec$ measured at the top of the crop canopy. In the case of dimmable lights the previous lighting intensities refer to the maximum value. Supplemental light intensities above 200 $\mu mol/m^2 \cdot sec$ are uncommon in the greenhouse industry because of the installation and operation costs and the challenges of managing the excess heat that is generated in those cases. The simulations include supplemental lighting intensity above 200 $\mu mol/m^2 \cdot sec$ for theoretical purposes only.

Besides the previous settings for the DSS, the lighting simulations include a Standard or Reference Case to which the results from the DSS are compared. There are no rules to implement the standard lighting and screen control strategies but some guiding principles may be followed:

1. To minimize lighting cost, the lighting window includes as many off peak hours as possible (considering the dark period constraint of a minimum of 6 hours of darkness)
2. To avoid equipment cycling (turn lights on and off or deploy and retract the shade screens frequently during cloudy days), lights are turned on or the shade screens are opened after light levels remain below a minimum threshold during certain amount of time (activation or proving period).
3. Also to avoid equipment cycling, the decision taken about the lights or the shade screens remains valid for a minimum period of time (minimum on time).

4. To avoid conflicting operations of the lighting and the shade screens (lights on when the shade screen is deployed during day time hours) the lighting and shade screen set points followed an appropriate order.

The lighting and shading set points used in the Reference Case when the targets are minimum time from sowing to final harvest and maximum crop yield were chosen following the control strategies commonly used in the industry (*Light and Lighting Control in Greenhouses*, 2010) and those used for tomato crops at the Rutgers New Jersey Agricultural Experiment Station (NJAES) and the Rutgers Ecocomplex Research and Demonstration Greenhouse.

Reference Case or Standard lighting and shading strategy when the targets are minimum time from sowing to final harvest and maximum crop yield:

1. System: lights non-dimmable and one single shade screen
2. Lighting window: allow the lights to be turned on only during the 18 consecutive hours starting six hours after sunset. The goals of this lighting window are to guarantee 6 hours of dark period (Demers et al., 1998; McAvoy et al., 1989) and maximize off peak hours.
3. Allow shade screens to open during daytime and close during nighttime hours (for temperature control purposes).
4. Open shade screens set point: open shade screens for the next hour if the average outside PAR flux has been below $1200 \mu\text{mol}/\text{m}^2 \cdot \text{sec}$ during the previous hour.
5. Lights on set point: turn lights on for the next hour if average outside PAR flux has been below $800 \mu\text{mol}/\text{m}^2 \cdot \text{sec}$ during the previous hour.
6. Lights off set point: turn lights off for the next hour if average outside PAR flux is above $1000 \mu\text{mol}/\text{m}^2 \cdot \text{sec}$ during the previous hour.

7. Close shade screens for the next hour if the outside PAR flux is above $1500 \mu\text{mol}/\text{m}^2 \cdot \text{sec}$ at any time (for temperature control purposes).

For all lighting simulations, the lighting system for the Reference Case was composed of non-dimmable lamps, and the shading system for both the DSS and the Reference Case consisted of a single shade screen able to block 50% of the direct and diffuse radiation when fully deployed.

The performance of the DSS at achieving minimum time from sowing to final harvest and maximum crop yield is tested during the summer and winter months (summer months: June (second half), July, August, September (first half), winter months: December (second half), January, February, March (first half)) during each simulation year with the goal of comparing the effect of extreme seasons (with respect to cumulative solar radiation received during the period) on the different metrics previously defined. Figures 8.2 to 8.17 show the results for the lighting simulations.

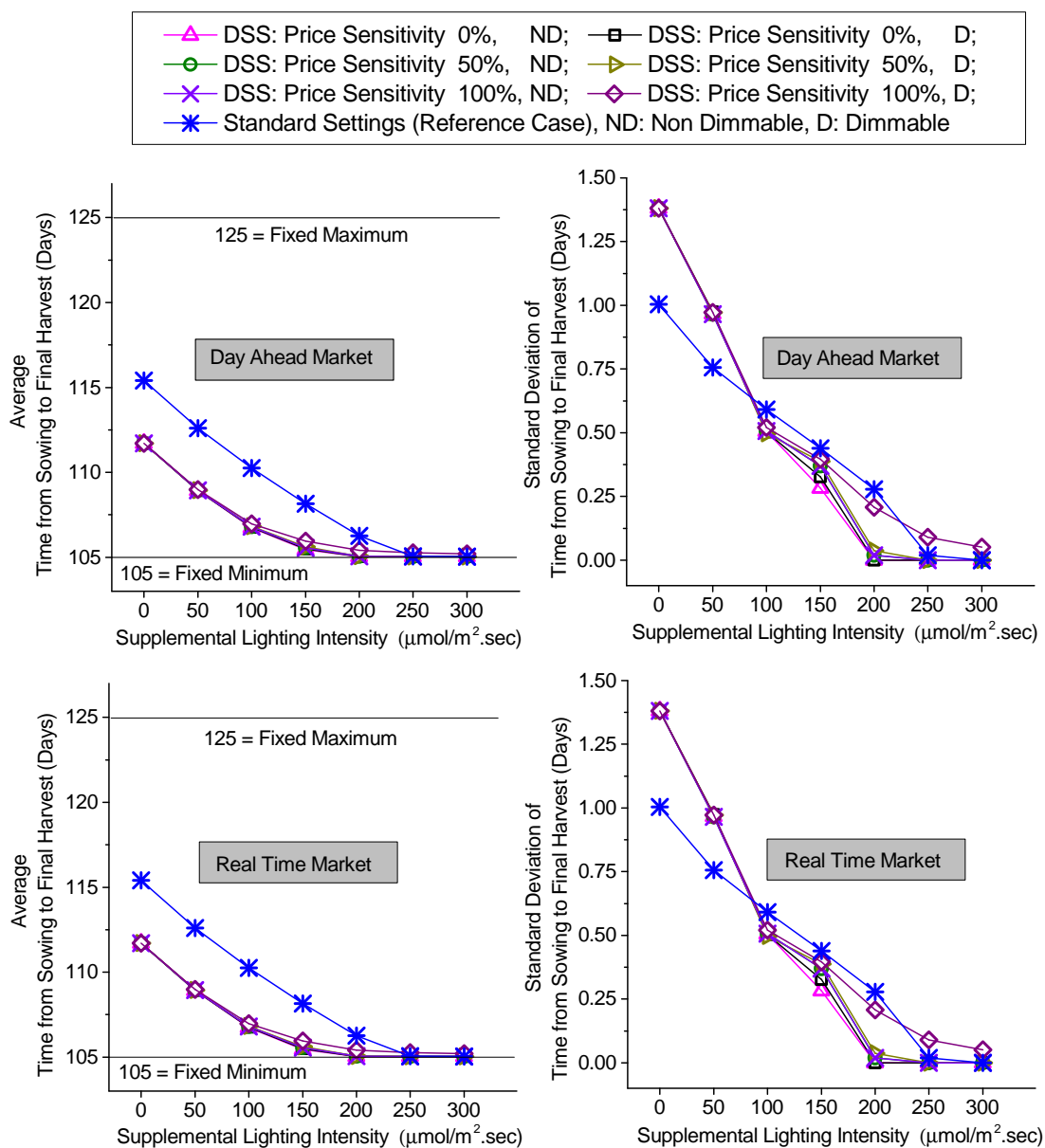


Figure 8.2: Average and standard deviation of time from sowing to final harvest. Time periods of simulations start on June 15th of each year from 2000 through 2004. The lighting system for the Reference Case consisted of non-dimmable lamps. The Shading system for DSS and Reference Case consisted of a single screen able to block 50% of the direct and diffuse radiation when fully deployed.

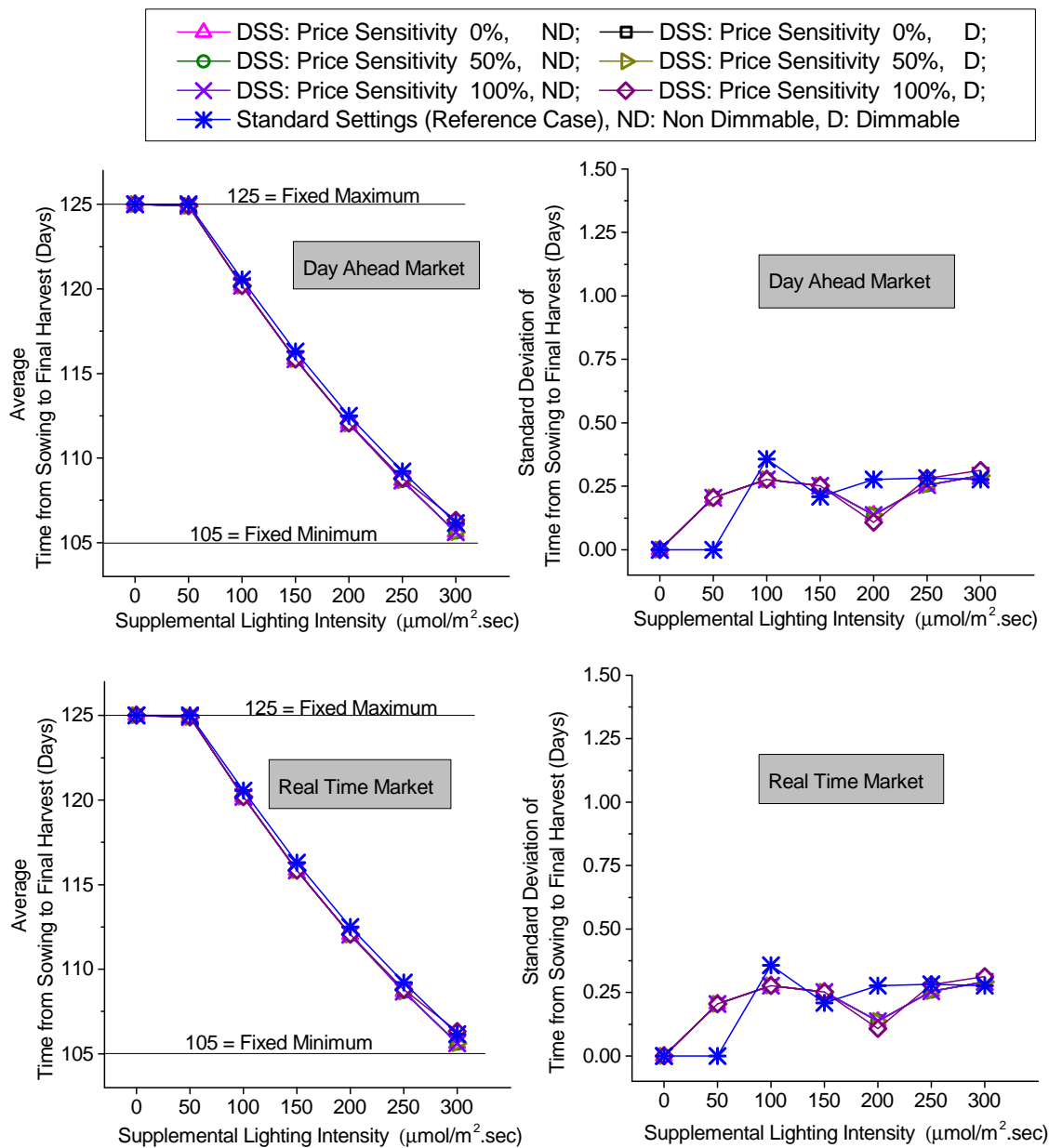


Figure 8.3: Average and standard deviation of time from sowing to final harvest. Time periods of simulations start on December 15th of each year from 2000 through 2004. The lighting system for the Reference Case consisted of non-dimmable lamps. The Shading system for DSS and Reference Case consisted of a single screen able to block 50% of the direct and diffuse radiation when fully deployed.

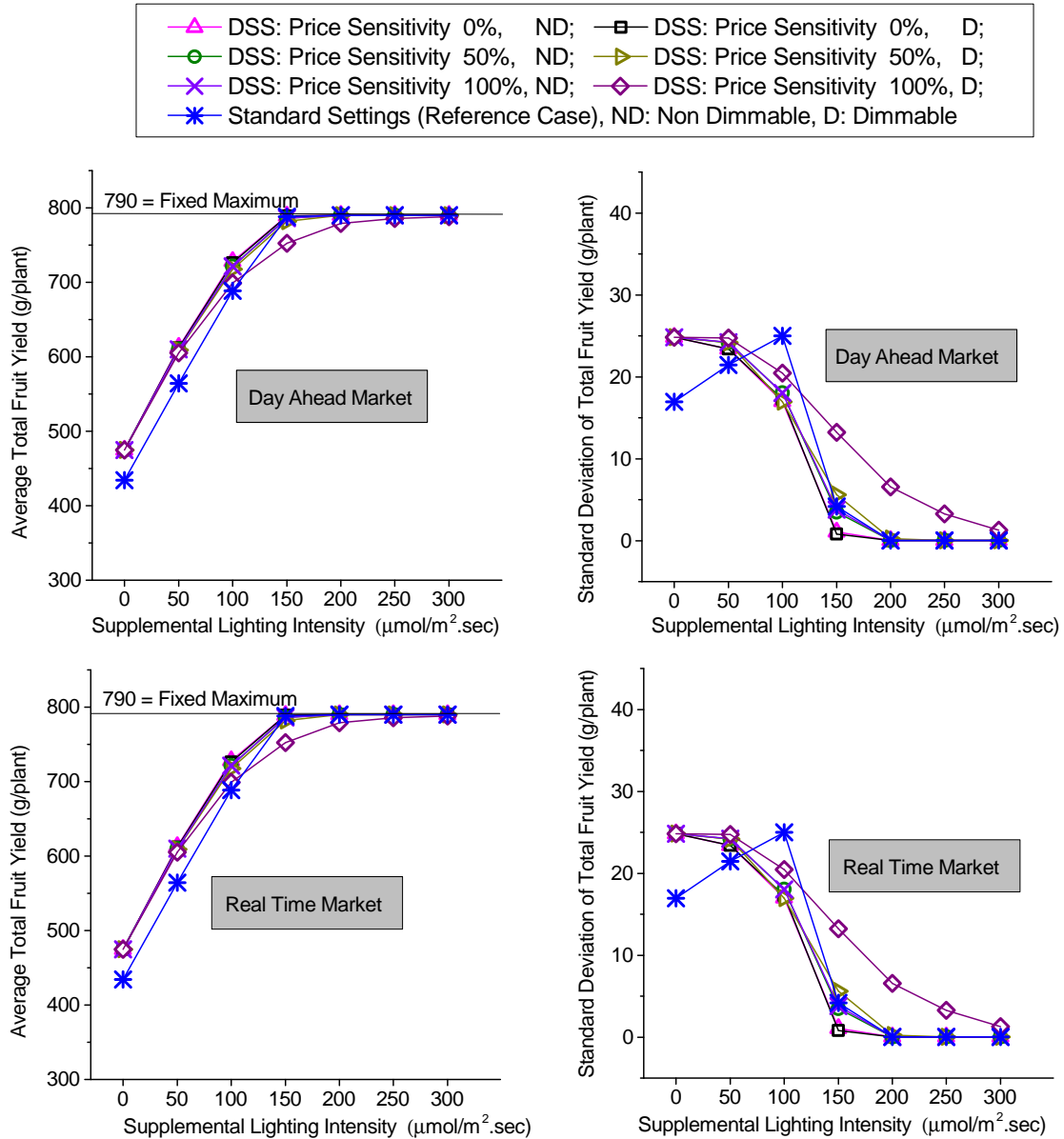


Figure 8.4: Average and standard deviation of total fruit yield. Time periods of simulations start on June 15th of each year from 2000 through 2004. The lighting system for the Reference Case consisted of non-dimmable lamps. The Shading system for DSS and Reference Case consisted of a single screen able to block 50% of the direct and diffuse radiation when fully deployed.

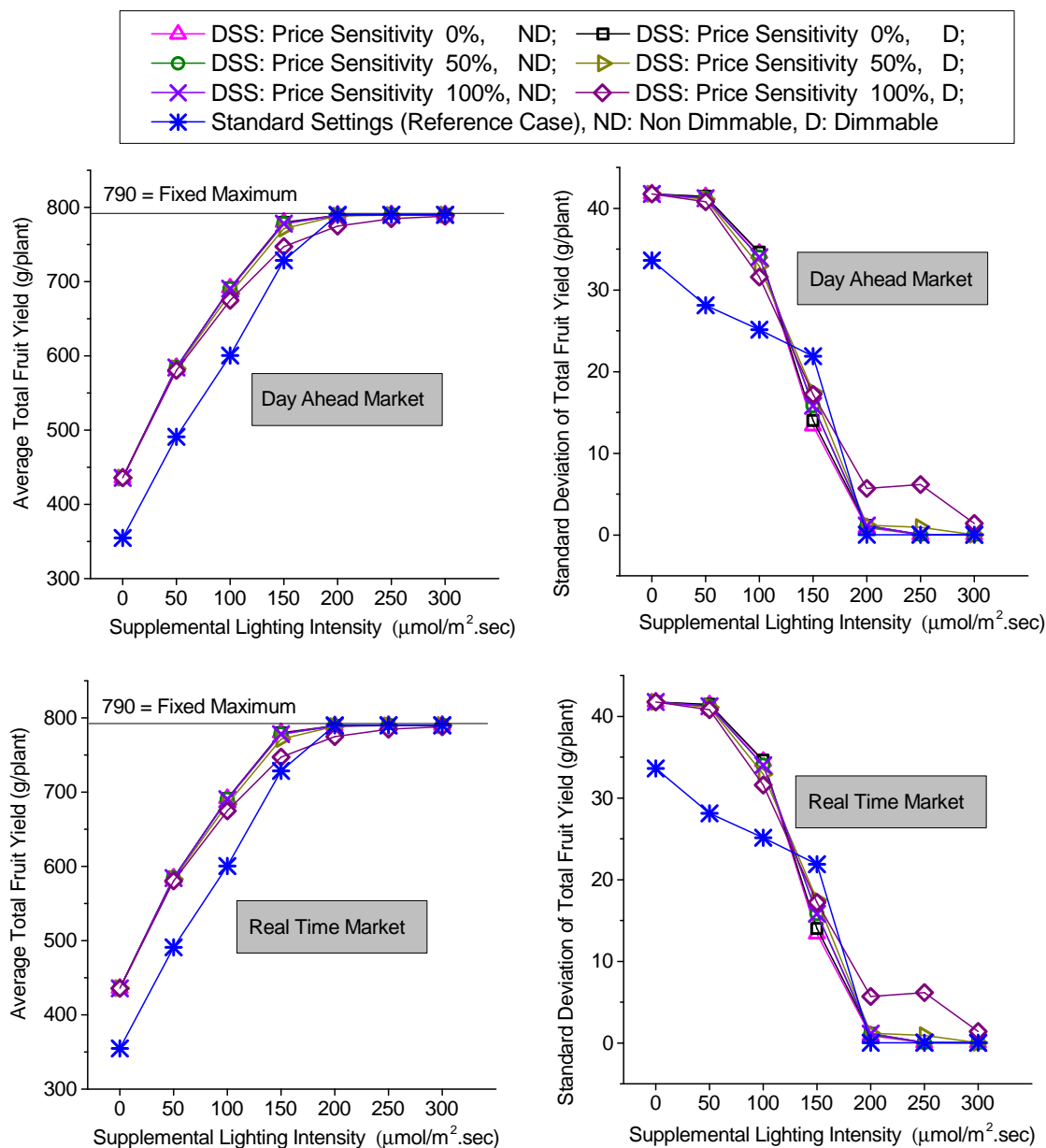


Figure 8.5: Average and standard deviation of total fruit yield. Time periods of simulations start on December 15th of each year from 2000 through 2004. The lighting system for the Reference Case consisted of non-dimmable lamps. The Shading system for DSS and Reference Case consisted of a single screen able to block 50% of the direct and diffuse radiation when fully deployed.

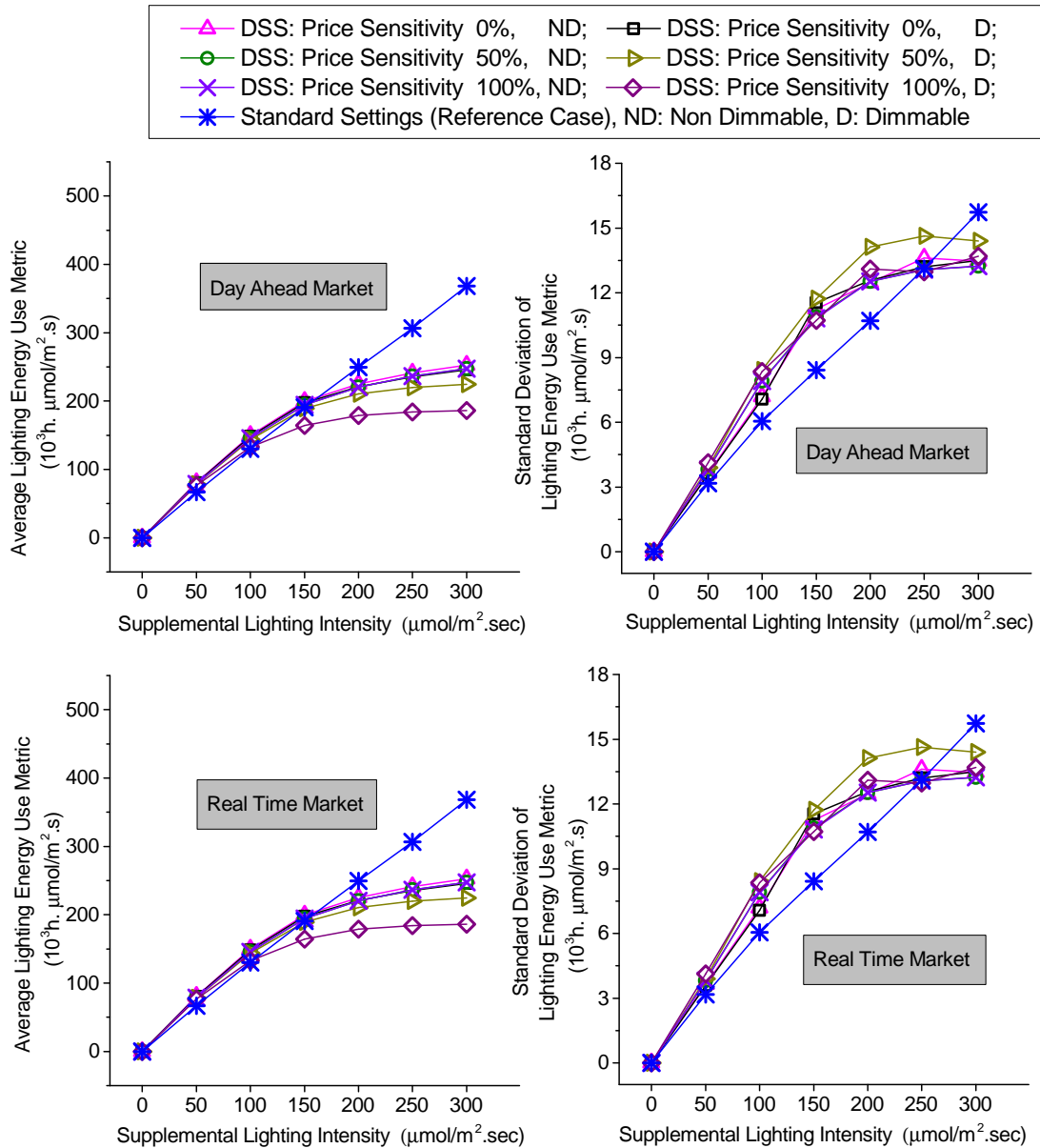


Figure 8.6: Average and standard deviation of lighting energy use. Time periods of simulations start on June 15th of each year from 2000 through 2004. The lighting system for the Reference Case consisted of non-dimmable lamps. The Shading system for DSS and Reference Case consisted of a single screen able to block 50% of the direct and diffuse radiation when fully deployed.

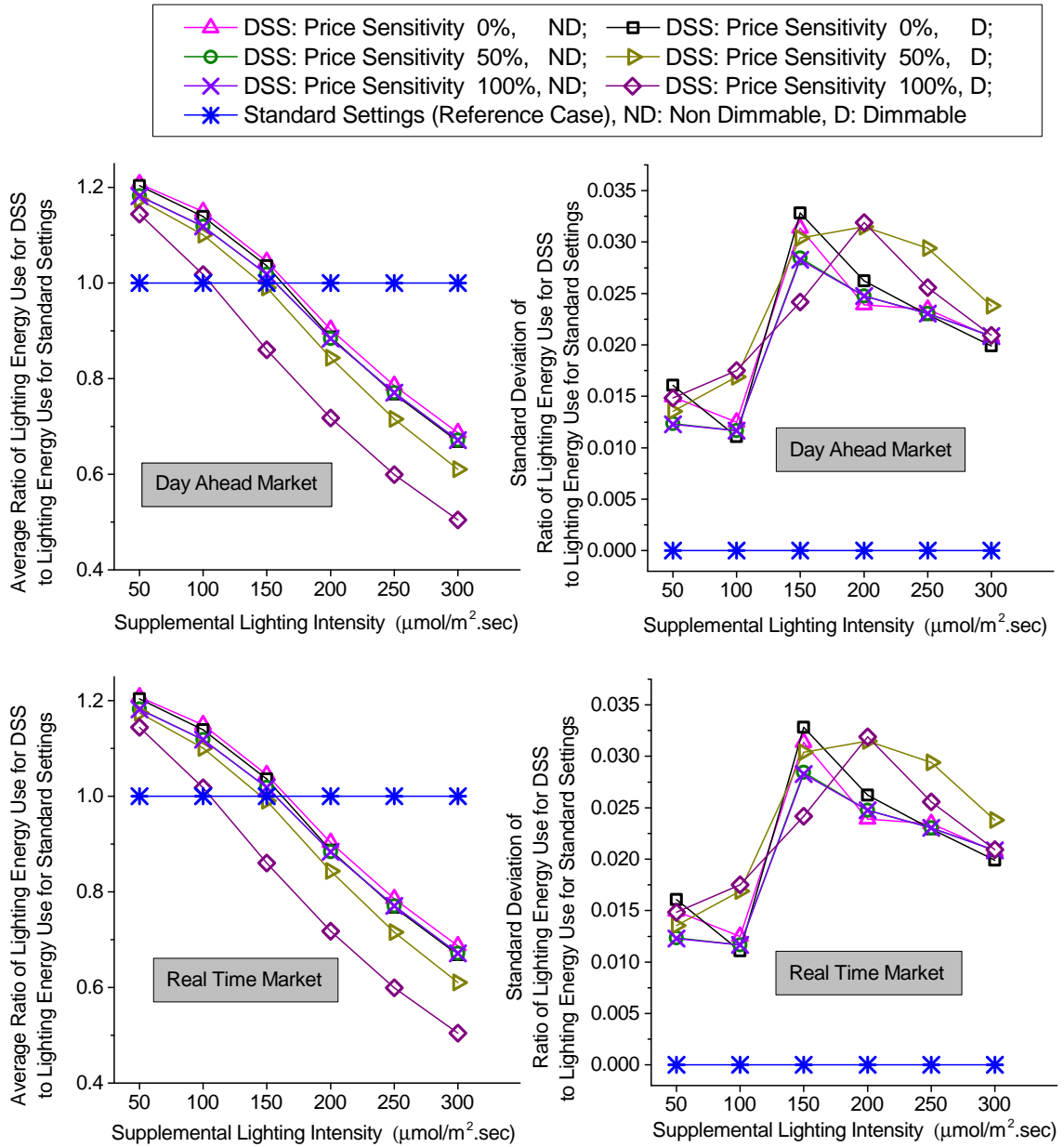


Figure 8.7: Average and standard deviation of the ratio of the lighting energy use for the DSS to the lighting energy use for the Reference Case. Time periods of simulations start on June 15th of each year from 2000 through 2004. The lighting system for the Reference Case consisted of non-dimmable lamps. The Shading system for DSS and Reference Case consisted of a single screen able to block 50% of the direct and diffuse radiation when fully deployed.

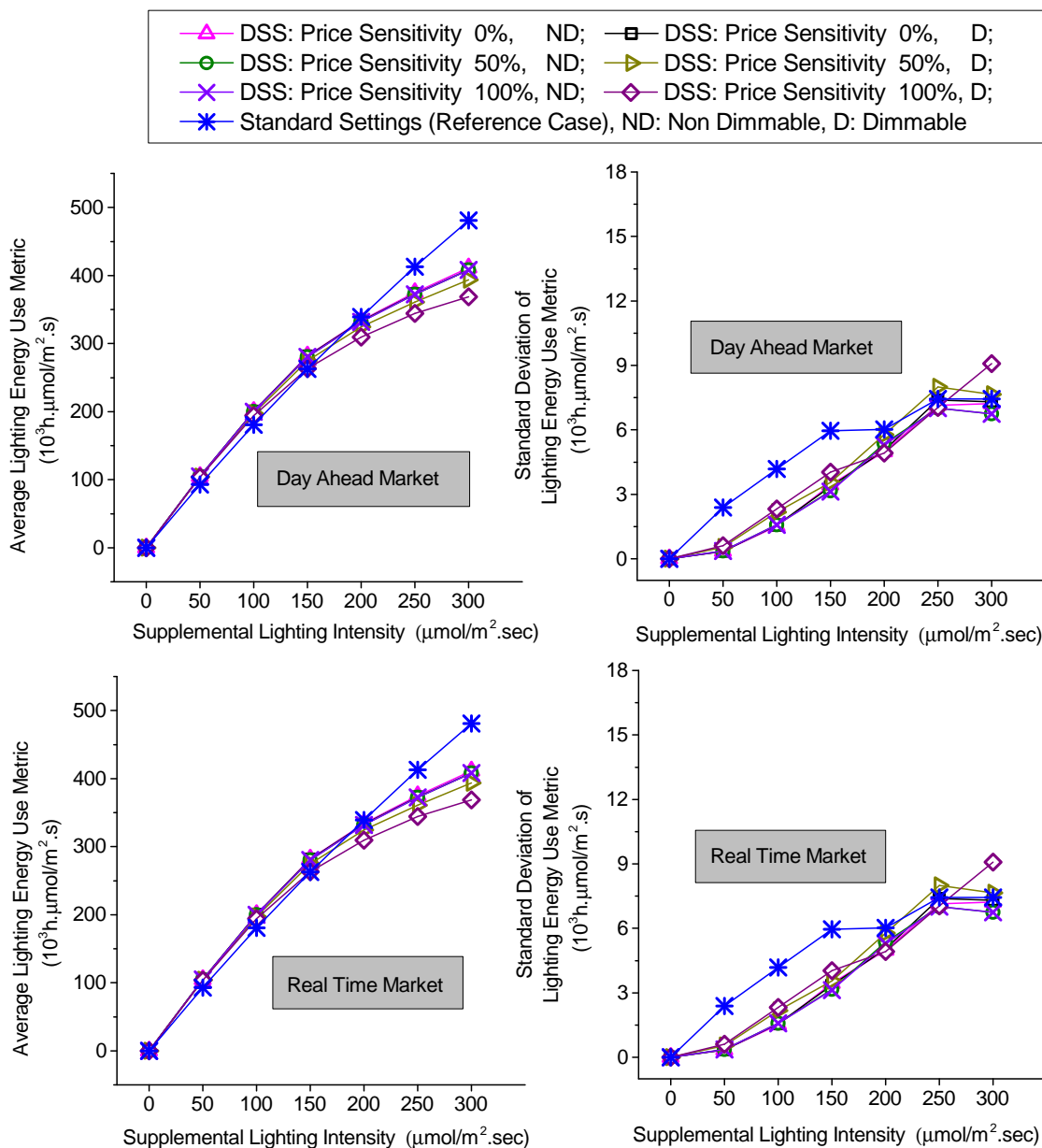


Figure 8.8: Average and standard deviation of lighting energy use. Time periods of simulations start on December 15th of each year from 2000 through 2004. The lighting system for the Reference Case consisted of non-dimmable lamps. The Shading system for DSS and Reference Case consisted of a single screen able to block 50% of the direct and diffuse radiation when fully deployed.

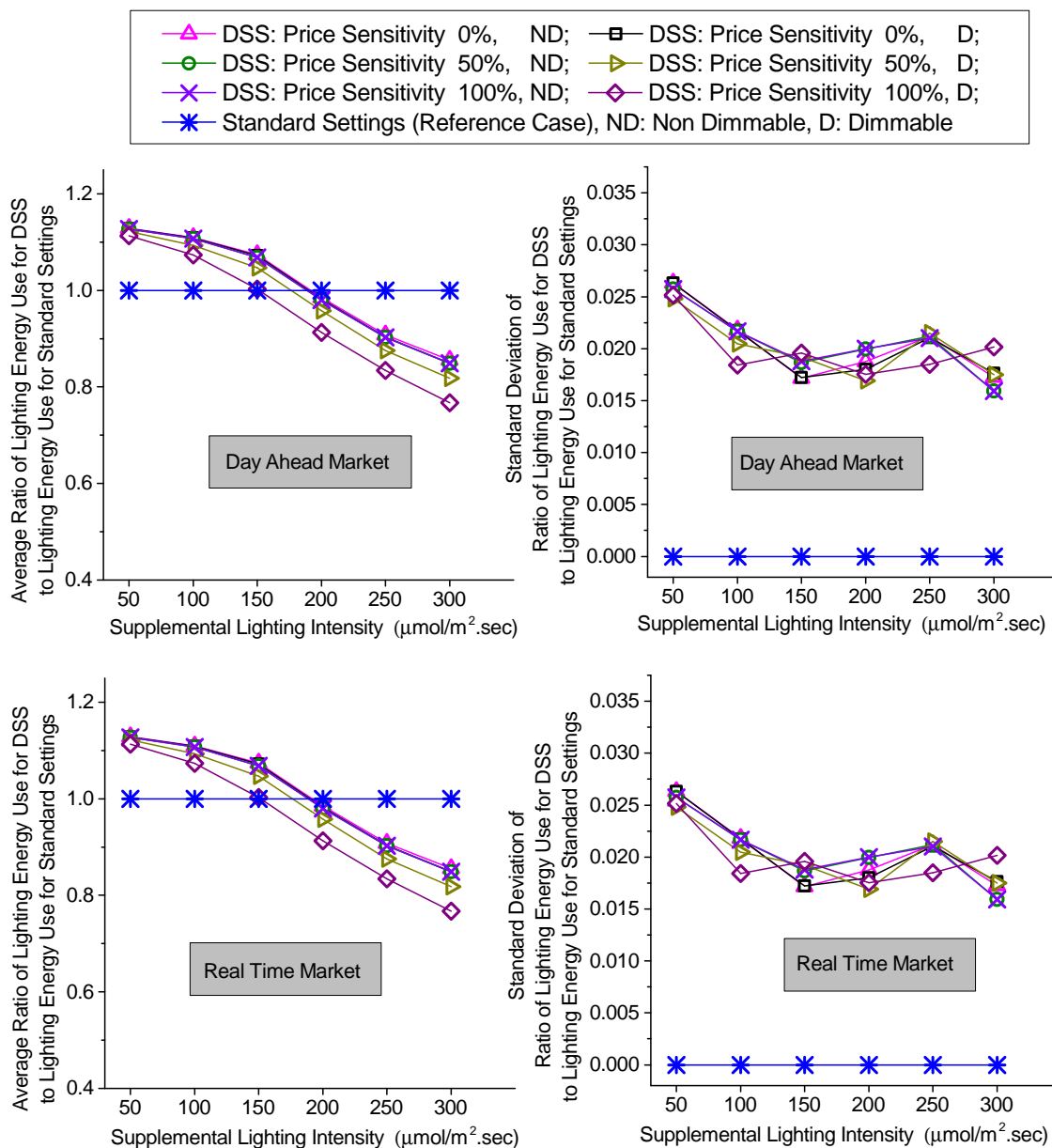


Figure 8.9: Average and standard deviation of the ratio of the lighting energy use for the DSS to the lighting energy use for the Reference Case. Time periods of simulations start on December 15th of each year from 2000 through 2004. The lighting system for the Reference Case consisted of non-dimmable lamps. The Shading system for DSS and Reference Case consisted of a single screen able to block 50% of the direct and diffuse radiation when fully deployed.

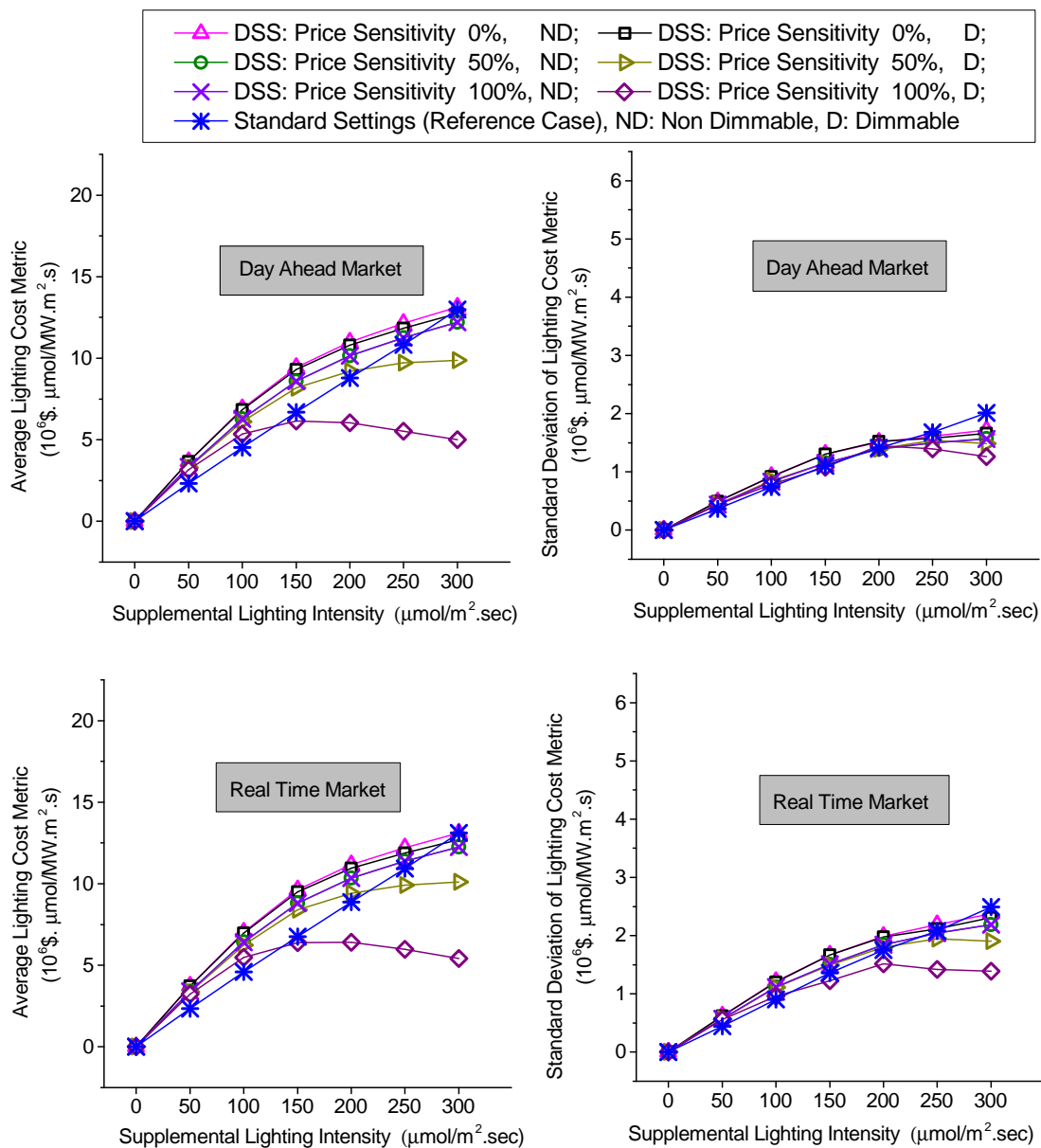


Figure 8.10: Average and standard deviation of lighting cost. Cost adjusted for inflation to year 2000 dollars. Simulation periods start on June 15th of each year from 2000 through 2004. The lighting system for the Reference Case consisted of non-dimmable lamps. The Shading system for DSS and Reference Case consisted of a single screen able to block 50% of the direct and diffuse radiation when fully deployed.

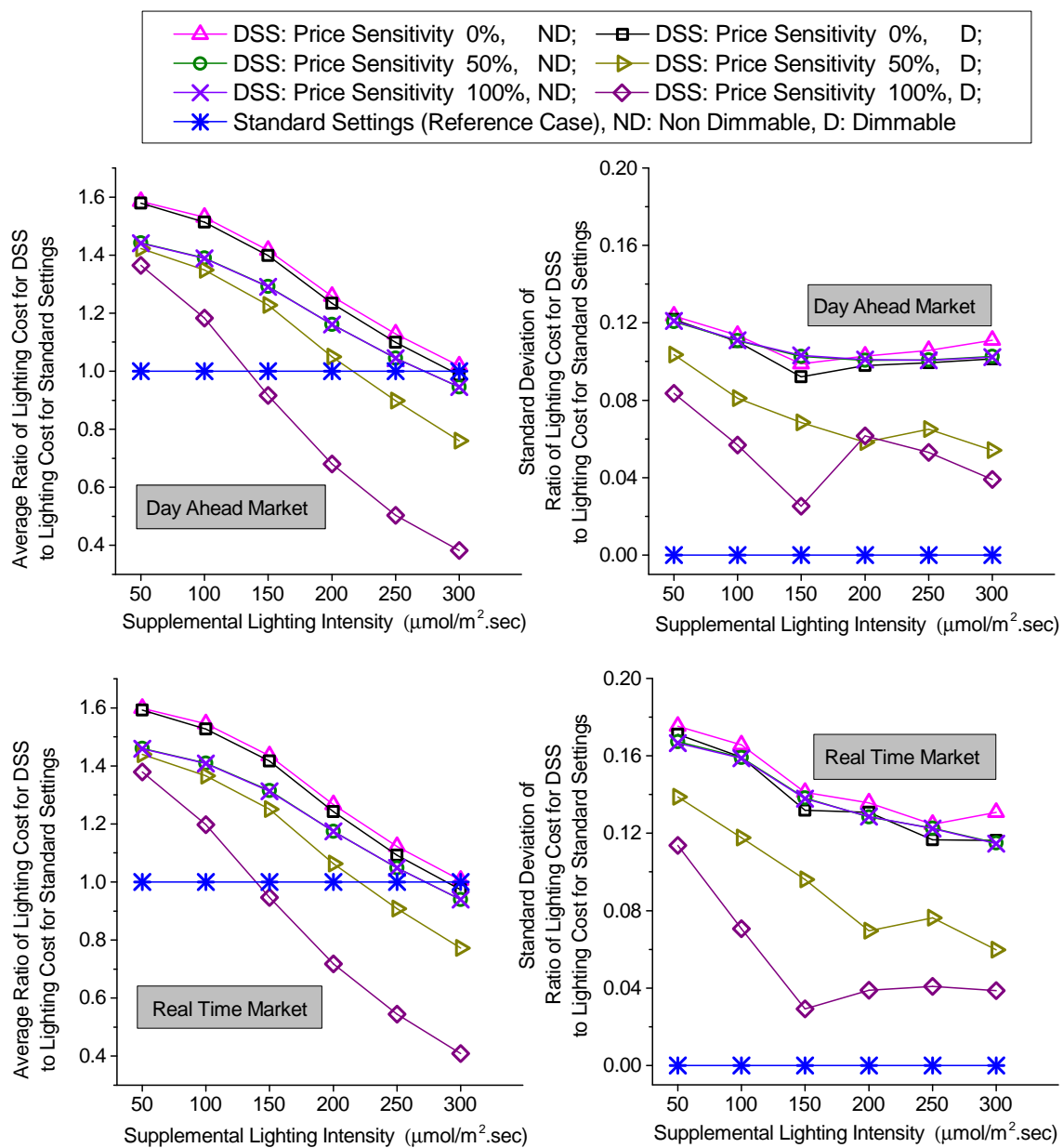


Figure 8.11: Average and standard deviation of the ratio of the lighting cost for the DSS to the lighting cost for the Reference Case. Simulation periods start on June 15th of each year from 2000 through 2004. The lighting system for the Reference Case consisted of non-dimmable lamps. The Shading system for DSS and Reference Case consisted of a single screen able to block 50% of the direct and diffuse radiation when fully deployed.

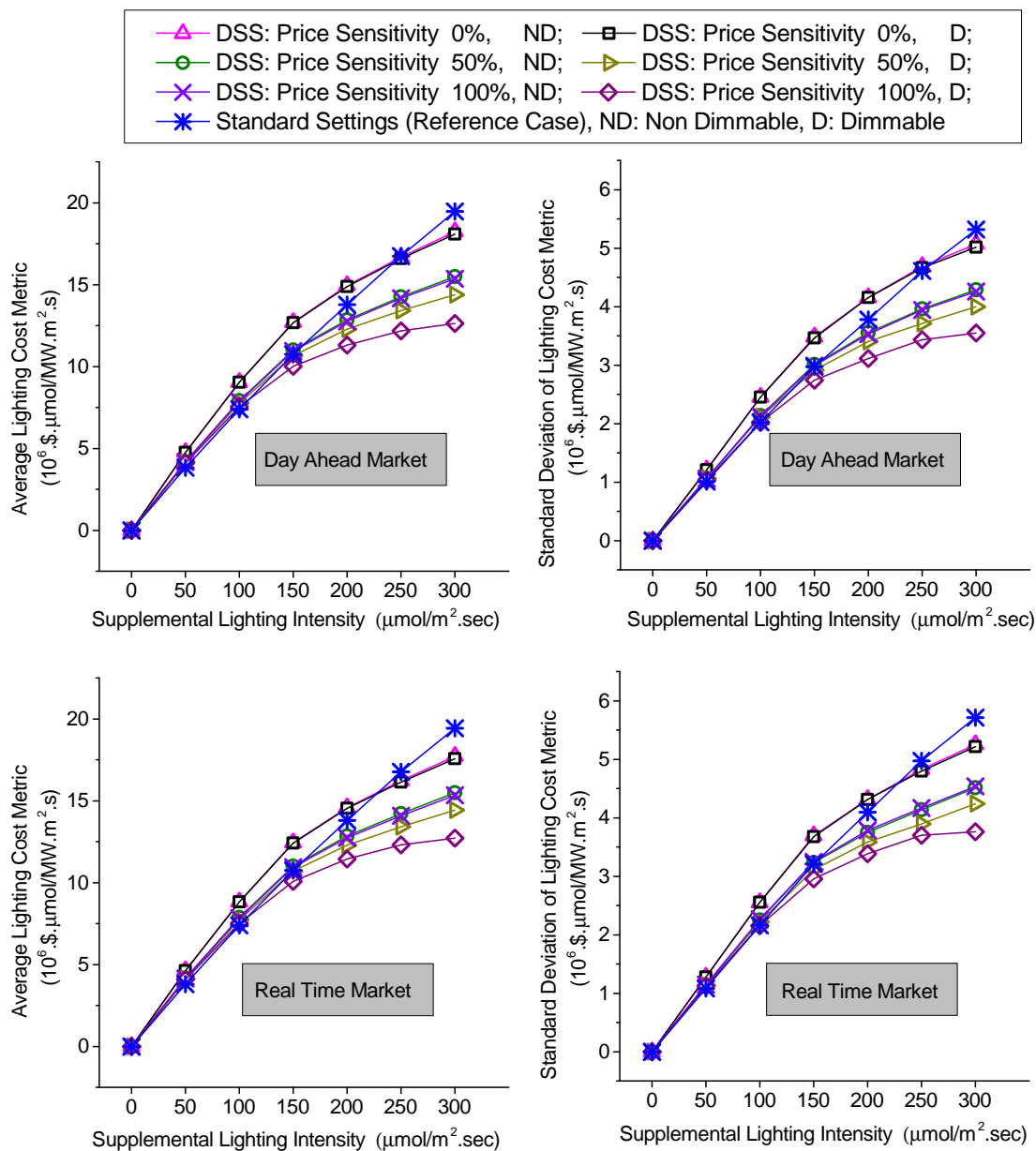


Figure 8.12: Average and standard deviation of lighting cost. Cost adjusted for inflation to year 2000 dollars. Simulation periods start on December 15th of each year from 2000 through 2004. The lighting system for the Reference Case consisted of non-dimmable lamps. The Shading system for DSS and Reference Case consisted of a single screen able to block 50% of the direct and diffuse radiation when fully deployed.

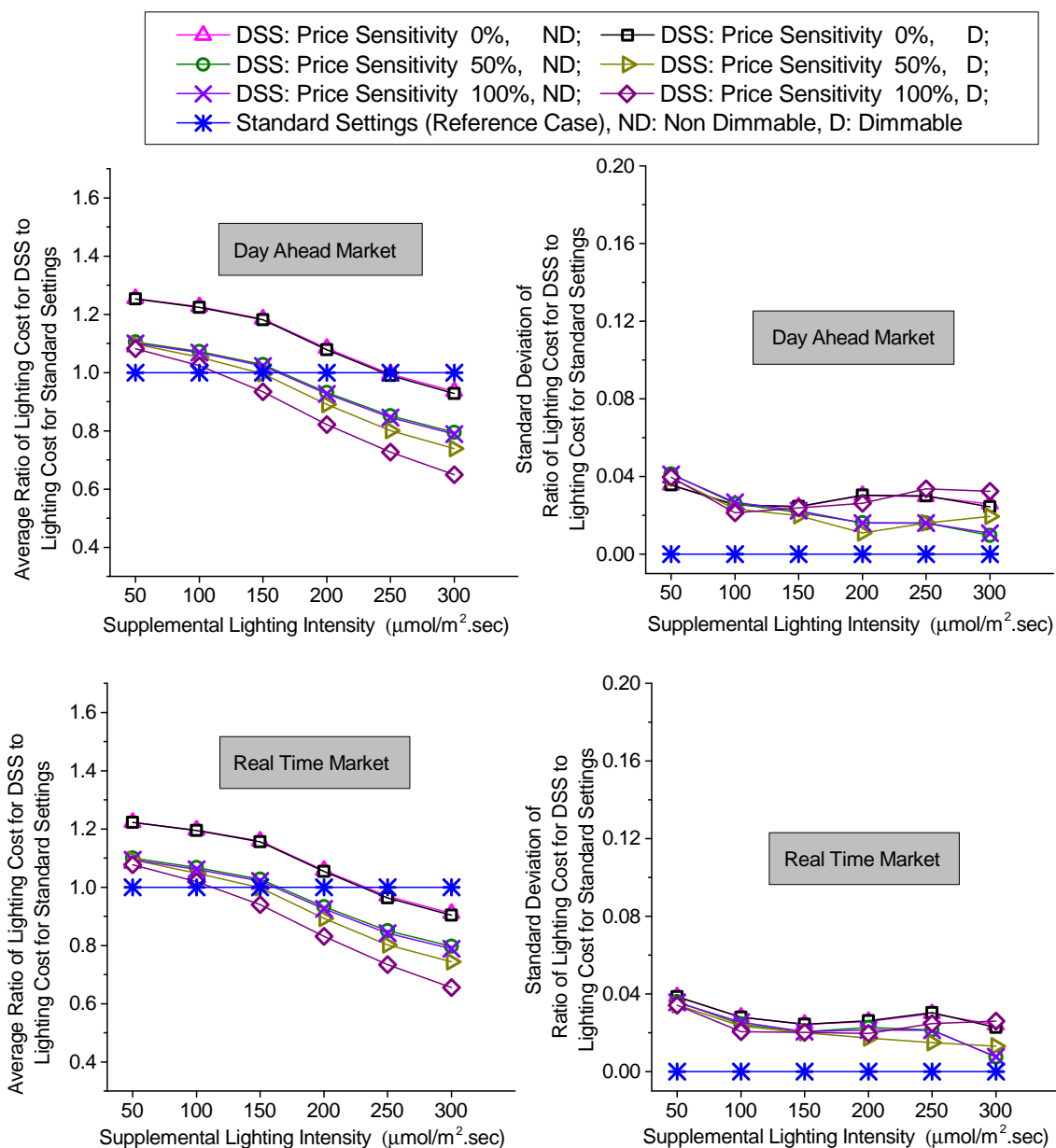


Figure 8.13: Average and standard deviation of the ratio of the lighting cost for the DSS to the lighting cost for the Reference Case. Simulation periods start on December 15th of each year from 2000 through 2004. The lighting system for the Reference Case consisted of non-dimmable lamps. The Shading system for DSS and Reference Case consisted of a single screen able to block 50% of the direct and diffuse radiation when fully deployed.

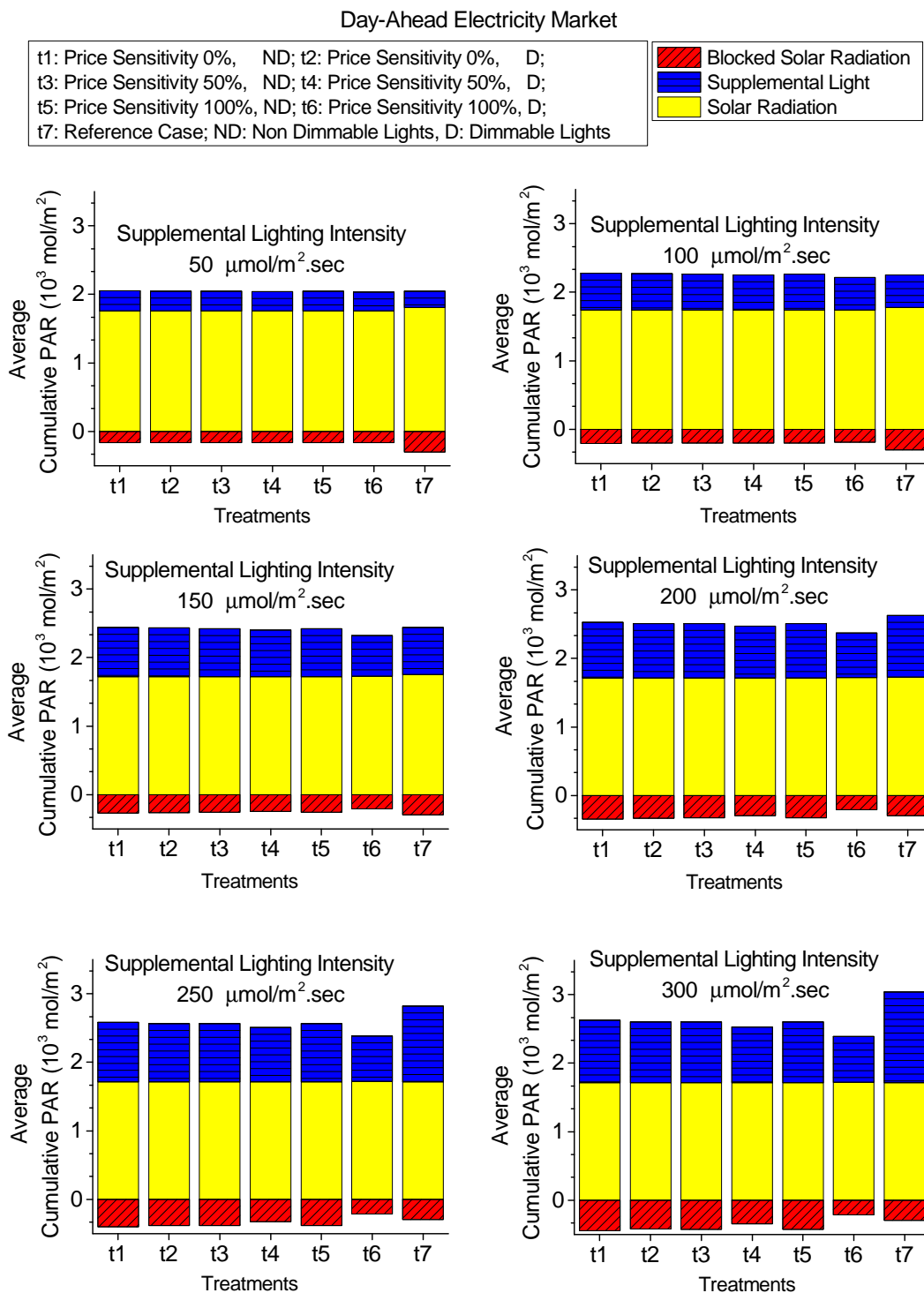


Figure 8.14: Radiation Budget. Lighting Simulations during Summer. Day-Ahead Market.

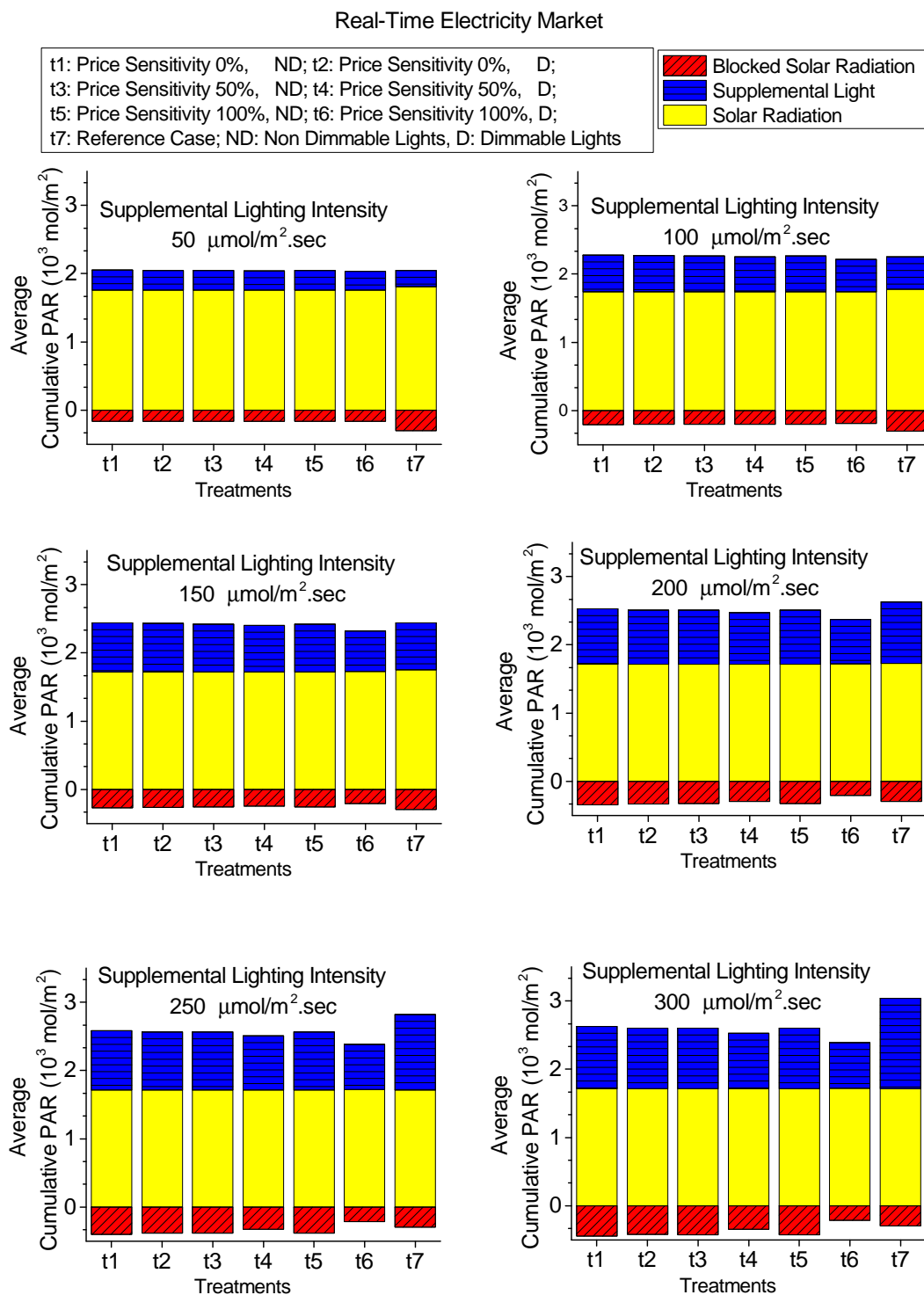


Figure 8.15: Radiation Budget. Lighting Simulations during Summer. Real-Time Market.

Day-Ahead Electricity Market

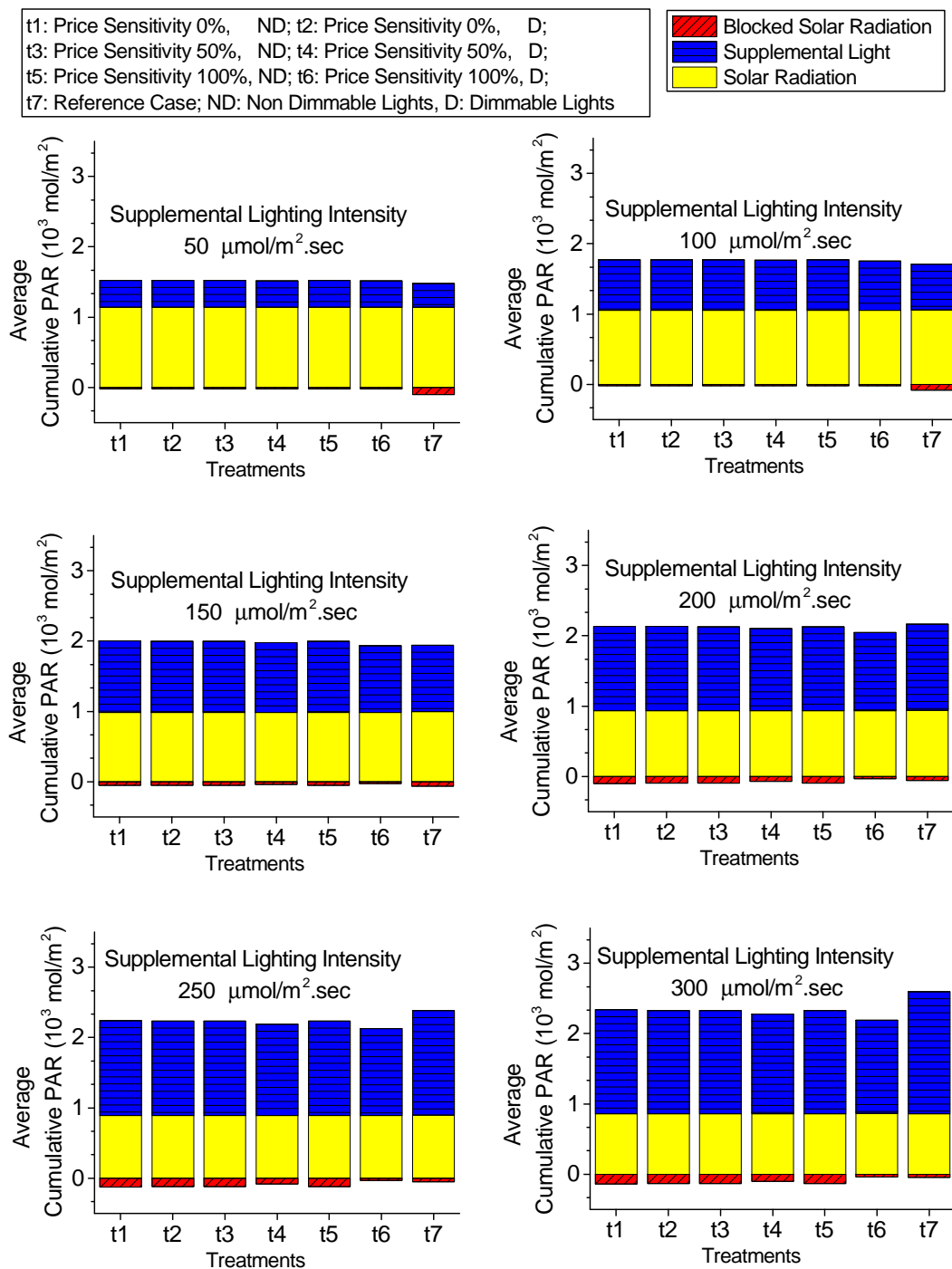


Figure 8.16: Radiation Budget. Lighting Simulations during Winter. Day-Ahead Market.

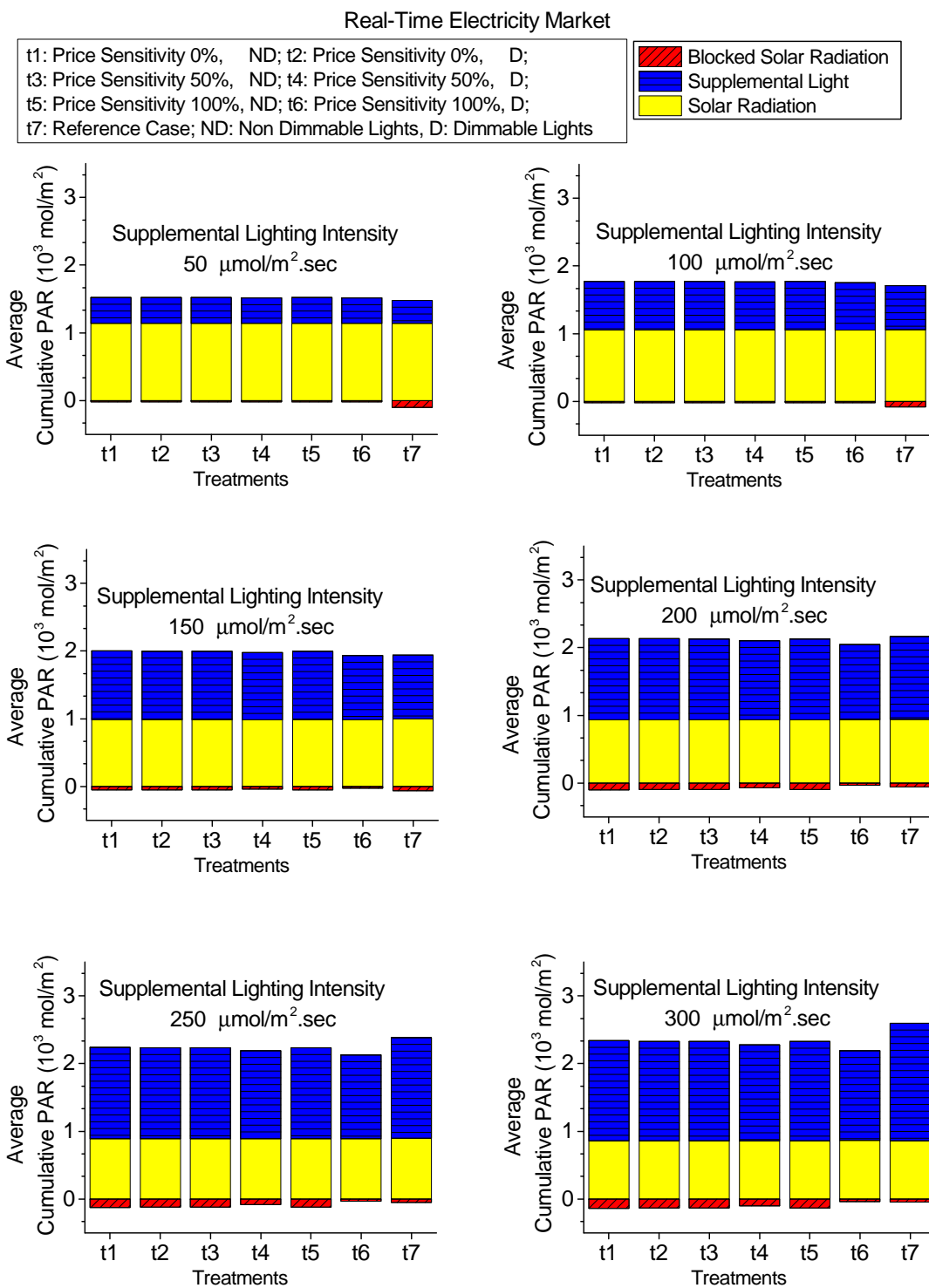


Figure 8.17: Radiation Budget. Lighting Simulations during Winter. Real-Time Market.

8.3 Performance of the DSS while Using the Shade Screens for the Hypothetical case of Maximum Time from Sowing to Final Harvest and Minimum Crop Yield Targets.

Although the shading system in a greenhouse typically consists of a single shade screen and in some cases of two (more than three shade screens is highly unlikely), the DSS system is designed to handle the general case when the shading system contains any number of shade screens. The simulations to test the performance of the DSS at using the shade screens (shading simulations) include the cases when the shading system is composed of 1, 2, and 3 identical shade screens (the term *identical screens* is used to indicate that each screen blocks the same amount of incoming light. When multiple screens are used in a real greenhouse, it is likely that each shade screen will have a different percent of shading). For each of these three screen configurations (shading system composed of 1, 2, or 3 identical screens) the shading simulations comprise the cases when the percentage of direct and diffuse radiation that each screen blocks is the same and equal to 0, 20, 40, 60, or 80 (for a total of 15 shading simulation runs for each year from 2000 through 2004).

The shading simulations are performed only during the summer months (June (second half), July, August, September (first half)) when the solar radiation is maximum and achieving maximum time from sowing to final harvest and minimum crop yield requires active use of the shading system. It is common to use the shade screens for both shading and energy conservation. In the present project, however, it is assumed that the shade screens are used solely for shading and for that reason the effect that the use of the shade screens for energy conservation may have in the current results is not analyzed.

When the shade screens are also used for energy conservation, solar radiation is not the only environmental factor that needs to be considered for their control, but also temperature. However, it is not expected that the use of the shade screens for

energy conservation may have a strong effect on the present simulation results because the shading simulations take place during the summer, when high temperatures and high solar radiation are correlated and deploying the shade screens for cooling and shading purposes tend to coincide.

The shading simulations also include a standard or Reference Case to which the results from the DSS are compared to. Designing the lighting and screen control strategy for the Reference Case when the targets are maximum time from sowing to final harvest and minimum crop yield, a purely theoretical scenario to analyze the performance of the DSS at using the shade screens to block unwanted radiation, requires additional analysis because these goals are opposite to the ones commonly used (minimum time from sowing to final harvest and maximum crop yield) and for which the previous standard lighting and screen control strategy was designed.

For the shading simulations, the control strategies for the Reference Case need to reduce the radiation available to the crop so that the time from sowing to final harvest is maximized and the crop yield is minimized. The radiation available to the crop may be reduced by lowering the set point values at which the shade screens are deployed and the lights are turn on and off (items 3, 4, and 5 from the strategy discussed in section 8.2).

The selection of the new set points in the lighting and shading control strategy for the Reference Case is based on two criteria: the Reference Case should provide results similar to the results provided by the DSS, and the reduction in the radiation available to the crop should not affect the normal development during the vegetative or production stages.

Since the Reference Case utilizes a single shade screen, the results from the DSS corresponding to a single shade screen configuration are used as a benchmark. The single shade screen configuration from the DSS is able to achieve more than 90 % of the time and yield targets when the shade screen is able to block 60 % or more of the solar radiation (Figures 8.18 and 8.19). Considering that the DSS is more flexible

than the Reference Case at controlling both the supplemental lighting and the shade screens and for that reason able to achieve better results, the requirement for the Reference Case is slightly relaxed to 90% of the time and yield targets when the shade screen is able to block 80% instead of 60% of the solar radiation.

As Table 8.2 shows, when the shade screen is able to block 80% of incoming radiation, the control strategies for the Reference Case is already able to achieve 90% of the time and yield targets of the shading simulations if the set point values at which the shade screens are deployed and the lights are turn on and off are $\frac{1}{4}$ of their values in the control strategies for the Reference Case in the lighting simulations. Since those set points already produce the desired results, it is not necessary to reduce their values any further and avoid blocking radiation beyond what is required.

Table 8.2: Performance of Reference Case when the shade screen is able to block 80% of incoming solar radiation and the targets are maximum time from sowing to final harvest and minimum crop yield.

Open Shade Screens Set Point ($\mu\text{mol}/\text{m}^2 \cdot \text{sec}$)	$\frac{1}{2} \cdot 1200$	$\frac{1}{4} \cdot 1200$	$\frac{1}{8} \cdot 1200$
Lights On Set Point ($\mu\text{mol}/\text{m}^2 \cdot \text{sec}$)	$\frac{1}{2} \cdot 800$	$\frac{1}{4} \cdot 800$	$\frac{1}{8} \cdot 800$
Lights Off Set Point ($\mu\text{mol}/\text{m}^2 \cdot \text{sec}$)	$\frac{1}{2} \cdot 1000$	$\frac{1}{4} \cdot 1000$	$\frac{1}{8} \cdot 1000$
Percent of Target Duration	94.13	100	100
Percent of Target Yield	80.15	94.08	98.95

Reference Case or Standard lighting and shading strategy for the theoretical scenario when the targets are maximum time from sowing to final harvest and minimum crop yield:

- System: lights non-dimmable and one single screen.
- Lighting window: allow the lights to be turned on only during the daytime hours. (for the present goals it is not necessary to provide supplemental lighting)

during the nighttime hours).

- Allow to open shade screens during daytime and close during nighttime hours (for temperature control purposes).
- Open shade screens set point: open shade screens for the next hour if the average outside PAR flux has been below $\frac{1}{4} \cdot 1200 \mu\text{mol}/\text{m}^2 \cdot \text{sec}$ during the previous hour.
- Lights on set point: turn lights on for the next hour if average outside PAR flux has been below $\frac{1}{4} \cdot 800 \mu\text{mol}/\text{m}^2 \cdot \text{sec}$ during the previous hour.
- Lights off set point: turn lights off for the next hour if average outside PAR flux is above $\frac{1}{4} \cdot 1000 \mu\text{mol}/\text{m}^2 \cdot \text{sec}$ during the previous hour.
- Deploy screens for the next hour if the outside PAR flux is above $1500 \mu\text{mol}/\text{m}^2 \cdot \text{sec}$ at any time (for temperature control purposes).

The *Percent of Target Duration*, $p(\text{time})$, and *Percent of Target Yield*, $p(\text{yield})$, in Table 8.2 are calculated in the following way:

$$p(\text{time}) = \frac{\text{Time}(\text{days}) - \text{Minimum Time}}{\text{Maximum Time} - \text{Minimum Time}} \cdot 100\% \quad (8.17)$$

$$p(\text{yield}) = \frac{\text{Maximum Yield} - \text{Yield}(\text{g/plant})}{\text{Maximum Yield} - \text{Minimum Yield}} \cdot 100\% \quad (8.18)$$

where:

$$\text{Maximum Time} = 125 \text{ days}$$

$$\text{Minimum Time} = 105 \text{ days}$$

$$\text{Maximum Yield} = 790 \text{ g/plant}$$

$$\text{Minimum Yield} = 52 \text{ g/plant}$$

For all shading simulations the shading system for the Reference Case is composed of a single shade screen and the lighting system for the DSS and Reference Case is composed of dimmable and non-dimmable lamps, respectively, and able to provide a maximum light intensity of $100 \mu mol/m^2 \cdot sec$. Figures 8.18 to 8.25 show the results for the shading simulations.

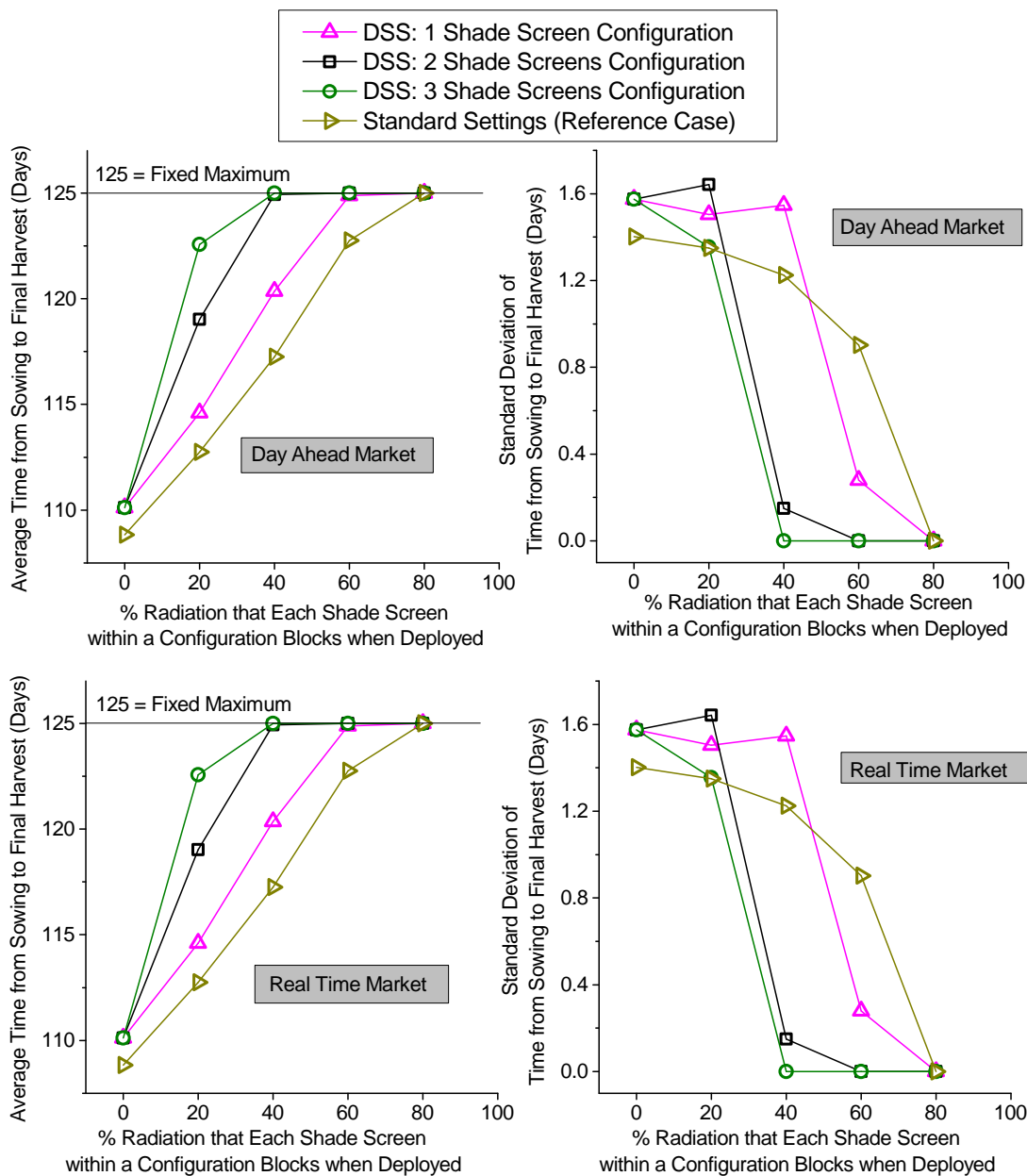


Figure 8.18: Average and standard deviation of time from sowing to final harvest. Time periods of simulations start on June 15th of each year from 2000 through 2004. The shading system for the Reference Case consisted of a single screen. The lighting system for DSS and Reference Case consisted of dimmable and non-dimmable lamps, respectively. The maximum light intensity that both lighting systems can provide is $100 \mu\text{mol}/\text{m}^2 \cdot \text{sec}$.

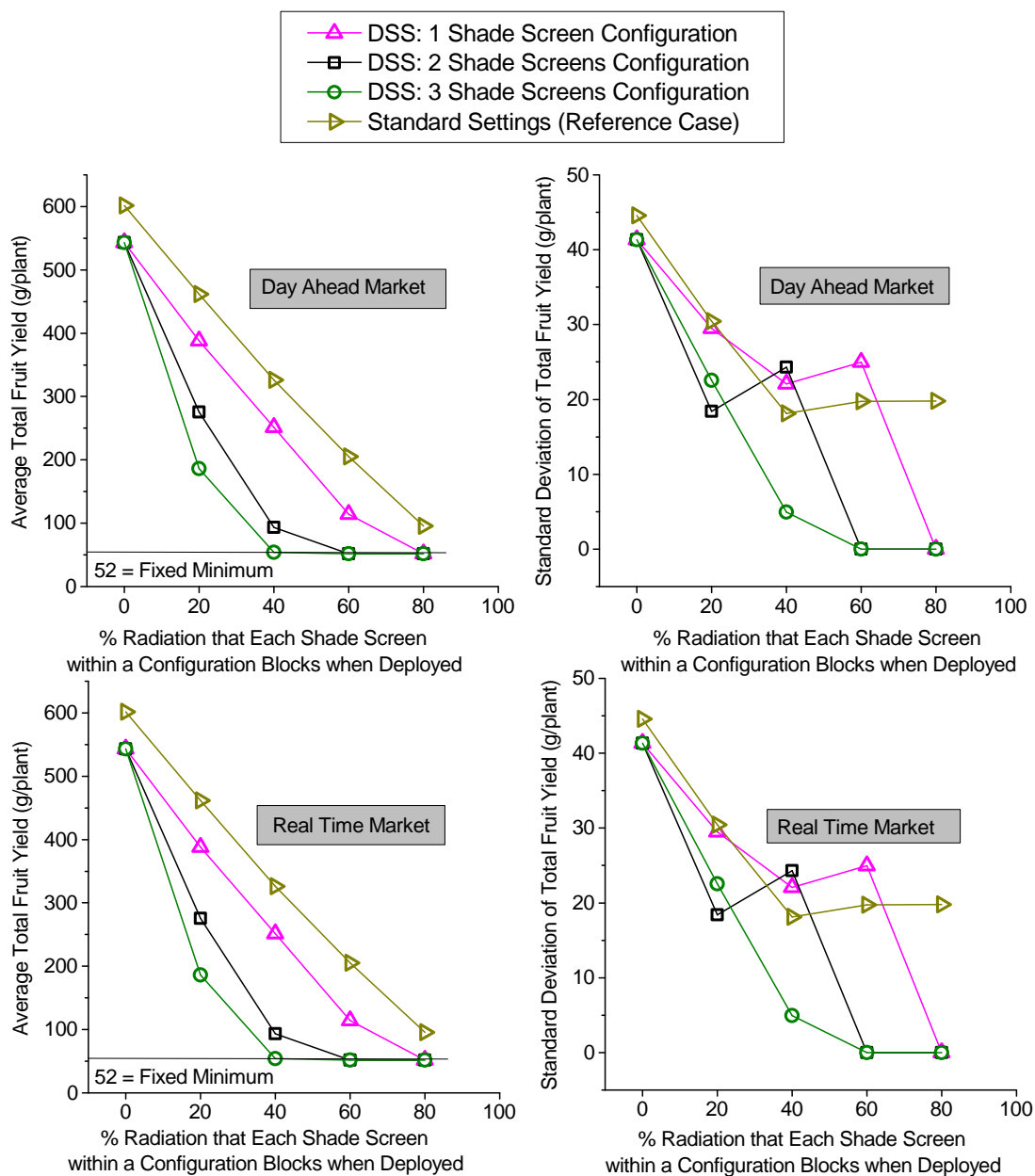


Figure 8.19: Average and standard deviation of total fruit yield. Time periods of simulations start on June 15th of each year from 2000 through 2004. The shading system for the Reference Case consisted of a single screen. The lighting system for DSS and Reference Case consisted of dimmable and non-dimmable lamps, respectively. The maximum light intensity that both lighting systems can provide is $100 \mu mol/m^2 \cdot sec$.

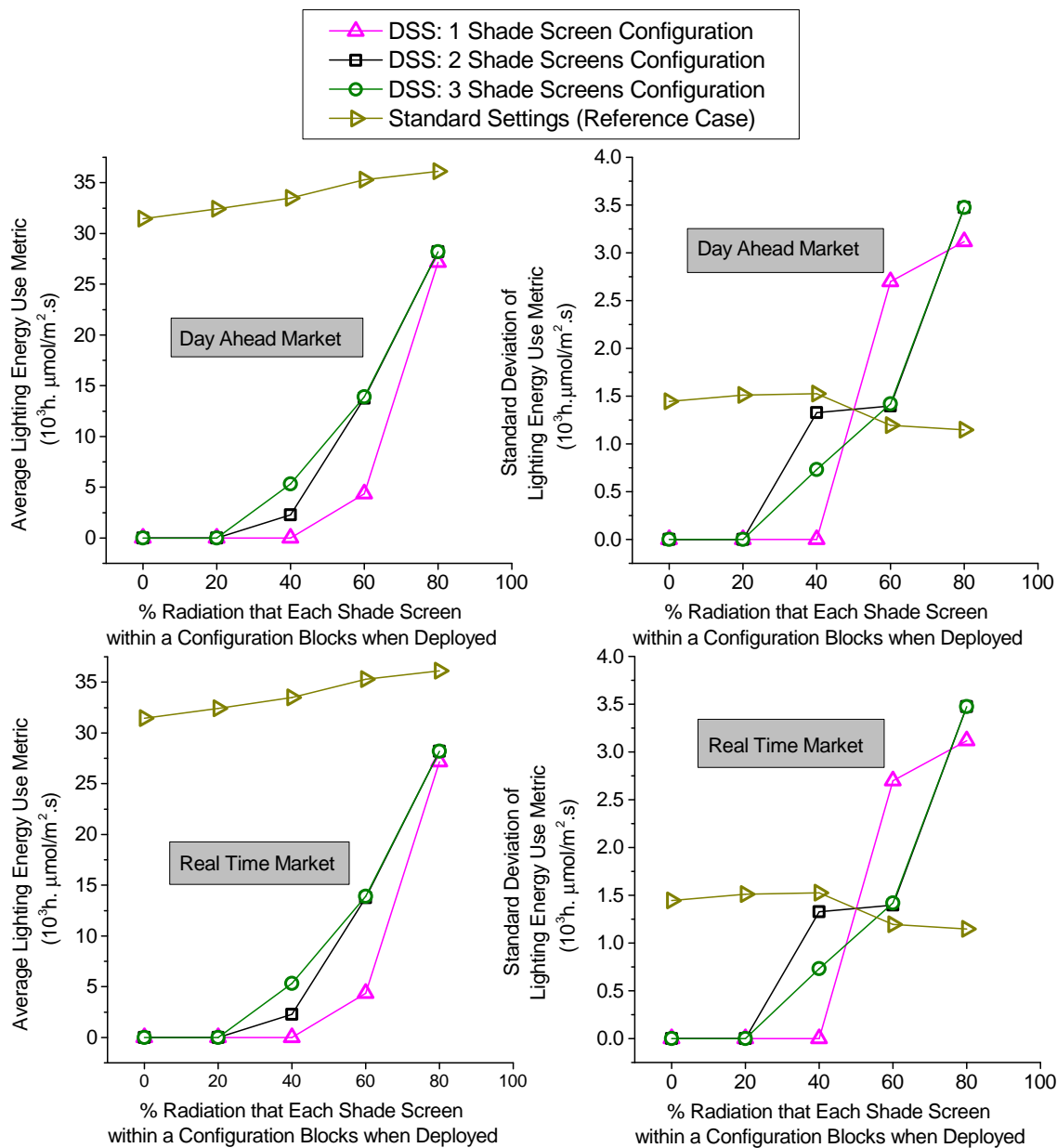


Figure 8.20: Average and standard deviation of lighting energy use. Time periods of simulations start on June 15th of each year from 2000 through 2004. The shading system for the Reference Case consisted of a single screen. The lighting system for DSS and Reference Case consisted of dimmable and non-dimmable lamps, respectively. The maximum light intensity that both lighting systems can provide is $100 \mu mol/m^2 \cdot sec$.

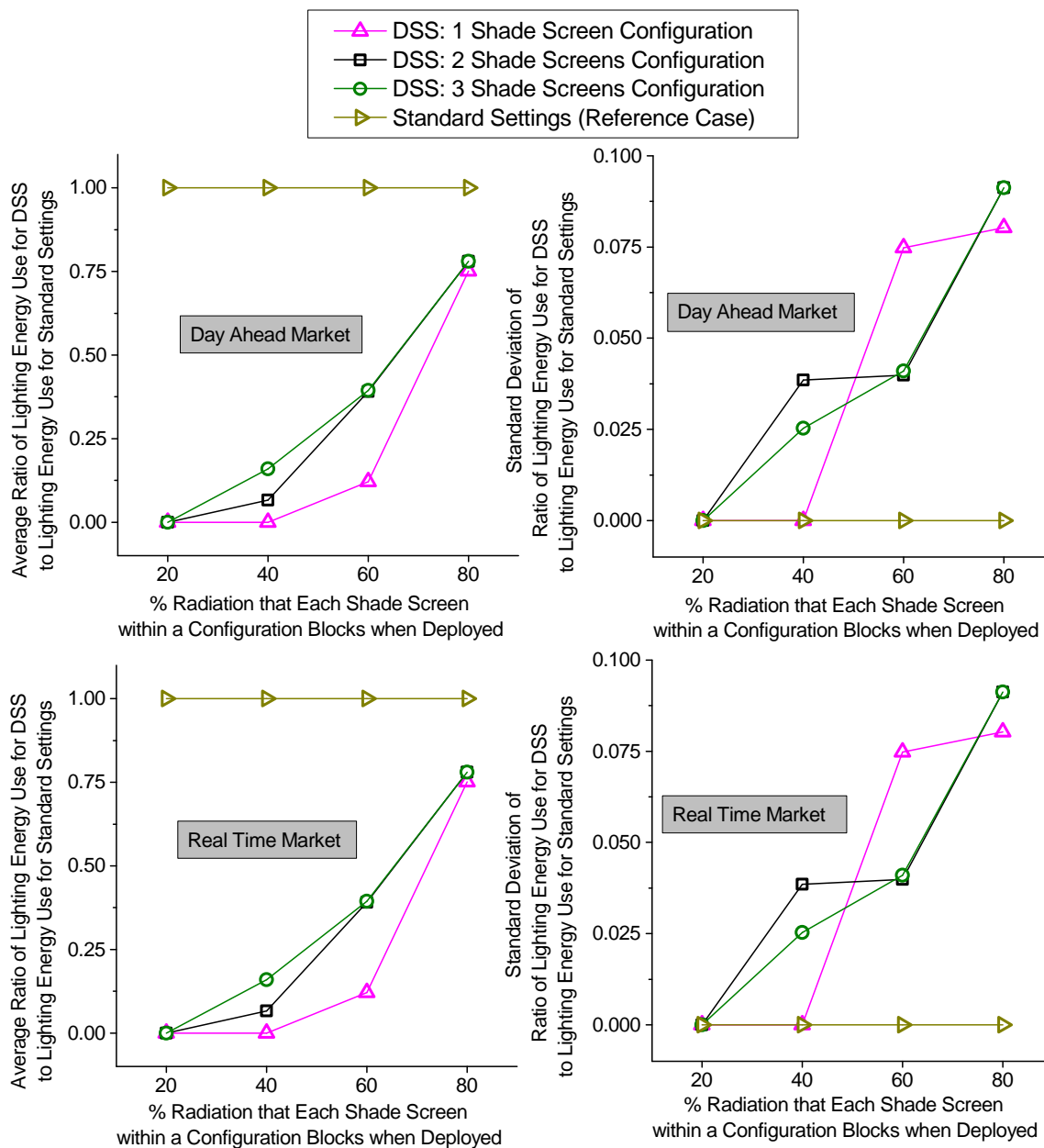


Figure 8.21: Average and standard deviation of the ratio of the lighting energy use for the DSS to the lighting energy use for the Reference Case. Time periods of simulations start on June 15th of each year from 2000 through 2004. The shading system for the Reference Case consisted of a single screen. The lighting system for DSS and Reference Case consisted of dimmable and non-dimmable lamps, respectively. The maximum light intensity that both lighting systems can provide is $100 \mu\text{mol}/\text{m}^2 \cdot \text{sec}$.

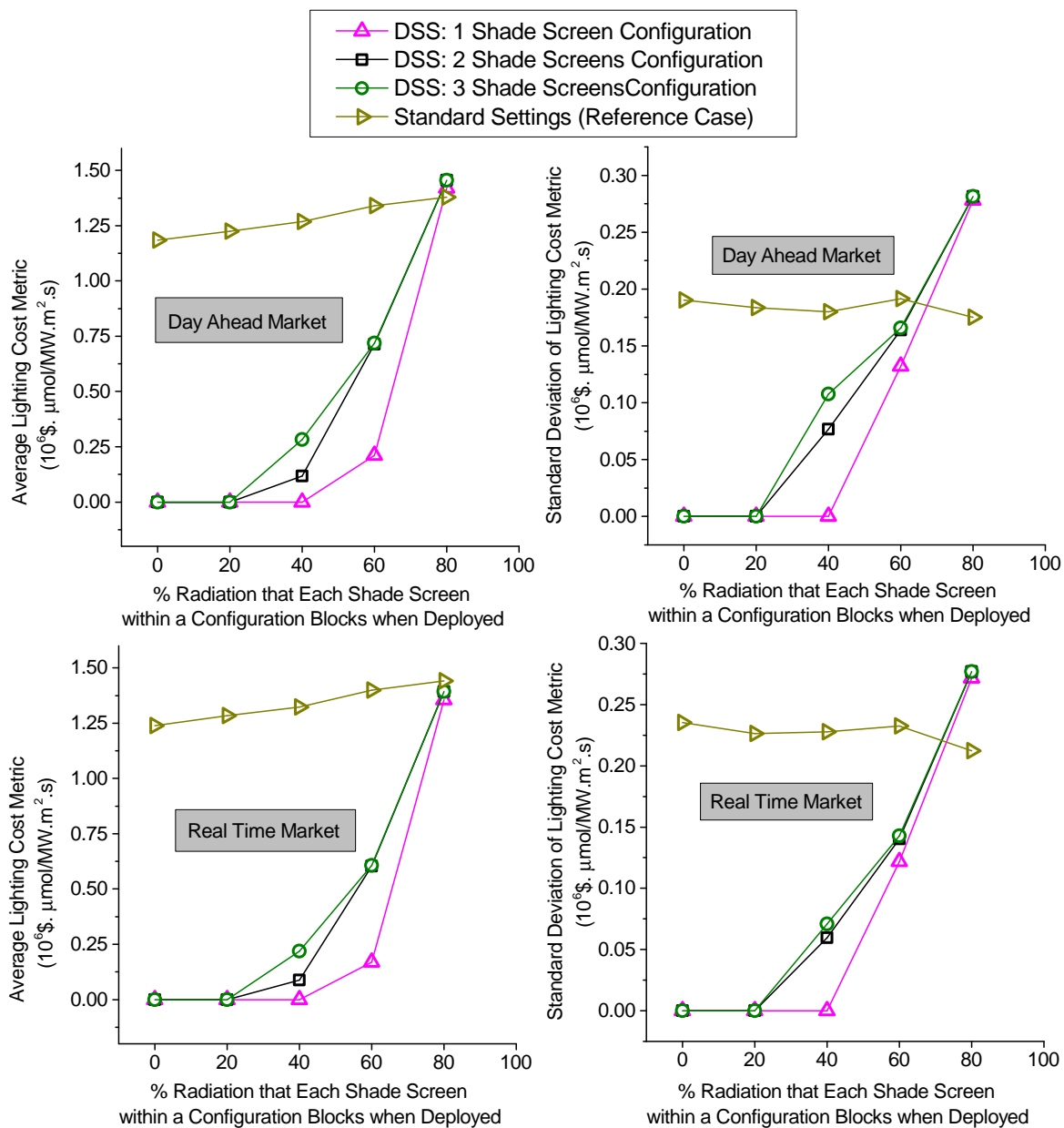


Figure 8.22: Average and standard deviation of lighting cost. Time periods of simulations start on June 15th of each year from 2000 through 2004. The shading system for the Reference Case consisted of a single screen. The lighting system for DSS and Reference Case consisted of dimmable and non-dimmable lamps, respectively. The maximum light intensity that both lighting systems can provide is $100 \mu mol/m^2 \cdot sec$.

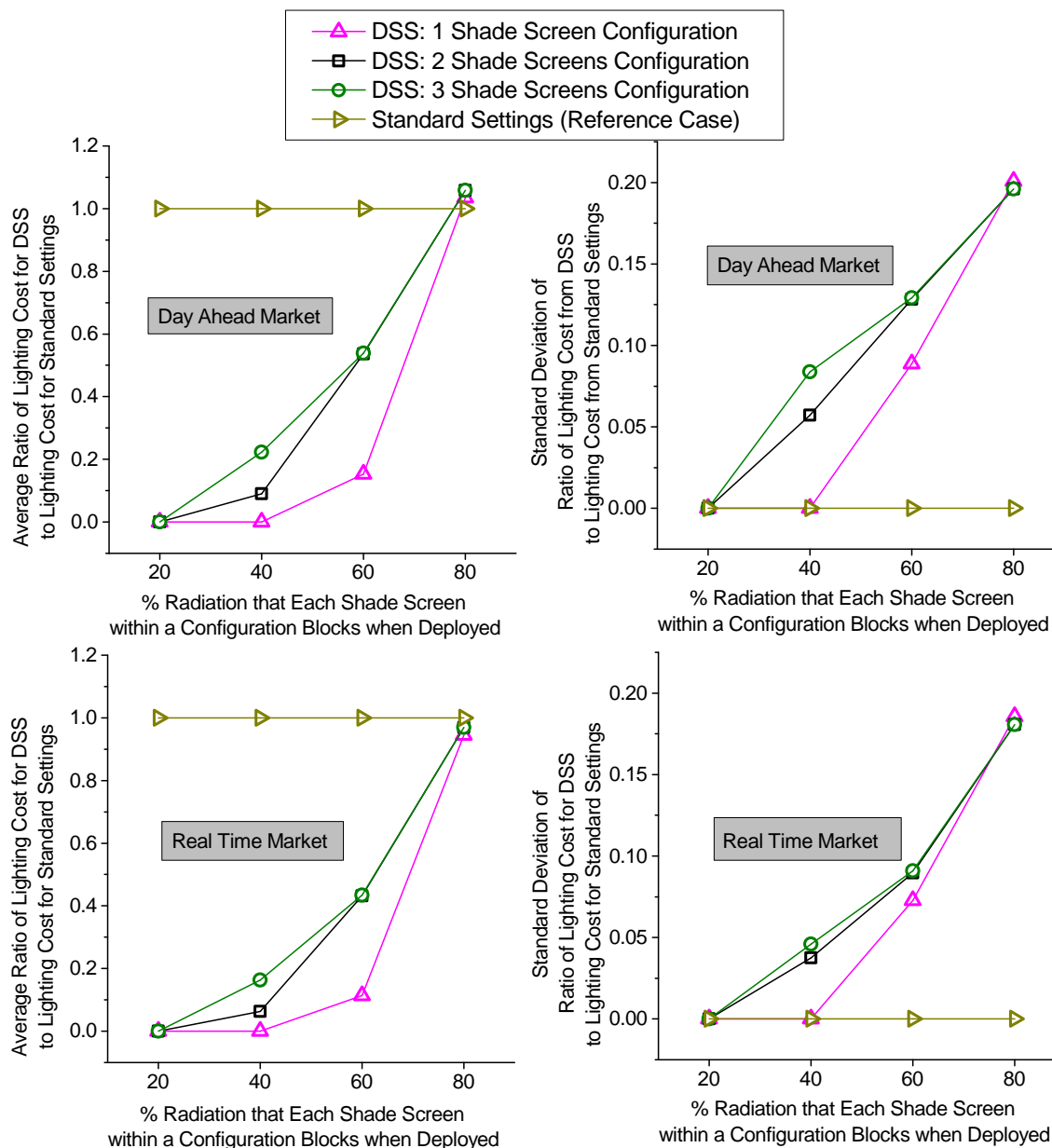


Figure 8.23: Average and standard deviation of the ratio of the lighting cost for the DSS to the lighting cost for the Reference Case. Time periods of simulations start on June 15th of each year from 2000 through 2004. The shading system for the Reference Case consisted of a single screen. The lighting system for DSS and Reference Case consisted of dimmable and non-dimmable lamps, respectively. The maximum light intensity that both lighting systems can provide is $100 \mu mol/m^2 \cdot sec$.

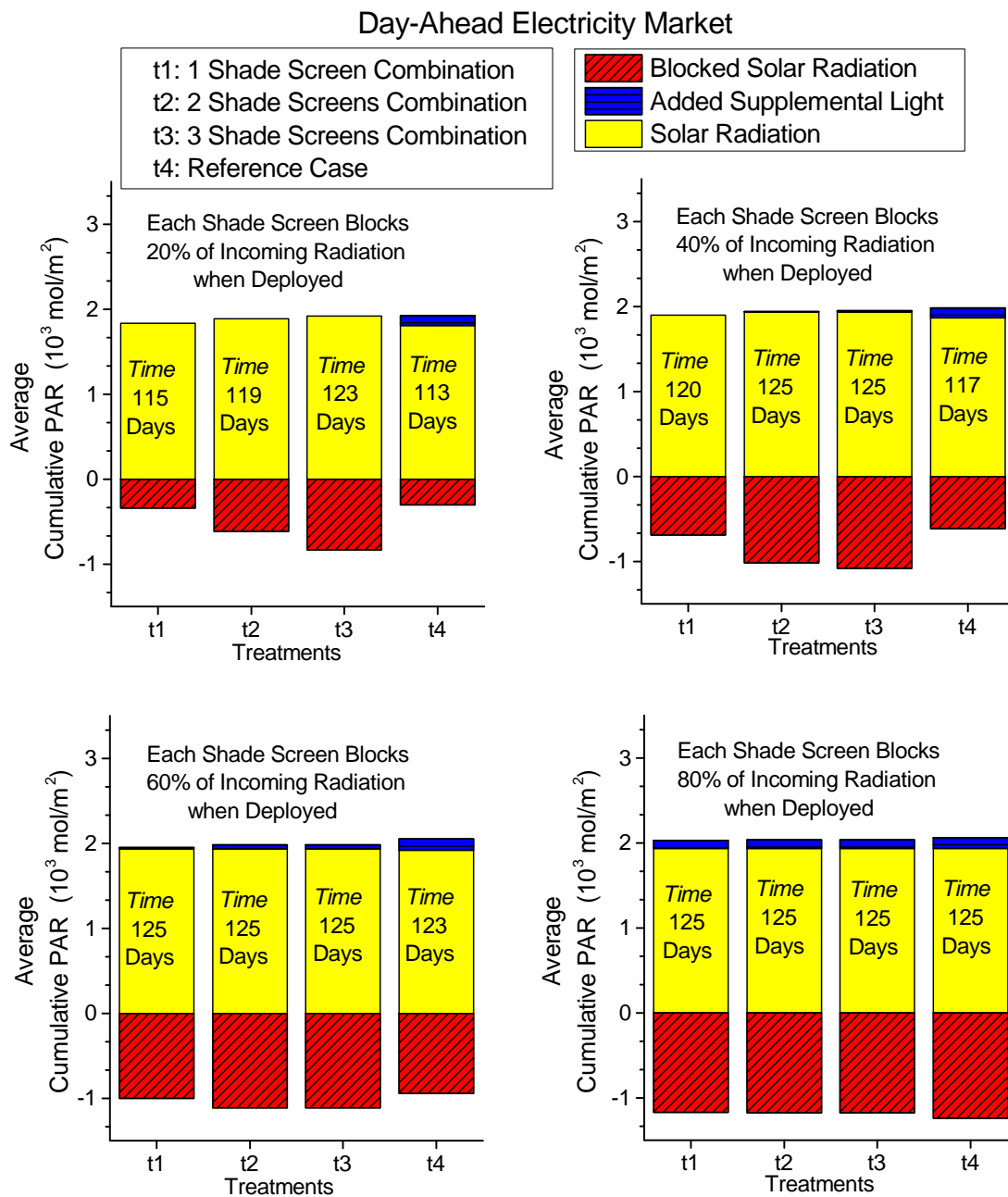


Figure 8.24: Radiation Budget. Shading Simulations during the summer months for the Day-Ahead electricity market. The treatments 1 to 3 correspond to the DSS. *Time* refers to the duration of the crop growth period from sowing to final harvest.

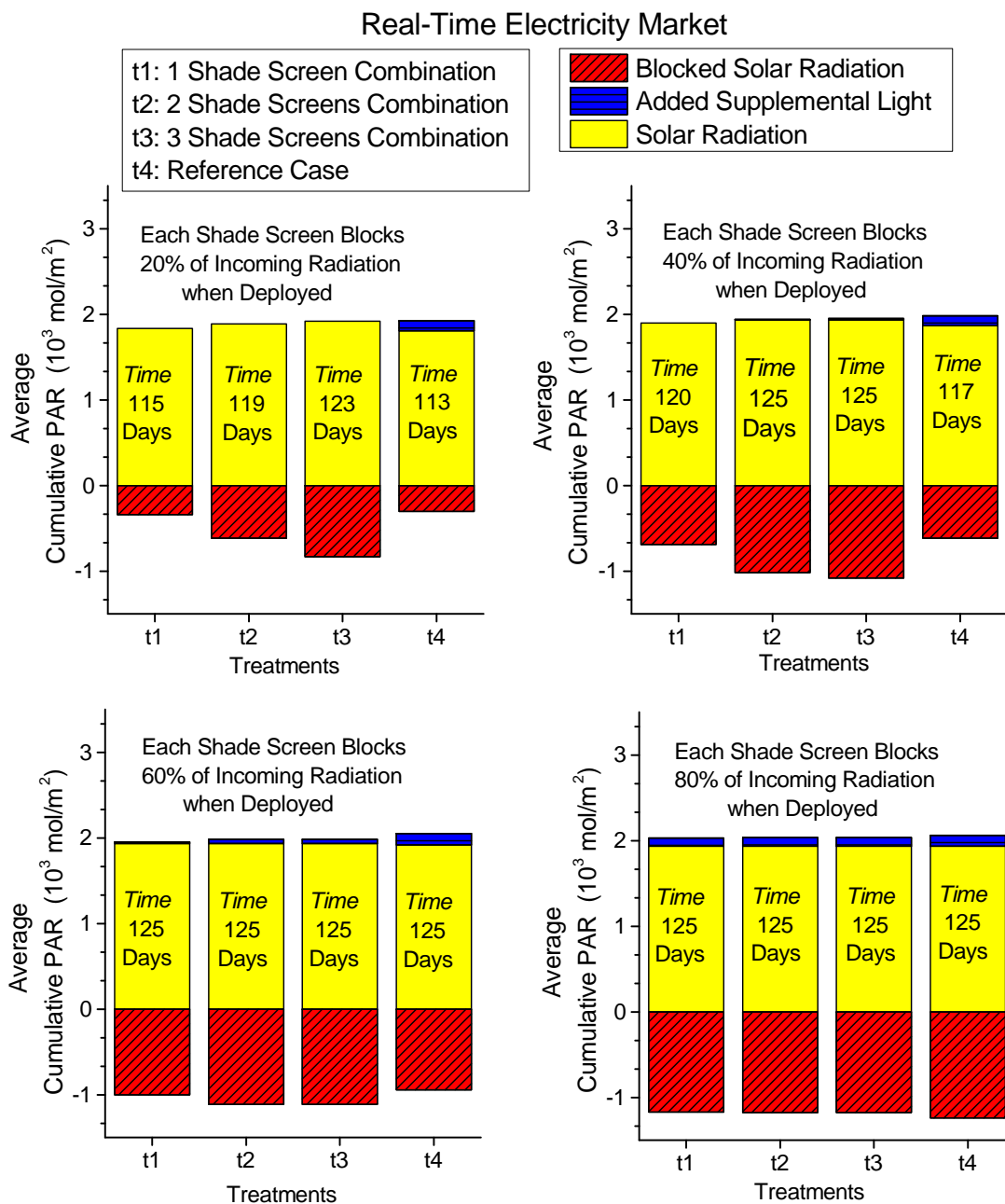


Figure 8.25: Radiation Budget. Shading Simulations during the summer months for the Real-Time Market. The treatments 1 to 3 correspond to the DSS. *Time* refers to the duration of the crop growth period from sowing to final harvest.

Chapter 9

Discussion

9.1 Performance of the DSS at Providing Supplemental Lighting. Minimum Time from Sowing to Final Harvest and Maximum Crop Yield Targets.

Time from Sowing to Final Harvest during the Summer Months.

The left panels of Figure 8.2 show that for all different settings, as the supplemental lighting intensity that the system can provide increases, the time from sowing to final harvest (*time*) decreases towards its minimum target value (105 *days*) in the same way whether or not the DSS is sensitive to electricity prices in the Day-Ahead or Real-Time electricity markets. It is also apparent that the Reference Case is less effective than the different settings from the DSS at achieving the *time* target when the supplemental lighting intensity is below $250 \mu mol/m^2 \cdot sec$.

Both the relationship observed between *time* and supplemental lighting intensity, and the independence of that relationship to the type of electricity market are expected results and serve as validation criteria for the DSS and Reference Case algorithms:

- The more radiation from supplemental light is available, the shorter the time is to reach the harvest.
- Total fruit yield (*yield*) and *time* are determined by the solar radiation and the hourly allocation of supplemental lighting, and the latter depends on the

grower's targets, past values and future prediction of solar radiation, and ranking of the electricity prices throughout the different hours. The Real-Time electricity prices follow the same ranking as the Day-Ahead electricity prices because they were modeled as a single linear relation using the Day-Ahead electricity prices as a predictor; so, all the factors that determine *time* and *yield* are the same for both types of electricity prices.

- *time* and *yield* for the Reference Case exhibit no dependency on the type of electricity market because the reference case is not sensitive to the electricity prices.
- The cost, on the contrary, exhibits some dependency on the type of electricity market because it depends directly on electricity prices.

The observed higher effectiveness of the DSS at achieving *time* values closer to the target than the Reference Case is a result of one factor: sensitivity of the screen selection algorithm from the Reference Case to large values of solar radiation. This is apparent during the summer months when the supplemental lighting intensity is $0 \mu mol/m^2 \cdot sec$ and neither the DSS nor the Reference Case provide supplemental lighting. In this case any difference between the values of *time* corresponding to the DSS and the Reference Case is determined by the differences between their shade screen selection algorithms. As the left panels of Figure 8.2 show, at $0 \mu mol/m^2 \cdot sec$ of supplemental lighting the *time* corresponding to the Reference Case is close to 116 *days* while the *time* corresponding to the different DSS settings is slightly below 112 *days*.

The operations of the DSS, including the deployment of the shade screens, are based on the periodical assessment of the crop needs depending on the grower's targets, and past values and future predictions of solar radiation. The operations of the Reference Case, on the contrary, are not based on the crop needs but only on recent and instantaneous values of solar radiation. For the present case when the

grower's target *time* is the minimum possible value, the Reference Case deploys the shade screens when the outside solar radiation is above $1500 \mu\text{mol}/\text{m}^2 \cdot \text{sec}$. This large value of outside solar radiation is frequently reached during the summer period, resulting in the Reference Case blocking more solar radiation than the DSS.

The standard deviation of *time* for both types of electricity markets show a similar trend of decreasing values with increasing supplemental lighting intensity (right panels of Figure 8.2) for the different settings. This result implies that the effect of the variability of the solar radiation throughout the different years is smoothed out as the system is able to provide more supplemental lighting. The standard deviation does not exhibit marked differences between the different settings. The relative standard deviation remains below 1.3%. The low relative standard deviation indicates that the different settings are robust or able to perform their goal of decreasing the time from sowing to final harvest with increasing supplemental lighting intensity independently of the year.

Time from Sowing to Final Harvest during the Winter Months.

Similar to *time* during the summer months, during the winter months *time* is also independent of the type of electricity market and decreases towards its minimum target value as the supplemental light maximum increases (left panels of Figure 8.3). However, except for these two expected similarities, the behavior of *time* during the winter period is markedly different from its behavior during the summer months.

Contrary to what was observed during the summer, during the winter period the *time* corresponding to the different settings of the DSS and to the Reference Case is similar. The left panels of Figure 8.3 also show that during the winter period, for a given value of supplemental lighting intensity, the value of *time* that corresponds to a given setting is larger than the value of *time* that corresponds to that same setting and supplemental lighting intensity during the summer period. Both features are consequences of the difference between the amount of solar radiation available during

the summer and winter months.

When the grower's target *time* is the minimum possible value, neither the DSS nor the Reference Case tends to deploy the shade screens during the winter period because of the low values of solar radiation. On the contrary, for this same reason, both systems tend to provide the maximum possible amount of radiation from supplemental lighting. As the left panels of Figure 8.3 show, the result is that for both the DSS and the Reference Case, *time* behaves in a similar way during the winter period.

Because less solar radiation is available during the winter than during the summer, the *time* achieved at a given value of supplemental lighting intensity for any of the settings, is closer to its target value during the summer than during the winter. In particular, when the supplemental lighting intensity is not higher than $50 \mu\text{mol}/\text{m}^2 \cdot \text{sec}$, during the winter period neither the DSS nor the Reference Case is able to decrease *time* from its maximum possible value (125 *days*). This is reflected in left panels of Figure 8.3 as a constant value of time (125 *days*) when the supplemental lighting intensity is either $0 \mu\text{mol}/\text{m}^2 \cdot \text{sec}$ or $50 \mu\text{mol}/\text{m}^2 \cdot \text{sec}$.

The right panels of Figure 8.3 show that during the winter period the standard deviation of *time* does not exhibit marked differences between the different settings. The trend of decreasing values of standard deviation with increasing supplemental lighting intensity, observed during the summer, is not present during the winter and the standard deviation remains relatively constant. Because less solar radiation is available during the winter than during the summer, even at low values of the supplemental lighting intensity, the system is able to reduce the variability of *time* originating from the variability of solar radiation. This also explains the lower values of the relative standard deviations observed during the winter compared to those observed during the summer: the relative standard deviation during the winter remains below 0.3%, compared to 1.3% during the summer.

Total Fruit Yield during the Summer Months.

The left panels of Figure 8.4 show that the total fruit yield (*yield*) exhibits the expected trend of increasing yield values with increasing values of supplemental lighting intensity in the same way for both types of electricity market. The relationship observed between *yield* and supplemental lighting intensity and the independence of that relationship of the type of electricity market are explained in the same way as in the case of *time*:

- As more radiation from supplemental light is available, the closer the *yield* is to its maximum target value.
- All the factors that determine *time* and *yield*: the grower's targets, past values and future prediction of solar radiation, and ranking of the electricity prices throughout the different hours; are the same for both types of electricity markets.
- The Reference Case is not sensitive to the type of electricity market.

The right panels of Figure 8.4 show that the standard deviation of *yield* for both types of electricity markets show a similar trend of decreasing values with increasing supplemental lighting intensity for the different cases, except for the Reference Case at 0, 50, and 100 $\mu\text{mol}/\text{m}^2 \cdot \text{sec}$. This result implies that the effect of the variability of the solar radiation throughout the different years is reduced as the system is able to provide more supplemental lighting.

Excluding the three irregular values from the Reference Case, the standard deviation does not exhibit major differences between the different settings. The relative standard deviation remains below 5.3%. As in the case of *time*, the low relative standard deviation of the different settings indicates that both the DSS and the Reference Case is robust (perform their goal independently of the yearly weather variations).

Total Fruit Yield during the Winter Months.

The behavior of *yield* during the winter and summer months does not exhibit fundamental differences (left panels of Figures 8.4 and 8.5). As expected, the behavior is independent of the type of electricity market. One difference that can be observed from the figures is that during the winter the DSS is slightly more effective than the Reference Case at achieving the *yield* target. As explained below, this is the result of slightly less outside solar radiation being available during the production period corresponding to the winter than during the production period corresponding to the summer.

Since the time period for the winter simulations start on December 15th and since the production period follows the seedling stage, the longer the duration of the seedling stage, the more the production period will be into the spring and the more solar radiation will be available to the crop during this period. Because the longest duration of the seedling stage achieved during the winter is 58 days, to which corresponds a total time from sowing to final harvest of 125 days (Figure 8.3), the production period corresponding to the winter simulations where the highest amount of solar radiation is available starts on Julian day 49 (one week plus 58 days after sowing on December 15th).

Following this same logic and since the summer simulations start on June 15th (Julian Day 166), the longer the duration of the seedling stage, the more the production period will be into the fall and the less solar radiation is available to the crop. Because the longest duration of the seedling stage achieved during the summer is 49 days, to which corresponds a total time from sowing to final harvest of 116 days (Figure 8.2), the production period corresponding to the summer simulations where the least amount of solar radiation is available starts on Julian day 222 (one week plus 49 days days after sowing on June 15th).

For the production period corresponding to the winter simulations when the highest amount of solar radiation is available, the average outside solar radiation over the

years from 2000 through 2004 was $1845 \text{ mol}/\text{m}^2$ and the average number of hours when the outside solar radiation was equal or above $1500 \text{ } \mu\text{mol}/\text{m}^2 \cdot \text{sec}$ was 77. For the production period corresponding to the summer simulations when the least amount of solar radiation is available, the average outside solar radiation over the years from 2000 through 2004 was $2019 \text{ mol}/\text{m}^2$ and the average number of hours when the outside solar radiation was equal or above $1500 \text{ } \mu\text{mol}/\text{m}^2 \cdot \text{sec}$ was 72.

The similar values for the average number of hours when the outside solar radiation was equal or above $1500 \text{ } \mu\text{mol}/\text{m}^2 \cdot \text{sec}$ implies that the Reference Case deploys the shade screens, due to high values of solar radiation, a similar number of times during the summer and winter production periods. However, since less radiation is available during the production period corresponding to the winter, the deployment of the shade screens during this time results in a larger gap between the radiation available to the crop during the summer and winter production periods, which is reflected in the figures that show that the Reference Case is less effective than the DSS at achieving the *yield* target during the winter compared to the summer.

The right panels of Figure 8.5 show that the standard deviation of *yield* for both types of electricity markets show a similar trend of decreasing values with increasing supplemental lighting intensity for the different cases. This result implies that the effect of the variability of the solar radiation throughout the different years is reduced as the system is able to provide more supplemental lighting. The standard deviation does not exhibit major differences between the different settings. The relative standard deviation remains below 10%. As in the case of *time*, the low relative standard deviation of the different settings indicates that both the DSS and the Reference Case is robust.

Lighting Energy Use during the Summer Months.

The lighting energy use (*energy use*) is presented in the results in two different ways, *energy use metric* in $\text{h} \cdot \mu\text{mol}/\text{m}^2 \cdot \text{sec}$ (left panels in Figures 8.6 and 8.8), and

relative energy use as the ratio of the *energy use* corresponding to the DSS to the *energy use* corresponding to the Reference Case (left panels in Figures 8.7 and 8.9).

During the summer, the *energy use metric* behaves in the same way for the Day-Ahead and Real-Time electricity markets (Figure 8.6). In the case of the DSS settings, the values of the *energy use metric* increases linearly with increasing supplemental lighting intensity in the range of 0 to 100 $\mu\text{mol}/\text{m}^2 \cdot \text{sec}$ and starts leveling off thereafter. The *energy use metric* corresponding to the Reference Case, on the contrary, increases linearly with increasing supplemental lighting intensity across the entire range of intensities.

The values of the *energy use metric* for the DSS show that the DSS adjusts the *energy use* based on the crop radiation needs determined by the grower's targets. The radiation that the system can provide when the supplemental lighting intensity is in the range of 0 to 100 $\mu\text{mol}/\text{m}^2 \cdot \text{sec}$ is not enough to achieve the targets and the DSS uses all available energy resulting in the linear relationship observed. But as the supplemental lighting intensity increases and more radiation is available to the system, the DSS uses only the energy that is needed to achieve the targets and the values of the *energy use metric* level off. For the Reference Case, on the contrary, the more energy that is available the more energy is used, because the Reference Case is not sensitive to the crop radiation needs but to the outside values of solar radiation, resulting in the linear relationship observed across the entire range of variation of supplemental lighting intensity.

The *relative energy use* values also behave in the same way for the Day-Ahead and Real-Time electricity markets. These values allow the comparison of the *energy use* corresponding to the DSS to the *energy use* corresponding to the Reference Case. The left panels in Figure 8.7 show that for low values of supplemental lighting intensity the *energy use* values corresponding to the DSS settings are slightly larger than the *energy use* corresponding to the Reference Case while for high values of supplemental lighting intensity the *energy use* values corresponding to the DSS settings are substantially

smaller than the *energy use* corresponding to the Reference Case.

Time and *yield* were not influenced by price sensitivity or dimmability of lights, but the left panels in Figure 8.7 show that these two variables have an impact on *energy use*. Among the settings implemented when using the DSS, the one that correspond to 100% price sensitivity and dimmable lights shows the lowest value of *relative energy use* for a given value of supplemental lighting intensity. The *relative energy use* at $150 \mu\text{mol}/\text{m}^2 \cdot \text{sec}$ for that DSS particular setting is around 85% of the *energy use* from the Reference Case, and at $200 \mu\text{mol}/\text{m}^2 \cdot \text{sec}$ it is close to 70% (Table 9.1).

High sensitivity to electricity prices forces the DSS to shift the supplemental lighting to the future hours were the electricity prices are predicted to be low. Deferring supplemental light from the present hour to the future increases the chances of lowering the net *energy use* because the supplemental lighting is not provided *now* but expected to be provided *later*. As the results show, the decrease in total energy use due to this effect is not enough to impact *time* and *yield* in a noticeable manner. The effect of dimmability of lights on *energy use* was expected: when lights are dimmable the system is able to adjust the lighting intensity to the value required according to the radiation target.

The standard deviation of the *energy use metric* and the *relative energy use* show the same behavior independently of the type of electricity market (right panels in Figures 8.6 and 8.7). The relative standard deviation of the *energy use metric* and the *relative energy use* remains below 7.5% and 4.5%, respectively. These low values of relative standard deviation indicate that the DSS and the Reference Case is robust or able to perform in the same way independently of the simulated year.

Lighting Energy Use during the Winter Months.

As the left panels of Figures 8.8 and 8.9 show, the behavior of *energy use* during the winter exhibits some differences compared to its behavior during the summer. From

Table 9.1: Ratio of the energy use for the DSS’s most energy efficient settings (50% and 100% price sensitivity with dimmable lights) and the energy use for the Reference Case during the summer months.

Supplemental Lighting Intensity $\mu\text{mol}/\text{m}^2 \cdot \text{sec}$	Day-Ahead Market		Real-Time Market	
	Price Sensitivity		Price Sensitivity	
	50%	100%	50%	100%
50	1.17	1.14	1.17	1.14
100	1.10	1.02	1.10	1.02
150	0.99	0.86	0.99	0.86
200	0.84	0.72	0.84	0.72
250	0.72	0.60	0.72	0.60
300	0.61	0.50	0.61	0.50

the graphs it is apparent that for all different settings, the value of the *energy use metric* that corresponds to a given supplemental lighting intensity is substantially larger during the winter than during the summer. It is also noticeable that the behavior of the *energy use metric* corresponding to the different DSS settings becomes more linear during the winter. The *energy use metric* shows that the difference between the *energy use* corresponding to the different DSS settings and the Reference Case is less pronounced during the winter than during the summer. Both, the *energy use metric* and *relative energy use* are independent from the type of electricity market.

These results are not unexpected and are consequences of less solar radiation being available during the winter compared to the summer. On average, over the simulated years, the maximum cumulative value of outside solar radiation during the whole crop growth period during the winter is $2859 \text{ mol}/\text{m}^2$, while the minimum cumulative value of solar radiation during the whole crop growth period during the summer period is $4120 \text{ mol}/\text{m}^2$.

Because the event that triggers the use of supplemental lighting in the case of the Reference Case is independent from the crop needs (the Reference Case turns the lights on when the outside solar radiation falls below $800 \mu\text{mol}/\text{m}^2 \cdot \text{sec}$.) and because low values of solar radiation during the winter are more frequent than during the

summer, for the Reference Case the relationship between *energy use* and supplemental lighting intensity remains linear during the winter, although the slope increases in the winter compared to the summer (for the same value of supplemental lighting intensity the corresponding value of the *energy use metric* is higher during the winter than during the summer).

The ability of the DSS to fine tune the use of supplemental light according not only to the available solar radiation but also to the crop needs and sensitivity to electricity prices is reflected in the energy use in the nonlinear behavior observed during the summer period. During the winter, however, when the supplemental lighting intensity is low, the DSS is not able to meet the crop needs even after maximizing the use of supplemental lighting. For this reason, the *energy use metric* corresponding to the DSS settings exhibits a nonlinear behavior only at high values of supplemental lighting intensity.

The *relative energy use* (left panels in Figure 8.9) shows that the *energy use* difference between the DSS and the Reference is not as pronounced during winter as during the summer. Still, for high values of supplemental lighting intensity the different settings from the DSS are more efficient than the Reference Case. In particular, the energy use corresponding to the 100% price sensitivity and dimmable lights settings from the DSS is 90% of the energy use corresponding to the Reference Case at $200 \mu\text{mol}/\text{m}^2 \cdot \text{sec}$ and close to 75% at $300 \mu\text{mol}/\text{m}^2 \cdot \text{sec}$. It is important to note that the ability of the DSS to lower the energy use is an added benefit, but the final goal of the DSS is to achieve the grower's time and yield targets while reducing the cost associated with the use of supplemental lighting (Table 9.2).

The standard deviation of the *energy use metric* and the *relative energy use* show the same behavior independently of the type of electricity market (right panels in Figures 8.8 and 8.9). The relative standard deviation of the *energy use metric* and the *relative energy use* remains below 2.7% and 2.6%, respectively. These low values of relative standard deviation indicate that the DSS and the Reference Case is robust

and able to perform in the same way independently of the simulated year.

Table 9.2: Ratio of the energy use for the DSS's most energy efficient settings (50% and 100% price sensitivity with dimmable lights) and the energy use for the Reference Case during the winter months.

Supplemental Lighting Intensity $\mu\text{mol}/\text{m}^2 \cdot \text{sec}$	Day-Ahead Market		Real-Time Market	
	Price Sensitivity		Price Sensitivity	
	50%	100%	50%	100%
50	1.12	1.11	1.12	1.11
100	1.09	1.07	1.09	1.07
150	1.05	1.00	1.05	1.00
200	0.96	0.91	0.96	0.91
250	0.88	0.83	0.88	0.83
300	0.82	0.77	0.82	0.77

Lighting Cost during the Summer Months.

Similar to *energy use*, the lighting cost (*cost*) is also presented in the results in two different ways, *cost metric* in $\$ \cdot \mu\text{mol}/\text{MW} \cdot \text{m}^2 \cdot \text{sec}$ (left panels in Figures 8.10 and 8.12 for summer and winter, respectively), and *relative cost* as a ratio of the *cost* corresponding to the DSS to the *cost* corresponding to the Reference Case (left panels in Figures 8.11 and 8.13 for summer and winter, respectively).

The values of *cost metric* were first adjusted for inflation to the year 2000 dollars and then averaged over the years corresponding to the simulation period. As the figures show, *cost* and *energy use* during the summer behave similarly: the *cost metric* corresponding to the Reference Case increases linearly with increasing supplemental lighting intensity across the entire range of this variable while the *cost metric* corresponding to the DSS increases linearly with increasing supplemental lighting intensity only across a portion of the range of variation of the supplemental lighting intensity.

As in the case of *energy use*, this effect is the result of the Reference Case being sensitive only to outside values of solar radiation as opposed to the DSS which is also sensitive to the crop needs and the electricity prices. The similarities between the

Day-Ahead and Real-Time electricity prices (Equation 5.6) is reflected in the results in similar behavior and values for the cost in both types of electricity markets.

The *relative cost* values also behave in the same way for the Day-Ahead and Real-Time electricity markets and allow the comparison of the *cost* corresponding to the DSS to the *cost* corresponding to the Reference Case without having to make inflation adjustments. The left panels in Figure 8.11 show that among the DSS settings, the one that corresponds to 100% price sensitivity and dimmable lights exhibits *cost* values below the *cost* corresponding the Reference Case for supplemental lighting intensity at or above $150 \mu\text{mol}/\text{m}^2 \cdot \text{sec}$.

At $200 \mu\text{mol}/\text{m}^2 \cdot \text{sec}$ the cost for that particular DSS setting is below 70% of the cost corresponding to the Reference Case and at $250 \mu\text{mol}/\text{m}^2 \cdot \text{sec}$ it is roughly 50%. At $250 \mu\text{mol}/\text{m}^2 \cdot \text{sec}$ and $300 \mu\text{mol}/\text{m}^2 \cdot \text{sec}$ the *cost* that corresponds to the DSS setting of 50% price sensitivity and dimmable lights also exhibits values below the *cost* corresponding to the Reference Case (Table 9.3). As explained before, high sensitivity to electricity prices forces the DSS to shift the supplemental lighting to the hours were the electricity prices are predicted to be low. When high sensitivity to electricity prices is combined with the possibility of precisely adjusting the lighting intensity to the value required, the cost associated with the use of supplemental lighting is substantially reduced. This is precisely what is observed in the results. It is important to remember that this discussion refers to the lighting cost during the summer months, when the lighting cost is just a fraction of the lighting cost during the winter months.

The relative standard deviation of the *cost metric* remains high for all the different settings (between 12.8% and 25.3%), however, this is not an indication of the settings not being robust but rather a result of the variability introduced by the *cost metric* being reported in dollars, even after adjusting for inflation. Because the *relative cost* values are not affected by inflation, their relative standard deviations are reliable indicators of the robustness of the DSS settings and they remain below 11 %.

Table 9.3: Ratio of the lighting cost for the DSS's most energy efficient settings (50% and 100% price sensitivity with dimmable lights) and the lighting cost for the Reference Case during the summer months.

Supplemental Lighting Intensity $\mu\text{mol}/\text{m}^2 \cdot \text{sec}$	Day-Ahead Market		Real-Time Market	
	Price Sensitivity		Price Sensitivity	
	50%	100%	50%	100%
50	1.42	1.36	1.44	1.38
100	1.35	1.18	1.37	1.20
150	1.23	0.92	1.25	0.95
200	1.05	0.68	1.06	0.72
250	0.90	0.50	0.91	0.54
300	0.76	0.38	0.77	0.41

Lighting Cost during the Winter Months.

As expected, the *cost metric* and *relative cost* during the winter (Figures 8.12 and 8.13) are similar for both types of electricity market while the differences observed between *cost* during the winter and cost during the summer are similar to the differences between *energy use* during the winter and *energy use* during the summer: the value of the *cost metric* that corresponds to a given supplemental lighting intensity is substantially larger during the winter than during the summer, and the behavior of the *cost metric* corresponding to the different DSS settings becomes more linear during the winter than during the summer. These differences are also consequences of the reduced level of solar radiation during the winter compared to the summer.

The behavior of the *relative cost* during the winter exhibits important differences from its behavior during the summer. As the left panels of Figure 8.13 show, at high values of supplemental lighting intensity (250 and 300 $\mu\text{mol}/\text{m}^2 \cdot \text{sec}$), all the different DSS settings are more cost efficient than the Reference Case. At 200 $\mu\text{mol}/\text{m}^2 \cdot \text{sec}$ only the DSS settings that correspond to 0% price sensitivity are slightly less efficient than the Reference Case. For the DSS setting of 100% price sensitivity and dimmable lights, the cost is around 83% of the cost corresponding to the Reference Case at 200 $\mu\text{mol}/\text{m}^2 \cdot \text{sec}$, and around 73% and 66% at 250 $\mu\text{mol}/\text{m}^2 \cdot \text{sec}$ and 300 $\mu\text{mol}/\text{m}^2 \cdot \text{sec}$.

sec, respectively (Table 9.4).

During the winter, the relative standard deviation of the *cost metric* is even higher than during the summer (between 25.3% and 28.2%). As has been explained, this is not an indication of the settings not being robust but rather a result of the variability introduced by the *cost metric* being reported in dollars, even after adjusting for inflation. However, the standard deviations of the *relative cost*, a reliable indicator of the robustness of the DSS because it is not affected by inflation, is substantially lower during the winter than during the summer (relative standard deviation below 5%). The lower standard deviation of the *relative cost* during the winter months is the result of a more consistent use of the supplemental lighting system during the winter compared to the summer.

Table 9.4: Ratio of the lighting cost for the DSS's most energy efficient settings (50% and 100% price sensitivity with dimmable lights) and the lighting cost for the Reference Case during the winter months.

Supplemental Lighting Intensity $\mu\text{mol}/\text{m}^2 \cdot \text{sec}$	Day-Ahead Market		Real-Time Market	
	Price Sensitivity		Price Sensitivity	
	50%	100%	50%	100%
50	1.10	1.08	1.09	1.08
100	1.05	1.02	1.05	1.02
150	1.00	0.93	1.00	0.94
200	0.89	0.82	0.89	0.83
250	0.80	0.73	0.80	0.73
300	0.74	0.65	0.74	0.66

Radiation budget during lighting simulations.

In a similar way to the previously analyzed metrics, the graphs of radiation budget (Figures 8.14, 8.15, 8.16, and 8.17) are independent of the type of electricity market. For both the summer and the winter months, these graphs show a substantially increase in the amount of cumulative added supplemental light as the supplemental lighting intensity increases for any of the settings. The associated slight reduction

in cumulative solar radiation is the result of the decrease of the duration of the crop growth period as a result of the increase of the supplemental lighting intensity. For a given value of supplemental lighting intensity, the slight differences observed in the cumulative solar radiation across the different settings is also the result of different duration of the corresponding crop growth periods.

The lowest values of cumulative added supplemental light and cumulative blocked solar radiation correspond to the 100% price sensitivity and dimmable lights settings from the DSS. On the contrary, the Reference Case exhibits the largest cumulative value of added supplemental light and/or blocked solar radiation. For any of the settings, the reduction in cumulative solar radiation during the winter compared to the summer and the increase in the corresponding cumulative added supplemental light is clearly apparent in these graphs. The cumulative values of blocked solar radiation decrease from summer to winter, an indication that the extreme values of solar radiation that trigger the deployment of the shade screens are less frequent during winter.

9.2 Performance of the DSS while Using the Shade Screens for the Hypothetical case of Maximum Time from Sowing to Final Harvest and Minimum Crop Yield Targets.

Time from Sowing to Final Harvest.

If during the summer time, the period of the year when more solar radiation is available, grower's harvest time and yield targets are set to their maximum and minimum values, respectively, the system is forced to use the shade screens more often. Although these targets are not practical, they make it possible to test the performance of the system at using the shade screens.

Figure 8.18 shows the simulation results for *time* under four different settings.

The left hand panels in the figure show that for each of the settings, as the percent of radiation blocked by each screen within a configuration increases, *time* also increases. It is also apparent that *time* behaves in the same way for both types of electricity market. Both of these results are expected and serve as validation of the screen selection algorithm and electricity price model.

As the left hand panels of Figure 8.18 show, the different DSS configurations are more effective than the Reference Case at blocking unwanted radiation. Except at 80% of blocked radiation (unless specified otherwise, the % of blocked radiation refers to the % of blocked radiation by each screen within a configuration and not to the total % of blocked radiation by the screens within a configuration), at every value of percent of blocked radiation, the *time* values corresponding to the DSS configurations are closer to the target *time* value than the those corresponding to the Reference Case. At 40% of blocked radiation, the single screen configuration from the DSS achieves close to 75% of the target *time* compared to around 60% in the case of the Reference Case.

The better performance of the DSS at operating the shade screens is the result of the differences between the screen selection algorithms for the DSS and the Reference Case. In the case of the DSS, the shade screens selection is based on the radiation need according to the target, received radiation by the crop up to the present, and prediction of future values of solar radiation. The Reference Case, on the contrary, deploys the shade screen based on instantaneous values of outside solar radiation.

Among the DSS configurations, the dual screen configuration shows improvements over the single screen configuration while the triple screen configuration is not markedly better than the dual screen configuration. Since the dual and triple screen configurations from the DSS both achieve 100% of the target *time* at just 40% of blocked radiation, the triple screen configuration seems unnecessary. The reasons for these results are evident, the more screens are available to the DSS, the easier it can block unwanted radiation.

The two and three screen configurations from the DSS show particularly low values of standard deviations at 40% of blocked radiation. In general, the relative standard deviation is low (the relative standard deviation is below 1.5% for all cases) and serve as an indication of the robustness of the DSS and Reference Case screen selection algorithms.

Total Fruit Yield.

As expected, *yield* decreases as the percent of radiation blocked by each screen within a configuration increases and *yield* behaves in the same way for both types of electricity market (Figure 8.19). It is also apparent from the figure that results in the case of yield are similar to the case of time: the different DSS configurations are more effective than the Reference Case at blocking unwanted radiation; and among the DSS configurations, the dual screen configuration shows improvements over the single screen configuration while the triple screen configuration is not markedly better than the dual screen configuration.

The reasons for these results are the same as in the case of *time*: the better performance of the DSS at operating the shade screens is the result of the differences between the screen selection algorithms for the DSS and the Reference Case. In the case of the DSS, the shade screens selection is based on the radiation need according to the time and yield targets, the received radiation by the crop up to the present, and the prediction of future values of solar radiation. The Reference Case, on the contrary, deploys the shade screen based on instantaneous values of outside solar radiation.

The relative standard deviation of *yield* is high for three cases: 26% for the DSS dual screen configuration at 40% of blocked radiation, 22% for the DSS one screen configuration at 60% of blocked radiation, and 21% for the Reference Case at 80% of blocked radiation. However, these three high values of relative standard deviation are the result of low values of the corresponding average *yield*: 93 *g/plant*, 114 *g/plant*,

and 96 *g/plant*, respectively.

Lighting Energy Use.

As in the case of the lighting simulations, in the shading simulations the lighting energy use (*energy use*) is presented in two different ways, *energy use metric* in $h \cdot \mu\text{mol}/\text{m}^2 \cdot \text{sec}$ (left panels in Figure 8.20), and *relative energy use* as the ratio of *energy use* corresponding to the DSS to *energy use* corresponding to the Reference Case (left panels in Figure 8.21).

These figures show a difference between the *energy use* corresponding to the Reference Case and the *energy use* corresponding to the different DSS settings. For any value of percent of radiation blocked, the corresponding value of *energy use* is larger for the Reference Case than for any of the DSS settings. The figures also show that for each of the DSS settings, the *energy use* increases with increasing percentage of radiation blocked. As expected, the *energy use* shows independence from the type of electricity market (section 9.1).

During the summer period, if the *time* and *yield* targets are set to their maximum and minimum values, respectively, the DSS operates mainly the shade screens because the goal is to block solar radiation. Only when the predicted values of solar radiation will result in less radiation than the minimum needed, the system operates the supplemental lighting. As a result, the DSS makes minimum use of supplemental light under this set of targets. However, if the percent of blocked radiation is 60% or 80%, when the DSS deploys the shade screens it blocks more radiation than needed, resulting in the use of supplemental light to compensate for the unintended blocked radiation. This is the reason why for each of the DSS settings, the *energy use metric* increases with increasing percentage of blocked radiation.

In the Reference Case, although the algorithm was modified to accommodate this new set of targets, it still uses supplemental lighting when the outside solar radiation falls below a threshold value, resulting in substantially higher values of *energy use*

compared to the DSS. It is important to note that in the present case when the *time* and *yield* targets are set to their maximum and minimum values, respectively, and the system needs to block unneeded radiation, the *energy use* for both the DSS and the Reference Case is just a fraction of the *energy use* during the summer or winter when the *time* and *yield* targets are set to their minimum and maximum values, respectively, and the system needs to provide additional radiation through supplemental lighting.

Because the average values of the *energy use metric* is very small for most cases, the relative standard deviation of the *energy use metric* is not a reliable measure of relative variability. However, since the *energy use metric* corresponding to the Reference Case is relatively constant, the standard deviation of the *relative energy use* becomes an indicator of relative variability, and as is shown in the right panels of Figure 8.21, it is below 0.1.

Lighting Cost.

The left panels in Figure 8.22 correspond to the *cost metric* in $\$/\mu\text{mol}/\text{MW}\cdot\text{m}^2\cdot\text{sec}$ and the left panels in Figure 8.23 to the *relative cost* or ratio of *absolute cost* from the DSS to *absolute cost* corresponding to the Reference Case.

The linearity observed in the relationship between Real-Time and Day-Ahead electricity prices (Equation 5.6) determines the similarities that the *cost* exhibits in the Real-Time and Day-Ahead electricity markets. In a similar way, because *cost* and *energy use* are directly related, their behavior is similar. For this reason, the particularities observed in the behavior of *cost* are explained in the same way as in the case of *energy use*:

- Because the Reference Case is only sensitive to instantaneous values of outside solar radiation as opposed to the DSS which operates based on the *time* and *yield* targets, for any value of percent of radiation blocked, the corresponding

cost value is significantly larger for the Reference Case than for any of the DSS settings.

- If the percent of blocked radiation is above 40%, when the DSS deploys the shade screens it blocks more radiation than needed, resulting in a *cost* increase due to the use of supplemental lighting to compensate for the unintended blocked radiation.

Similarly to *energy use*, in the present case when the *time* and *yield* targets are set to their maximum and minimum values, respectively, and the system needs to block unneeded radiation, the *absolute cost* for both the DSS and the Reference Case is just a fraction of the *absolute cost* during the summer or winter when the *time* and *yield* targets are set to their minimum and maximum values, respectively, and the system needs to provide additional radiation through supplemental lighting.

Because the *relative cost* is not affected by inflation and because the *relative cost* corresponding to the Reference Case is relatively constant, its standard deviation is a good indicator of variability. As it is shown in the right hand panels of Figure 8.23, the standard deviation of the *relative cost* is below 0.2.

Radiation Budget.

The goal of the *shading simulations* is to evaluate the performance of both the DSS and the Reference Case at blocking solar radiation and for this reason are performed only during the summer months. The radiation budget graphs (Figures 8.24, and 8.25) clearly show the increase in cumulative blocked solar radiation as the percentage of radiation that each screen within a configuration blocks increases and as the number of shade screens within a configuration also increases. The differences observed in the cumulative solar radiation across the different treatments is the result of different duration of the corresponding crop growth periods. The graphs show that the radiation budget is independent of the type of electricity market.

Except for the case when the percentage of radiation that each screen within a configuration blocks is 80%, all the DSS configurations are more effective than the Reference Case at blocking solar radiation. In every case the Reference Case exhibits some cumulative value of added supplemental light, an undesired effect in these simulations. When the percentage of radiation that each screen within a configuration blocks is 20% and 40%, the values of cumulative added supplemental light is zero or negligible for all the DSS treatments. The presence of some added supplemental lighting for the other cases is the result of the DSS blocking solar radiation beyond what is necessary to achieve maximum *time* and minimum *yield*.

Chapter 10

Summary and Conclusions

The use of supplemental lighting is a major expense for greenhouse tomato growers in the northeast of the U.S. because during winter months light is often the principal limiting factor for tomato production. Managing the use of supplemental lighting to achieve the grower's goals while minimizing the cost of electricity is a challenging task for a greenhouse operator for several reasons:

- Minimizing the cost of electricity and achieving the grower's goals of timing and yield act in opposite directions: the more supplemental lighting is used to achieve grower's goals, the higher the associated electricity cost,
- The price of electricity is not constant (i.e., varies hourly),
- The present crop needs are based on past and predicted values of different environmental factors that have an effect on the crop development, among them: Photosynthetically Active Radiation (PAR), carbon dioxide concentration, nutrients, temperature, and relative humidity.

For the present study a Decision Support System (DSS) was developed to manage the use of supplemental lighting for a tomato crop grown at the Rutgers EcoComplex Research and Demonstration Greenhouse located at the Burlington County Resource Recovery Complex, Columbus, NJ. The supplemental lighting system is powered by the electricity generated by an on-site 250 kW landfill gas-fired microturbine. Since most of the generated power is exported to the grid when it is not used in the greenhouse for supplemental lighting, optimizing the use of supplemental lighting can maximize the revenue from the exported electricity.

The DSS prioritizes crop needs and maximizes the value of the exported electricity by providing supplemental lighting during hours when the electricity prices are the lowest. The optimal lighting schedule to meet both goals is found by using the following main elements:

- A crop model that relates duration of growth period and yield to cumulative PAR energy,
- Predicted values of incoming solar radiation and electricity prices,
- An optimization algorithm that uses the output from the crop growth model, past and predicted values of solar radiation, and predicted values of electricity prices, to make a decision on a user defined time step basis to meet the grower's goals while maximizing the returns from the exported electricity.

The crop model used in this project was developed by Giniger et al. (1988) for a single truss tomato cropping system. The crop model assumes that cumulative PAR energy is the only input variable and the values of the other factors are kept within determined ranges (a valid assumption for a greenhouse environment). For implementation in a computer environment, this model has the advantage of consisting of a set of only two linear equations, one for the seedling or vegetative stage (period from emergence to flowering), and the other for the production stage (period from flowering to harvest).

Solar radiation is modeled through a linear relation using sky cover and solar radiation for a clear sky as regressor variables. The model is based on historic weather data from the National Solar Radiation Database (NSRDB), a discrete database spanning from 1991 to 2005 for 1,454 weather stations throughout the United States. Using this model and values for sky cover generated using the NSRDB, a long term prediction of hourly values of solar radiation for the different Julian days of the year was generated. The long term prediction of solar radiation is constantly updated with

short term predictions based on values of sky cover provided by the National Digital Forecast Database (NDFD). This approach has the advantage that solar radiation values for a clear sky require only the latitude and longitude of the location while forecast values of sky cover are readily available for any location in the United States.

The DSS was developed for the general case when the electricity is exported to the Day-Ahead or Real-Time wholesale electricity markets. Using historic data on electricity prices, available from PJM Interconnection (Regional Transmission Organization, RTO, that coordinates the movement of wholesale electricity in all or parts of 13 states, including New Jersey and Pennsylvania, and the District of Columbia), and historic data of meteorological variables, available from the NSRDB, two linear regressions were fit to model Day-Ahead and Real-Time electricity prices. In the Day-Ahead price model, the regressors are indicator variables (binary variables to indicate season, weekdays, and holidays) and quantitative variables based on meteorological quantities (cooling and heating degree hours). The Real-Time prices were modeled through a single linear regression with the Day-Ahead prices as the regressor.

Using these models and the values of the regressors generated using the available historic data, a long term prediction of Day-Ahead and Real-Time electricity price hourly values was generated for the different Julian days. Every time the Decisions Module is executed, the long term prediction of Day-Ahead electricity prices is updated: first, with a short term prediction based on the most recent forecast of meteorological variables (available from the NDFD website); and second, with the Day-Ahead electricity prices values settled for the next day (available from PJM).

According to this strategy, the DSS relies not on the prediction of Day-Ahead electricity prices but on their future values as reported by PJM. Only if the DSS has no access to those values because of an extraordinary event (e.g., power outage, values not available from the website), the prediction values of Day-Ahead electricity prices are used. The updated prediction of Day-Ahead prices is then used to update the long term prediction of Real-Time prices.

The DSS is executed on a time step defined by the user. For convenience and because of availability of certain historic data, it was chosen as one hour for simulation purposes. At the moment of execution, the DSS uses the output from the crop model (radiation need based on past values of solar radiation and grower's goals, and time window to provide it) and the updated prediction of solar radiation and electricity prices to make a decision about providing supplemental lighting or deploying the shade screens. The decision about providing supplemental lighting is based on an algorithm that ranks the future hours according to their corresponding electricity prices and the sensitivity to electricity prices defined by the user. The supplemental lighting is then assigned to the future hours according to their rankings. The shade screen selection algorithm was developed for the general case when the system is composed of an arbitrary number of screens.

The sensitivity to electricity prices is an input variable that provides the possibility of defining the level of cost optimization. At 100% price sensitivity the ranking of the future hours is solely based on the electricity prices and maximum emphasis is placed on cost optimization at achieving the crop timing and yield targets. At 0% price sensitivity, the ranking of the future hours is solely based on their proximity to the present and maximum emphasis is placed on immediacy at achieving the crop timing and yield targets.

The DSS was tested by simulation using five years (2000-2004) of historic electricity prices and meteorological data. The DSS simulation results were compared to the simulation results from a Reference Case based on conventional practices. In general, the results show that the performance of the DSS at achieving even extreme *time* and *yield* targets (minimum *time* and maximum *yield* targets during winter, and maximum *time* and minimum *yield* targets during summer) is similar in some cases and superior in others to the performance of the Reference Case. However, the results of using the DSS exhibit substantial energy and cost savings compared to using the Reference Case.

When the grower's goals are minimum *time* and maximum *yield*, at a supplemental lighting intensity of $200 \mu\text{mol}/\text{m}^2 \cdot \text{sec}$ the lighting energy use while implementing the DSS could be from 30% (during the summer) to 10% (during the winter) less compared to the energy use of the Reference Case. Also at a supplemental lighting intensity of $200 \mu\text{mol}/\text{m}^2 \cdot \text{sec}$, the supplemental lighting cost while implementing the DSS could be from 30% (during the summer) to 20% (during the winter) less compared to the lighting cost of the Reference Case. At higher values of supplemental lighting intensity ($250 \mu\text{mol}/\text{m}^2 \cdot \text{sec}$ and $300 \mu\text{mol}/\text{m}^2 \cdot \text{sec}$), the simulation results show that the energy and cost savings are even higher.

When the grower's goals are maximum *time* and minimum *yield*, a purely theoretical scenario to test the performance of the DSS at blocking unwanted radiation, the results showed that the DSS configurations were more effective than the Reference Case. In particular, the DSS implemented with a dual screen configuration (with each screen able to block 40% of incoming radiation) exhibited the best combination of *time*, *yield*, *energy use*, and *cost* results.

In general, the DSS provided substantial energy and cost savings compared to the Reference Case implemented following industry guidelines, and the possibility of having more control over the grower targets. The DSS is not location specific, it can be implemented in any location within the continental U.S.A. as long as the particulars of the local electricity market are taken into account. Although the DSS was developed for the particular case when the electricity is generated on-site and sold in the wholesale electricity market, it can be readily extended to the case of a commercial grower that uses grid electricity for supplemental lighting. In this scenario, by optimizing the use of supplemental lighting with the help of the DSS, the associated cost of electricity is minimized.

10.1 Future Work

The simulation results showed the effectiveness of the DSS but this is only the first step and it should be followed by the implementation of the DSS in a greenhouse. Only then can different details and situations that were not considered for the simulations become visible and their importance properly weighed. For simulation purposes, it was not necessary to develop a graphical user interface (GUI) or the live connectivity to the different online databases that the DSS requires; however, the implementation of the DSS in a greenhouse will require both.

There are several areas in which the DSS can be particularly improved. The descriptive crop model used restricts the application of the DSS to only one type of crop under very specific conditions. An explanatory crop model could accommodate more than one crop, offer more flexibility for the conditions under which it can be applied, and allow for evaluation of the impact of other factors in addition to solar radiation on crop growth and development.

The accuracy that the DSS can achieve for the grower's timing and yield targets can not be greater than the accuracy for these variables provided by the crop model. Since an explanatory model takes into account more of the factors that have an effect on the crop growth, it could potentially offer better accuracy for timing of production and yield, and as a consequence a DSS based on an explanatory model could achieve better accuracy for the grower's timing and yield targets.

However, the use of an explanatory model introduces important challenges:

- Although it may be possible to indirectly obtain the values of timing of production and yield from other variables in the model, explanatory models usually do not provide straightforward output values of these variables,
- Each of the variables on which the explanatory model depends requires an independent model to predict its values,

- The complexity of an explanatory model should not be such that its computational requirements exceed those for the intended use of the DSS.

The prediction of electricity prices is another area in which the DSS could be improved. Because the DSS relied only marginally on the prediction of electricity prices, the model used for prediction of electricity prices was relatively simple. A more sophisticated model that takes into account some of the particulars of the electricity prices (non linearity, extreme values) could potentially increase the ability of the DSS to decrease the supplemental lighting cost.

The DSS was written in the MATLAB language for the advantages that this numerical computing environment offered. However, MATLAB is not an open source product and that limits the implementation of the DSS to computers where this application is installed. Rewriting the code in a general purpose programming language like C++ will make future improvements easier and facilitate its distribution.

Appendices

Appendix A

Cost and Greenhouse Gas (GHG) Emissions Analysis

A main goal of the present study was to develop the algorithm of a Decision Support System (DSS) that, compared to the standard greenhouse lighting and shading control strategies (Reference Case), provides substantial cost and energy savings for greenhouse tomato production. In order to compare the effectiveness of the DSS algorithm to the Reference Case it was necessary to define metrics that only depend on the lighting intensity that the supplemental lighting system can provide at the top of the crop canopy independently of the particular lighting system configuration (type of lamps, mounting height, and floor area covered per lamp). For this reason, the lighting system configuration was not specified in any analysis previously done in the present study.

A cost and greenhouse gas (GHG) emissions analysis, however, requires that the lighting system configuration is specified. The cost and GHG emissions analysis performed here was based on the lighting simulations results for the case when the excess electricity is sold in the Real-Time electricity market. The lighting simulations refer to a real scenario in which a grower tends to minimize the crop growth period and maximize the harvest yield and for those reasons the DSS makes maximum use of the lighting system and thus the associated energy use and cost are the highest. Although the Real-Time electricity market was chosen for the analysis because small power producers are likely to sell excess electricity in this market, the results are transferable to the Day-Ahead electricity market because the behaviour of the DSS and the Reference case is almost identical in both markets (see Chapter 8).

The DSS lighting system configuration for the cost and GHG emissions analysis was based on the case with 100% price sensitivity and dimmable lights settings because they showed the largest energy and cost savings compared to the Reference Case introduced in the lighting simulations in the Results Chapter. Since these settings require that the lamps be continuously dimmable, the implementation of the DSS lighting system configuration was based on the use of LED lamps.

Two cases of lighting system configurations were considered for the Reference Case, one based on High Pressure Sodium (HPS) lamps, and another on Ceramic Metal Halide (CMH) lamps. Both the HPS and CMH lamps are commonly used in greenhouse lighting systems. The specific LED, HPS, and CMH lamps selected for the present study (Table A.1) were the ones that, according to Nelson and Bugbee (2013) provided the highest efficiency in converting electric power into Photosynthetic Photon Flux, PPF (the PPF is used to refer to the total radiation in the PAR range produced by the lamp).

In addition to the types of lamps, the lighting system configuration also requires that the mounting height and the floor area covered per lamp be specified for the different cases of supplemental lighting intensity at the top of the crop canopy used in the simulations: 0, 50, 100, 150, 200, 250, and 300 $\mu\text{mol}/\text{m}^2 \cdot \text{sec}$. For a given mounting height, the necessary lamps per unit floor area to achieve any of the previous values of lighting intensity is specific to the type of lamp used. For the lamps selected for this study, however, no data was found to establish a relationship between the supplemental lighting intensity at the top of the crop canopy and the associated floor area covered per lamp.

The approach followed in this study was to use the estimated values of lighting intensity at the top of the crop canopy throughout a 1-acre greenhouse for different lighting configurations using 400 Watt HPS lamps, Table A.2, obtained by Both (2004). These data were then used to generate values of lighting intensity at the top of the crop canopy for the lamps selected for the present study assuming that the

Table A.1: LED, HPS, and CMH fixtures selected for the cost and GHG emissions analysis (Nelson & Bugbee, 2013).

Type	LED Red/Blue [†]	HPS Electronic Ballast	CMH 3100 K (Agro)
Manufacturer	Lighting Sciences Group	PARsource	Cycloptics
Voltage (V)	120	208	208
Power* (W)	391	1024	337
PPF Output** ($\mu\text{mol}/\text{sec}$)	626	1328	483
PPF Efficiency ($\mu\text{mol}/\text{J}$)	1.60	1.30	1.44

[†] Maximum output of Red and Blue light only.

* Power consumption for the whole fixture.

** Integrated total PPF output per fixture.

total PPF output for a 400 W HPS lamp is 410 $\mu\text{mol}/\text{sec}$ (PPF output for the 400 W HPS fixture with magnetic ballast (manufactured by Sunlight Supply) according to Nelson and Bugbee (2013)), and that for a given mounting height (1.52 m (5 feet) for the present study) and floor area covered per lamp, the corresponding lighting intensity at the top of the crop canopy is proportional to the total lamp PPF output independently of the type of lamp. For example, for a lighting system based on LED lamps with a PPF output of 626 $\mu\text{mol}/\text{sec}$ per lamp, a mounting height of 1.52 m, and a floor area covered per lamp of 10.56 m^2/lamp , the lighting intensity at the top of the crop canopy would be $52 \cdot \frac{626}{410} \mu\text{mol}/\text{m}^2 \cdot \text{sec} = 79.40 \cdot \mu\text{mol}/\text{m}^2 \cdot \text{sec}$. The generated values for the supplemental lighting intensity for the selected lamps are shown in Table A.3.

With the data from Table A.3 it is possible to fit a linear regression between the lamps per unit floor area and the supplemental lighting intensity for the different lamps (left column in Figures A.1 to A.3), and use the resulting linear regression coefficients to predict, for each lamp, the number of lamps per unit floor area required to achieve the supplemental lighting intensity at the top of the crop canopy considered in the simulations. The predicted values for the number of lamps per unit floor area

Table A.2: Supplemental lighting intensity at the top of the crop canopy throughout a 1-acre greenhouse for different lighting configurations using 400 Watt HPS lamps (Both, 2004).

floor area covered/lamp		Supplemental Lighting Intensity ($\mu\text{mol}/\text{m}^2 \cdot \text{sec}$)	
($\text{feet}^2/\text{lamp}$)	(m^2/lamp)	mounting height 2.44 m (8 feet)	mounting height 1.52 m (5 feet)
113.70	10.56	49	52
74.50	6.92	75	80
55.40	5.15	100	107
35.10	3.26	149	162
27.30	2.54	202	213

Mounting height: distance between the bottom of the fixture reflector and the top of the crop canopy.

Table A.3: Generated values for the supplemental lighting intensity at the top of the crop canopy for the selected LED, HPS, and CMH lamps when the mounting height is 1.52 m (5 feet).

m^2/lamp	Generated Values for the Supplemental Lighting Intensity ($\mu\text{mol}/\text{m}^2 \cdot \text{sec}$)		
	LED (626 $\mu\text{mol}/\text{sec}$)	HPS (1328 $\mu\text{mol}/\text{sec}$)	CMH (483 $\mu\text{mol}/\text{sec}$)
10.56	79.40	168.43	61.26
6.92	122.15	259.12	94.24
5.15	163.37	346.58	126.05
3.26	247.35	524.72	190.84
2.54	325.21	689.91	250.92

and the price of the corresponding lighting fixture are used in the return on investment (ROI) analysis.

In a similar way, using the data shown in Tables A.1 and A.3, it is possible to fit a linear regression between the power consumption per unit floor area and the lighting intensity for the different lamp configuration (right column in Figures A.1 to A.3); and then use the resulting linear regression coefficients, the corresponding relative values of supplemental lighting energy use and cost (energy and cost metrics, E_m and C_m , respectively) from the lighting simulation results, and Equations A.1 and

A.2 relating the absolute and relative values of lighting energy use and cost introduced in the Results Chapter to find, for each lamp configuration, the yearly average values of absolute lighting energy use and cost per unit floor area corresponding to each supplemental lighting intensity at the top of the crop canopy considered in the simulations.

$$E/A = \lambda \cdot E_m \quad (\text{A.1})$$

$$C/A = \lambda \cdot C_m \quad (\text{A.2})$$

For the calculation of the yearly average values of absolute lighting energy use and cost per unit floor area, it is assumed that the tomato cropping system operates continuously in a batch mode so that only 6% of the available production area of the greenhouse space is allocated to seedling production and the remaining 94% is simultaneously used by four crop blocks in the production stage, each with a staggered 2-week harvest period, for a total of 26 crop blocks in a year (Giniger et al., 1988). For any of the crop blocks, the yearly average relative lighting energy use and cost are calculated averaging the corresponding winter and summer values from the lighting simulation results.

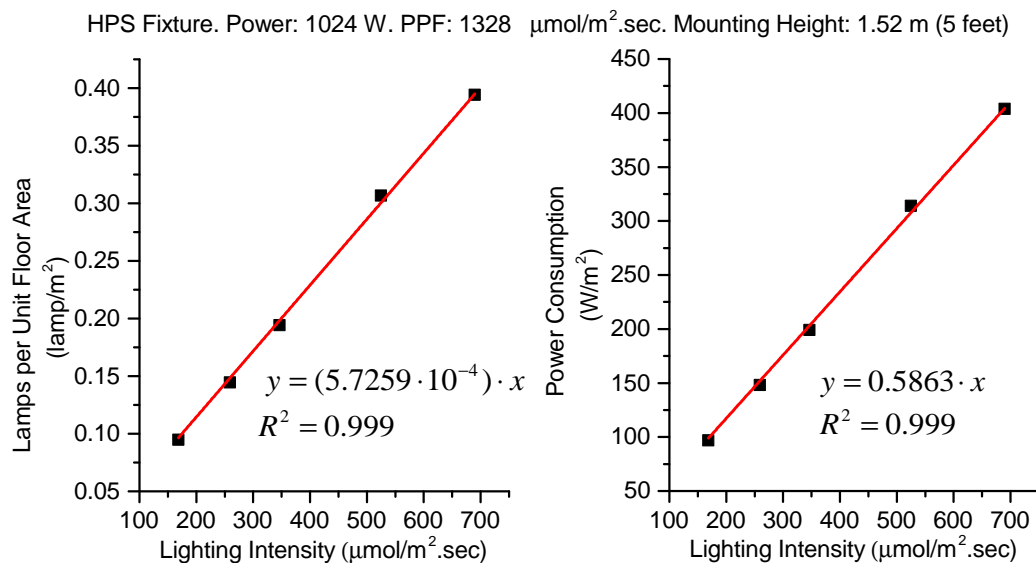


Figure A.1: Number of lamps and power consumption per unit floor area vs. lighting intensity for the selected HPS fixture mounted at 1.52 m (5 feet) above the crop canopy.

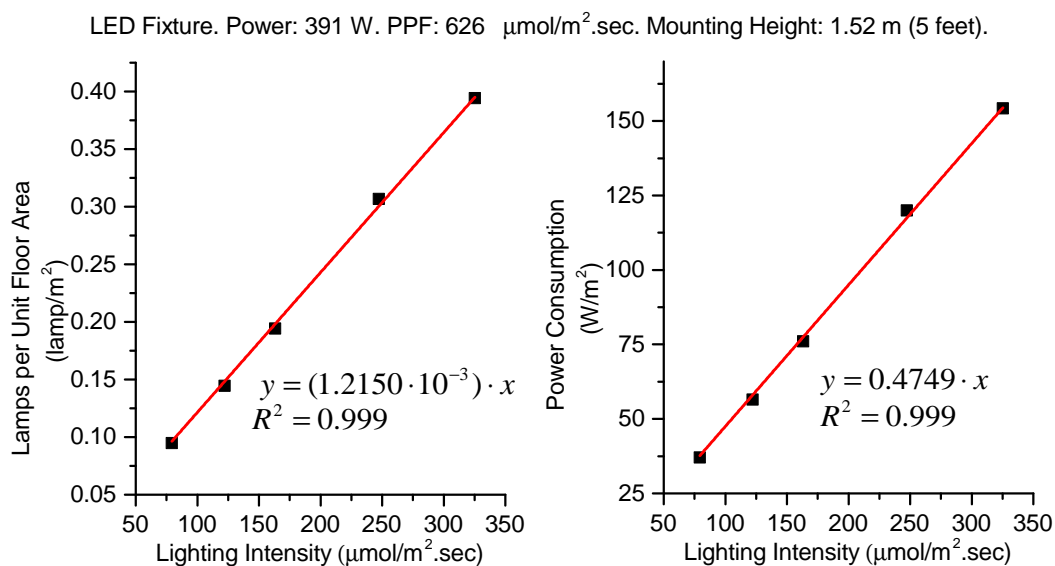


Figure A.2: Number of lamps and power consumption per unit floor area vs. lighting intensity for the selected LED fixture mounted at 1.52 m (5 feet) above the crop canopy.

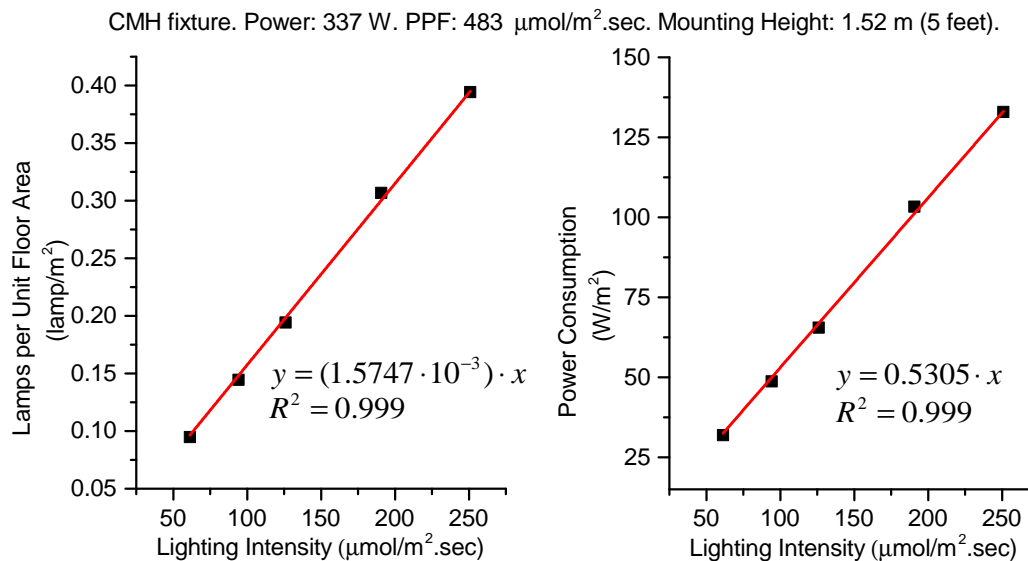


Figure A.3: Number of lamps and power consumption per unit floor area vs. lighting intensity for the selected CMH fixture mounted at 1.52 m (5 feet) above the crop canopy.

The goal of the cost and GHG emissions analysis is to compare a lighting system operating according to the DSS at 100% price sensitivity and dimmable lights settings using LED lamps to a lighting system operating according to the standard greenhouse lighting and shading control strategies using HPS lamps in one case, and on CMH in another. The comparison is made across the different cases of supplemental lighting intensity at the top of the crop canopy considered in the simulations and includes the yearly average values of supplemental lighting energy use and cost savings, GHG emissions reduction, and return on investment. The estimate for the reduction in GHG emissions from reduced energy use is based on the Emissions & Generation Resource Integrated Database (eGRID) that states that the U.S. annual non-baseload CO_2 output emission rate is $7.0555 \cdot 10^{-4}$ metric tons CO_2 per kWh of electricity produced.

The yearly return on investment refers to the replacement of the HPS or CMH lamps operated according to the standard lighting and shading control strategies for

LED lamps operated according to the DSS at 100% price sensitivity and dimmable lights settings. For this reason, it is based only on the purchase cost difference and yearly average lighting cost savings between the lighting systems. The lighting cost savings do not include the potential revenues from the NJ Class I Renewable Energy Credits (REC) because of the low REC prices in the financial market during the last few years (last reported values in July 2010 were below 3\$/MWh according to the NJ Clean Energy Program (*New Jerseys Renewable Portfolio Standard Rules. 2010 Annual Report, 2011*)).

Cost and GHG Emissions analysis results. DSS and Reference Case based on LED and HPS lamps, respectively.

Table A.4: Configuration and yearly average values of supplemental lighting energy use, cost, and GHG emissions for a lighting system operated according to the DSS at 100% price sensitivity and dimmable lights settings using selected LED lamps (Table A.1), and another operated according to the standard lighting and shading control strategies using selected HPS lamps (Table A.1).

Lighting Intensity ($\mu mol/m^2 \cdot sec$)	Lamps/Area ($lamps/m^2$)		Energy Use* (MWh/m^2)		Cost* ($2013\$/m^2$)		GHG Emissions* (Kg/m^2)**	
	LED	HPS	LED	HPS	LED	HPS	LED	HPS
50	0.06	0.03	0.18	0.16	9.67	8.43	127.55	113.25
100	0.12	0.06	0.33	0.32	17.36	17.01	233.94	227.59
150	0.18	0.09	0.43	0.48	21.37	25.47	303.14	340.63
200	0.24	0.11	0.48	0.64	22.17	33.90	337.28	453.46
250	0.30	0.14	0.50	0.80	21.76	42.43	355.01	566.91
300	0.36	0.17	0.52	0.96	21.17	50.73	367.48	679.92

* Supplemental lighting system yearly average values.

** Kg of CO_2 that would have the same global warming potential as the greenhouse gasses emitted (CO_2 equivalent).

Table A.5: Actual and projected lighting fixtures purchase cost per unit area for a lighting system operated according to the DSS at 100% price sensitivity and dimmable lights settings using selected LED lamps (Table A.1), and another operated according to the standard lighting and shading control strategies using selected HPS lamps (Table A.1).

Lighting Intensity ($\mu\text{mol}/\text{m}^2 \cdot \text{sec}$)	Lighting Fixtures Purchase Cost (2013\$/ m^2)					
	Prices per LED Fixture					Price per HPS Fixture
	\$1200*	\$1000†	\$800†	\$600†	\$400†	\$380*
50	72.90	60.75	48.60	36.45	24.30	10.88
100	145.80	121.50	97.20	72.90	48.60	21.76
150	218.69	182.25	145.80	109.35	72.90	32.65
200	291.59	242.99	194.40	145.80	97.20	43.53
250	364.49	303.74	242.99	182.25	121.50	54.41
300	437.39	364.49	291.59	218.69	145.80	65.29

* Actual prices as of June 2013 (Nelson & Bugbee, 2013).

† Projected prices anticipating future price drops.

Table A.6: Return on investment for a lighting system operated according to the DSS at 100% price sensitivity and dimmable lights settings using selected LED lamps (Table A.1). The reference case is a lighting system operated according to the standard lighting and shading control strategies using selected HPS lamps (Table A.1). The return on investment analysis is based only on the purchase costs (the installation costs are considered similar for both lighting systems).

Lighting Intensity ($\mu\text{mol}/\text{m}^2 \cdot \text{sec}$)	Return on Investment ($\%/year$)					
	LED Fixture Prices					HPS Fixture Price
	\$1200*	\$1000 [†]	\$800 [†]	\$600 [†]	\$400 [†]	\$380*
50	-2.00	-2.48	-3.28	-4.84	-9.23	Reference
100	-0.29	-0.36	-0.47	-0.69	-1.32	Reference
150	2.20	2.74	3.62	5.34	10.18	Reference
200	4.73	5.88	7.77	11.47	21.85	Reference
250	6.67	8.29	10.96	16.17	30.82	Reference
300	7.95	9.88	13.06	19.27	36.73	Reference

* Actual prices as of June 2013 (Nelson & Bugbee, 2013).

[†] Projected prices anticipating future price drops.

Cost and GHG Emissions analysis results. DSS and Reference Case based on LED and CMH lamps, respectively.

Table A.7: Configuration and yearly average values of supplemental lighting energy use, cost, and GHG emissions for a lighting system operated according to the DSS at 100% price sensitivity and dimmable lights settings using selected LED lamps (Table A.1), and another operated according to the standard lighting and shading control strategies using selected CMH lamps (Table A.1).

Lighting Intensity ($\mu\text{mol}/\text{m}^2 \cdot \text{sec}$)	Lamps/Area (lamps/m^2)		Energy Use* (MWh/m^2)		Cost* ($2013\$/\text{m}^2$)		GHG Emissions* (Kg/m^2)**	
	LED	CMH	LED	CMH	LED	CMH	LED	CMH
50	0.06	0.08	0.16	0.15	8.75	7.63	115.41	102.47
100	0.12	0.16	0.30	0.29	15.71	15.39	211.68	205.94
150	0.18	0.24	0.39	0.44	19.34	23.05	274.30	308.22
200	0.24	0.31	0.43	0.58	20.06	30.68	305.19	410.32
250	0.30	0.39	0.45	0.73	19.69	38.40	321.23	512.98
300	0.36	0.47	0.47	0.87	19.15	45.91	332.52	615.23

* Supplemental lighting system yearly average values.

** Kg of CO_2 that would have the same global warming potential as the greenhouse gasses emitted (CO_2 equivalent).

Table A.8: Actual and projected lighting fixtures purchase cost per unit area for a lighting system operated according to the DSS at 100% price sensitivity and dimmable lights settings using selected LED lamps (Table A.1), and another operated according to the standard lighting and shading control strategies using selected CMH lamps (Table A.1).

Lighting Intensity ($\mu\text{mol}/\text{m}^2 \cdot \text{sec}$)	Lighting Fixtures Purchase Cost (2013\$/ m^2)					
	Prices per LED Fixture					Price per CMH Fixture
	\$1200*	\$1000†	\$800†	\$600†	\$400†	\$700*
50	72.90	60.75	48.60	36.45	24.30	55.11
100	145.80	121.50	97.20	72.90	48.60	110.23
150	218.69	182.25	145.80	109.35	72.90	165.34
200	291.59	242.99	194.40	145.80	97.20	220.46
250	364.49	303.74	242.99	182.25	121.50	275.57
300	437.39	364.49	291.59	218.69	145.80	330.68

* Actual prices as of June 2013 (Nelson & Bugbee, 2013).

† Projected prices anticipating future price drops.

Table A.9: Return on investment for a lighting system operated according to the DSS at 100% price sensitivity and dimmable lights settings using selected LED lamps (Table A.1). The reference case is a lighting system operated according to the standard lighting and shading control strategies using selected CMH lamps (Table A.1). The return on investment analysis is based only on the purchase costs (the installation costs are considered similar for both lighting systems).

Lighting Intensity ($\mu\text{mol}/\text{m}^2 \cdot \text{sec}$)	Return on Investment (%/year)					
	LED Fixture Prices					CMH Fixture Price
	\$1200*	\$1000†	\$800†	\$600†	\$400†	\$700*
50	-6.30	-19.89	NA	NA	NA	Reference
100	-0.90	-2.85	NA	NA	NA	Reference
150	6.95	21.94	NA	NA	NA	Reference
200	14.92	47.09	NA	NA	NA	Reference
250	21.04	66.40	NA	NA	NA	Reference
300	25.07	79.13	NA	NA	NA	Reference

* Actual prices as of June 2013 (Nelson & Bugbee, 2013).

† Projected prices anticipating future price drops.

NA refers to the case when the purchase cost of the LED system is lower than the reference case.

Although the results shown in Tables A.4 to A.9 are based on assumptions that need more thorough analysis, they are a starting point to consider the environmental and economic effects, in the case of greenhouse tomato production, of replacing a lighting system based on traditional HPS or CMH lamps operated according to the standard lighting and shading control strategies with a lighting system based on LED lamps operated according to the strategies determined by the DSS.

The present analysis is not intended to answer the question of which value of lighting intensity the lighting system should provide. It is assumed that the grower already knows the desired intensities based on other considerations, such as the increase in revenues from extra yield from supplemental lighting depending on the greenhouse geographic location and product prices. What this analysis shows is that if the value of lighting intensity that a lighting system should provide is known, it is possible to determine which of the evaluated lighting systems is preferable from an environmental or economic point of view.

Tables A.4 and A.7 show that for supplemental lighting intensities above 100 $\mu\text{mol}/\text{m}^2 \cdot \text{sec}$ the LED system provides substantial reductions of GHG emissions compared to the HPS or CMH systems. The higher the required intensity of the lighting system, the higher the reduction. For supplemental lighting intensities above 200 $\mu\text{mol}/\text{m}^2 \cdot \text{sec}$, the reduction of GHG emissions from the LED system compared to the HPS or CMH systems for a 1-acre greenhouse is above 400 metric tons, which is equivalent to the annual greenhouse gas emissions from 83 passenger vehicles (using EPA estimate).

The return on investment analysis includes the current prices of the HPS and CMH fixtures, and a series of prices for the LED fixtures, the highest of which correspond to the current price (\$1200). The reason for this is that while the HPS and CMH lamps are mature technologies, LED lamps are relatively new in the greenhouse lighting industry and their cost is expected to decrease. Table A.6 shows that the return on investment for the LED system compared to the HPS system increases as the lighting intensity increases or the price of the LED fixture decreases. The increase of the return on investment as the price of the LED fixture decreases is an expected result, but the increase of the return on investment as the lighting intensity increases is an indication that the lighting cost savings for the LED system increases faster than the extra purchase cost, a result determined by the efficiency of the DSS at minimizing cost.

Compared to the HPS system, the returns on investment for the LED system are relatively low for the current price of the LED fixture. As Table A.6 shows, even when the required lighting intensity is $300 \mu\text{mol}/\text{m}^2 \cdot \text{sec}$, it takes more than 10 years to recover the additional purchase cost of an LED system at the current price of the LED fixture ($\text{ROI} = 7.95\%/year$). If the price of the LED fixture decreases by a factor of 2, the return on investment for the LED system approaches $20\%/year$ (which means that in around five year the additional purchase cost is recovered) when the required lighting intensity is $300 \mu\text{mol}/\text{m}^2$. In a similar way, if the price of the LED fixture decreases by a factor of 3, the return on investment for the LED system is above $20\%/year$ when the required lighting intensity is $200 \mu\text{mol}/\text{m}^2$.

The LED system becomes more attractive compared to the CMH system than to the HPS system. Table A.7 shows that even at the current price of the LED fixture, the return on investment for the LED system is above $20\%/year$ when the required lighting intensity is $250 \mu\text{mol}/\text{m}^2$. If the price of the LED fixture decreases from the current price, \$1200, to only \$1000, the return on investment for the LED system is above $20\%/year$ when the required lighting intensity is just $150 \mu\text{mol}/\text{m}^2$. For further decreases of the price of the LED fixture, the purchase cost of the LED system is lower than the purchase cost of the CMH system, which is represented in Table A.7 by *NA* since those cases do not represent investment.

Appendix B

Decision Support System Programming Code

To access the MATLAB programming code for the Decision Support System (DSS), auxiliary data (weather data, solar radiation measurements at the greenhouse, electricity prices), and results data, contact me at:

arielm@eden.rutgers.edu or amartinc1271@hotmail.com

All the code is contained in the folder *MATLAB* and the data in the folder *MATLAB_DATA*. The folder *MATLAB* contains more than 75 user defined functions and several scripts (a function and a script are series of statements: a function accepts input and output arguments but a script does not). The DSS comprises four types of simulations and to each of them corresponds a MATLAB script:

- DSS simulation for using supplemental lighting.
Corresponding script: *s_simulation_splight.m*
- DSS simulation for using the shade screens.
Corresponding script: *s_simulation_screens.m*
- Reference Case simulations for using supplemental lighting.
Corresponding script: *s_simulation_splightstandard.m*
- Reference Case simulation for using the shade screens.
Corresponding script: *s_simulation_screenstandard*

Running these scripts requires the installation of the MATLAB software. Once the software is installed, it is necessary to download the folders *MATLAB* and *MATLAB_DATA* to the *Documents* folder on the computer that will run the simulations.

In the scripts, it is possible to specify the values of different variables (e.g., year of simulation, electricity market, supplemental light values, sensitivity to electricity prices) according to the desired levels. The program sends the simulation results to the folder *dat_modeling* within *MATLAB_DATA* (the *dat_modeling* folder should be created and empty before the simulations are run).

The *MATLAB* folder also contains the functions necessary to run the previous scripts. Unless self explanatory, the functions contain a description of their use and arguments. Although running the scripts or functions requires the installation of MATLAB, the code could be viewed and analyzed using the free application development environment *Visual Studio Express Edition* (<http://www.microsoft.com/visualstudio/eng/products/visual-studio-express-products>).

Appendix C

DSS Auxiliary Data and Simulation Results

The folder *MATLAB_DATA* contains different subfolders to store the auxiliary data and the simulation results. The auxiliary data include the historic weather data from the National Solar Radiation Database (NSRDB), the electricity price data, and solar radiation data measured at the greenhouse used for the present study (inside and outside the greenhouse building).

The weather data is found within the subfolder *dat_meteorol* and consists of the historic data from the NSRDB for the weather stations within the geographic region of the electricity market Regional Transmission Organization (PJM for the present study). The weather data is used by the DSS to create the model to predict solar radiation.

The subfolder *dat_electmarket* contains the historic electricity price data for the different utility companies under PJM. This data is used to model the electricity prices. The solar radiation data measured at the greenhouse is contained within the subfolder *dat_sensors*. This data is used to model the solar radiation values inside the greenhouse from the solar radiation values values outside.

The hourly simulation results are stored within the subfolder *simulation_hourly*. For each year from 2000 through 2004 there are 10 files in Excel format containing the simulation results for the four different cases previously described in Appendix B. The name of the files corresponding to the year 2000 are presented as a way to explain the convention used to name the files:

2000_lightsum_da_hourly.xls: year 2000 DSS hourly simulation results while using supplemental lighting during the summer. Case of excess electricity exported

to the Day Ahead Electricity Market.

2000_lightsum_rt_hourly.xls: year 2000 DSS hourly simulation results while using supplemental lighting during the summer. Case of excess electricity exported to the Real Time Electricity Market.

2000_lightwin_da_hourly.xls: year 2000 DSS hourly simulation results while using supplemental lighting during the winter. Case of excess electricity exported to the Day Ahead Electricity Market.

2000_lightwin_rt_hourly.xls: year 2000 DSS hourly simulation results while using supplemental lighting during the winter. Case of excess electricity exported to the Real Time Electricity Market.

2000_screens_dart_hourly.xls: year 2000 DSS hourly simulation results while using the shade screens. Cases of excess electricity exported to the Day Ahead and Real Time Electricity Markets.

std2000_lightsum_da_hourly.xls: year 2000 Reference Case hourly simulation results while using supplemental lighting during the summer. Case of excess electricity exported to the Day Ahead Electricity Market.

std2000_lightsum_rt_hourly.xls: year 2000 Reference Case hourly simulation results while using supplemental lighting during the summer. Case of excess electricity exported to the Real Time Electricity Market.

std2000_lightwin_da_hourly.xls: year 2000 Reference Case hourly simulation results while using supplemental lighting during the winter. Case of excess electricity exported to the Day Ahead Electricity Market.

std2000_lightwin_rt_hourly.xls: year 2000 Reference Case hourly simulation results while using supplemental lighting during the winter. Case of excess electricity exported to the Real Time Electricity Market.

std2000_screens_dart_hourly.xls: year 2000 Reference Case hourly simulation results while using the shade screens. Cases of excess electricity exported to the Day Ahead and Real Time Electricity Markets.

Each of these files contains multiples sheet. A single sheet corresponds to a specific set of values of different variables. For example, within the file *2000_lightsum_da_hourly.xls*, the sheet *da2000st100_pdvslf200_1sc50* corresponds to the following case:

da: Day-Ahead electricity prices

2000: year 2000

st100: 100 percent sensitivity to electricity prices

pdv: prediction variable (duration of the decision time interval. See section 7.3.5)

slf200: supplemental lighting fixed (non-dimmable lights) at $200 \mu\text{mol}/\text{m}^2 \cdot \text{secec}$

1sc50: a single shade screen blocking 50 percent of incoming radiation.

The same nomenclature is used throughout all the sheets in the different files. The columns headings within each sheet are self explanatory.

The files within the subfolder *simulation_results* contain the final *crop growth period, yield, energy use, energy use ratio, cost, and cost ratio*, for the different simulations. The files within *simulation_results* are named following a similar convention as before, e.g.

2000_lightsum_da_results.xls: year 2000 final results for the DSS and the Reference Case while using supplemental lighting during the summer. Case of excess electricity exported to the Day Ahead Electricity Market.

2000_screens_rt_results.xls: year 2000 final results for the DSS and the Reference Case while using the shade screens. Case of excess electricity exported to the Real Time Electricity Market.

The sheets within these files correspond to *crop growth period, yield, energy use, energy use ratio, cost, and cost ratio*. Within each sheet, the column headings follow a nomenclature similar to the sheet nomenclature previously explained. The rows within a sheet correspond to the different values of the variables that correspond to

the type of simulation: for the lighting simulations the rows correspond to values of supplemental lighting intensity, for the shading simulations the rows correspond to percent of incoming radiation blocked by each screen within a configuration.

The averages of the yearly results are contained in files with similar names. For example, the file *avge.lightwin_rt_results.xls* corresponds to the average (over the years 2000-2004) of the final results for the DSS and the Reference Case while using the supplemental lighting during the winter when the excess electricity exported to the Real Time Electricity Market.

References

- 109th US Congress. (2005). Energy policy act of 2005. *Public Law 58. U.S. Government Printing Office.*
- Aggarwal, S. K., Saini, L. M., & Kumar, A. (2009). Electricity price forecasting in deregulated markets: A review and evaluation. *International Journal of Electrical Power & Energy Systems*, 31(1), 13-22.
- Albright, L. D. (2005). *Energy Management for Controlled Environment Agriculture (CEA) Tomato Production.* Cornell University. Report Submitted to NYSERDA. Retrieved on 01, 07, 2012. (<http://www.cornellcea.com/attachments/TomatoFinalReport.pdf>)
- Albright, L. D., Both, A. J., & Chiu, A. J. (2000). Controlling greenhouse light to a consistent daily integral. *Transactions of the ASAE*, 43(2), 421-431.
- Ångström, A. (1924). Solar and terrestrial radiation. Report to the international commission for solar research on actinometric investigations of solar and atmospheric radiation. *Quarterly Journal of the Royal Meteorological Society*, 50(210), 121-126.
- Archived Consumer Price Index Detailed Report Information.* (2012). Bureau of Labor Statistics. Retrieved on 01, 07, 2012. (http://www.bls.gov/cpi/cpi_dr.htm)
- Bhargava, H. K., Power, D. J., & Sun, D. (2007). Progress in web-based decision support technologies. *Decision Support Systems*, 43(4), 1083-1095.
- Bhargava, H. K., Sridhar, S., & Herrick, C. (1999). Beyond spreadsheets: tools for building decision support systems. *Computing Practices*, 32(3), 31-39.
- Both, A. J. (2004). Greenhouse supplemental lighting using HID lamps. *Greenhouse*

Product News, 14(12), 48–53.

- Brinsfield, R., Yaramanoglu, M., & Wheaton, F. (1984). Ground-level solar-radiation prediction model including sky cover effects. *Solar Energy*, 33(6), 493-499.
- Bristow, K. L., & Campbell, G. S. (1984). On the relationship between incoming solar radiation and daily maximum and minimum temperature. *Agricultural and Forest Meteorology*, 31(2), 159-166.
- Carrier, M., Gosselin, A., & Gauthier, L. (1994). Description of a crop growth model for the management of supplemental lighting in greenhouses. *Horticultural Technology*, 4(4), 383-389.
- Catalao, J. P. S., Mariano, S., Mendes, V. M. F., & Ferreira, L. (2007). Short-term electricity prices forecasting in a competitive market: A neural network approach. *Electric Power Systems Research*, 77(10), 1297-1304.
- Conejo, A. J., Plazas, M. A., Espinola, R., & Molina, A. B. (2005). Day-ahead electricity price forecasting using the wavelet transform and ARIMA models. *IEEE Transactions on Power Systems*, 20(2), 1035-1042.
- Contreras, J., Espinola, R., Nogales, F. J., & Conejo, A. J. (2003). ARIMA models to predict next-day electricity prices. *IEEE Transactions on Power Systems*, 18(3), 1014-1020.
- Cook, R., & Calvin, L. (2005). *Greenhouse Tomatoes Change the Dynamics of the North American Fresh Tomato Industry*. USDA. Economic Reserach Report No. 2. Retrieved on 01, 07, 2012. (<http://www.ers.usda.gov/publications/err-economic-research-report/err2.aspx>)
- Davies, J. A., & McKay, D. C. (1988). Estimating solar-radiation from incomplete cloud data. *Solar Energy*, 41(1), 15-18.
- Dayan, E., Van Keulen, H., Jones, J. W., Zipori, I., Shmuel, D., & Challa, H. (1993a). Development, calibration and validation of a greenhouse tomato growth-model .1. description of the model. *Agricultural Systems*, 43(2), 145-163.
- Dayan, E., Van Keulen, H., Jones, J. W., Zipori, I., Shmuel, D., & Challa, H. (1993b).

- Development, calibration and validation of a greenhouse tomato growth-model .2. field calibration and validation. *Agricultural Systems*, 43(2), 165-183.
- Demers, D.-A., Dorais, M., Wien, C. H., & Gosselin, A. (1998). Effects of supplemental light duration on greenhouse tomato (*Lycopersicon esculentum* Mill.) plants and fruit yields. *Scientia horticultrae*, 74(4), 295-306.
- Duffie, J. A., & Beckman, W. A. (2006). *Solar Engineering of Thermal Processes* (3rd ed.). John Wiley & Sons.
- Garcia, C. E., Prett, D. M., & Morari, M. (1989). Model predictive control: Theory and practice - A survey. *Automatica*, 25(3), 335-348.
- Gary, C., Jones, J. W., & Tchamitchian, M. (1998). Crop modelling in horticulture: state of the art. *Scientia Horticulturae*, 74(1-2), 3-20.
- Giniger, M. S., McAvoy, R. J., Giacomelli, G. A., & Janes, H. W. (1988). Computer-simulation of a single truss tomato cropping system. *Transactions of the ASAE*, 31(4), 1176-1179.
- Guirguis, H. S., & Felder, F. A. (2004). Further advances in forecasting day-ahead electricity prices using time series models. *KIEE International Transactions on Power Engineering*, 4(3), 159-166.
- Hanson, C. L., Cumming, K. A., Woolhiser, D. A., & Richardson, C. W. (1994). Microcomputer program for daily weather simulation in the contiguous United States. *US Department of Agriculture, Agricultural Research Service, ARS-114. USDA, Washington, DC.*
- Hargreaves, G. L., Hargreaves, G. H., & Riley, J. P. (1985). Irrigation water requirements for senegal river basin. *Journal of Irrigation and Drainage Engineering*, 111(3), 265-275.
- Heuvelink, E. (1996). Dry matter partitioning in tomato: Validation of a dynamic simulation model. *Annals of Botany*, 77(1), 71-80.
- Heuvelink, E. (1999). Evaluation of a dynamic simulation model for tomato crop growth and development. *Annals of Botany*, 83(4), 413-422.

- Heuvelink, E. P., & Challa, H. (1989). Dynamic optimization of artificial lighting in greenhouses. In *Acta Horticulturae (ISHS) 260. International Symposium on Growth and Yield Control in Vegetable Production* (pp. 401–412).
- Hoogenboom, G. (2000). Contribution of agrometeorology to the simulation of crop production and its applications. *Agricultural and Forest Meteorology*, *103*(1-2), 137-157.
- Hunt, L. A., Kuchar, L., & Swanton, C. J. (1998). Estimation of solar radiation for use in crop modelling. *Agricultural and Forest Meteorology*, *91*(3-4), 293-300.
- Johnson, G. L., Hanson, C. L., Hardegree, S. P., & Ballard, E. B. (1996). Stochastic weather simulation: Overview and analysis of two commonly used models. *Journal of Applied Meteorology*, *35*(10), 1878-1896.
- Jones, J. W., Dayan, E., Allen, L. H., Van Keulen, H., & Challa, H. (1991). A dynamic tomato growth and yield model (TOMGRO). *Transactions of the ASAE*, *34*(2), 663-672.
- Jones, J. W., Kenig, A., & Vallejos, C. E. (1999). Reduced state-variable tomato growth model. *Transactions of the ASAE*, *42*(1), 255-265.
- Kano, A., & Van Bavel, C. H. M. (1988). Design and test of a simulation-model of tomato growth and yield in a greenhouse. *Journal of the Japanese Society for Horticultural Science*, *56*(4), 408-416.
- Kasten, F., & Czeplak, G. (1980). Solar and terrestrial radiation dependent on the amount and type of cloud. *Solar Energy*, *24*(2), 177-189.
- Kenig, A., & Jones, J. W. (1997). *TOMGRO V3.0: A Dynamic Model of Tomato Growth and Yield*. Ch. II-5 In: Optimal environmental control for indeterminate greenhouse crops. Eds. Seginer I., Jones J.W., Gutman P. Vallejos C.E., BARD Research Report No. IS-1995-91RC. Haifa, Israel.
- Kutner, M. H., Nachtsheim, C., & Neter, J. (2004a). *Applied Linear Regression Models* (4th ed.). McGraw-Hill Irwin.
- Kutner, M. H., Nachtsheim, C., & Neter, J. (2004b). *Applied Linear Regression*

- Models* (4th ed.). McGraw-Hill Irwin.
- Lentz, W. (1998). Model applications in horticulture: a review. *Scientia Horticulturae*, 74(1-2), 151-174.
- Liebig, H. P. (1989). Development of planning models-methodological aspects. *Acta Horti.*, 248, 159-166.
- Light and Lighting Control in Greenhouses*. (2010). Argus Control Systems Ltd. Retrieved on 01, 07, 2012. (<http://www.arguscontrols.com/resources/Light-and-Lighting-Control-in-Greenhouses.pdf>)
- Mandal, P., Senjyu, T., Urasaki, N., Funabashi, T., & Srivastava, A. K. (2006). Electricity price forecasting for PJM day-ahead market. In *Power Systems Conference and Exposition, 2006. PSCE'06. 2006 IEEE PES* (p. 1321-1326). IEEE.
- Mandal, P., Senjyu, T., Urasaki, N., Funabashi, T., & Srivastava, A. K. (2007). A novel approach to forecast electricity price for PJM using neural network and similar days method. *IEEE Transactions on Power Systems*, 22(4), 2058-2065.
- Marcelis, L. F. M., Heuvelink, E., & Goudriaan, J. (1998). Modelling biomass production and yield of horticultural crops: a review. *Scientia Horticulturae*, 74(1-2), 83-111.
- Marsh, L. S., & Albright, L. D. (1991). Economically optimum day temperatures for greenhouse hydroponic lettuce production. i. a computer model. *Transactions of the ASAE*, 34(2), 550-556.
- Masters, G. M. (2004). *Renewable and Efficient Electric Power Systems* (1st ed.). Wiley-IEEE Press.
- Maxwell, E. L. (1998). METSTAT the solar radiation model used in the production of the national solar radiation data base (NSRDB). *Solar Energy*, 62(4), 263-279.
- McAvoy, R. J. (1988). *Development of a Management Strategy for a Single Truss Tomato Production System*. PhD. dissertation. Rutgers University, New Brunswick, NJ.

- McAvoy, R. J., Janes, H. W., Giacomelli, G. A., & Giniger, M. S. (1989). Validation of a computer-model for a single-truss tomato cropping system. *Journal of the American Society for Horticultural Science*, 114(5), 746-750.
- Monteith, J. L. (1996). The quest for balance in crop modeling. *Agronomy Journal*, 88(5), 695-697.
- Montgomery, D. C., Peck, E. A., & Vining, G. G. (2001). *Introduction to Linear Regression Analysis* (3rd ed.). Wiley.
- Nelson, J. A., & Bugbee, B. (2013). *Supplemental greenhouse lighting: Return on investment for LED and HPS fixtures*. Manuscript in preparation. Retrieved on 08, 20, 2013. (http://cpl.usu.edu/files/publications/factsheet/pub__4964212.pdf)
- New Jerseys Renewable Portfolio Standard Rules. 2010 Annual Report*. (2011). Office of Clean Energy. New Jerseys Board of Public Utilitie. Retrieved on 09, 22, 2013. (http://www.njcleanenergy.com/files/file/Renewable_Programs/Draft_2010_Annual_Report_for_New_Jersey_041311_version.pdf)
- Nicks, A. D., & Gander, G. A. (1993). *Using CLIGEN to stochastically generate climate data inputs to WEPP and other water resource models* (Tech. Rep. No. 93-4018). USGS Water-Resources Investigations Report.
- Nogales, F. J., Contreras, J., Conejo, A. J., & Espinola, R. (2002). Forecasting next-day electricity prices by time series models. *IEEE Transactions on Power Systems*, 17(2), 342-348.
- Perez, R., Moore, K., Wilcox, S., Renn, D., & Zelenka, A. (2007). Forecasting solar radiation - preliminary evaluation of an approach based upon the National Forecast Database. *Solar Energy*, 81(6), 809-812.
- Perry, K. B., Wu, Y. H., Sanders, D. C., Garrett, J. T., Decoteau, D. R., Nagata, R. T., ... McLaurin, W. J. (1997). Heat units to predict tomato harvest in the southeast USA. *Agricultural and Forest Meteorology*, 84(3-4), 249-254.
- PJM LOAD/ENERGY FORECASTING MODEL*. (2007). PJM. Retrieved on 12,

- 07, 2012. (<http://www.pjm.com/planning/resource-adequacy-planning/~media/planning/res-adeq/load-forecast/forecast-model-whitepaper.ashx>)
- PJM Manual 19: Load Forecasting and Analysis*. (2012). PJM. Retrieved on 12, 07, 2012. (<http://www.pjm.com//media/documents/manuals/m19.ashx>)
- Reddy, S. J. (1987). The estimation of global solar radiation and evaporation through precipitation: a note. *Solar Energy*, *38*(2), 97-104.
- Richardson, C. W. (1981). Stochastic simulation of daily precipitation, temperature, and solar radiation. *Water Resources Research*, *17*(1), 182-190.
- Richardson, C. W. (1984). *WGEN: a model for generating daily weather variables* (Tech. Rep. No. ARS-8 August 1984). Agricultural Research Service, Washington, DC.
- Seginer, I., & McClendon, R. W. (1992). Methods for optimal control of the greenhouse environment. *Transactions of the ASAE*, *35*(4), 1299-1307.
- Shim, J. P., Warkentin, M., Courtney, J. F., Power, D. J., Sharda, R., & Carlsson, C. (2002). Past, present, and future of decision support technology. *Decision Support Systems*, *33*(2), 111-126.
- Supit, I., & Van Kappel, R. R. (1998). A simple method to estimate global radiation. *Solar Energy*, *63*(3), 147-160.
- Szkuta, B. R., Sanabria, L. A., & Dillon, T. S. (1999). Electricity price short-term forecasting using artificial neural networks. *IEEE Transactions on Power Systems*, *14*(3), 851-857.
- Threlkeld, J., & Jordan, R. (1958). Direct radiation available on clear days. *ASHRAE Transactions*, *64*.
- Ting, K. C., & Giacomelli, G. A. (1987). Availability of solar photosynthetically active radiation. *Transactions of the ASAE*, *30*(5), 1453-1457.
- Ting, K. C., Giacomelli, G. A., & Fang, W. (1993). *Decision support system for single truss tomato production*. XXV CIOSTA - CIGR V Congress, May 10-13,

- Wageningen, The Netherlands, 1993.
- Weron, R. (2006). *Modeling and Forecasting Electricity Loads and Prices: A Statistical Approach* (1st ed.). John Wiley & Sons, Ltd.
- Wilcox, S. (2012). *National Solar Radiation Database 1991-2010 Update: Users Manual*. Technical Report. NREL/TP-5500-54824. Retrieved on 01, 07, 2012. (<http://www.nrel.gov/docs/fy12osti/54824.pdf>)
- Wilks, D. S. (1999). Simultaneous stochastic simulation of daily precipitation, temperature and solar radiation at multiple sites in complex terrain. *Agricultural and Forest Meteorology*, *96*(1-3), 85-101.
- Wilks, D. S., & Wilby, R. L. (1999). The weather generation game: a review of stochastic weather models. *Progress in Physical Geography*, *23*(3), 329-357.
- Wolf, S., Rudich, J., Marani, A., & Rekah, Y. (1986). Predicting harvesting date of processing tomatoes by a simulation-model. *Journal of the American Society for Horticultural Science*, *111*(1), 11-16.
- Yamin, H. Y., Shahidehpour, S. M., & Li, Z. (2004). Adaptive short-term electricity price forecasting using artificial neural networks in the restructured power markets. *International Journal of Electrical Power & Energy Systems*, *26*(8), 571-581.